UNIVERSITY OF OKLAHOMA

GRADUATE COLLEGE

MUTATIONAL ANALYSIS OF BACTERIAL CONDENSINS

A DISSERTATION

SUBMITTED TO THE GRADUATE FACULTY

In partial fulfillment of the requirements for the

Degree of

DOCTOR OF PHILOSOPHY

By

WEIFENG SHE

Norman, Oklahoma

2011

MUTATIONAL ANALYSIS OF BACTERIAL CONDENSINS

A DISSERTATION APPROVED FOR THE
DEPARTMENT OF CHEMISTRY AND BIOCHEMISTRY

BY

_____

Dr. Valentin V. Rybenkov, Chair

_____

Dr. Helen I. Zgurskaya

_____

Dr. Susan J. Schroeder

_____

Dr. Philip E. Klebba

_____

Dr. Anne K. Dunn

ACKNOWLEDGEMENTS

Finally, I have an opportunity to express my greatest gratitude to all those who made my dissertation possible and gave me enormous help during my graduate study and because of whom I will cherish my graduate experience forever.

I own my deepest gratitude to Dr. Rybenkov for his help and great support in guiding me through my graduate studies. He not only taught me how to do experiments, but also encouraged me to think the question through the scientific view. I am especially thankful to Dr. Zgurskaya for her help during my studies, especially during my proposal defense, journal club and my dissertation. I would like to thank my committee members Dr. Schroeder, Dr. Klebba and Dr. Dunn for their encouraging words, and time and attention during graduate work.

I would like to show my gratitude to Dr. Petrushenko for her constant help and suggestions in my research, and to other colleagues, Qinghong Wang, Yuanbo Cui, Yun Liu, Chien-hung Lai and Zhiqiang Sun for sharing their enthusiamsms and comments on my work. It is an honor for me to thank all other members of Dr. Rybenkov and Dr. Zgurskaya's laboratories, especially Dr. Tikhonova Elena.

I would like to show heartfelt thanks to my parents, my wife Xiaoru, for their endless support, patience, love and understanding.

TABLE OF CONTENTS

Table of Contents

List of Figures

List of Tables

Abstract

Genetic information is carried on chromosomes in all organisms and chromosome is at the center of all life processes. The chromosome must be properly folded to fit into the cells. Moreover, replication and segregation of chromosomes to daughter cells must be precisely controlled and coordinated during the cell cycle. Any failure in chromosome dynamics could lead to developmental diseases and cancer. The mechanism of chromosome organization remains unsolved. Structural maintenance of chromosome (SMC) proteins are involved in all the aspects of the higher-order chromosome dynamics in organisms ranging from bacteria to human (Hirano, 2005; Nasmyth and Haering, 2005). Because SMC proteins are so important, studying SMC proteins will not only help us better understand chromosome organization, but also understand mechanisms of related human diseases.

MukBEF is the bacterial condensin required for correct folding of the *Escherichia coli* chromosome (Niki et al., 1991; Petrushenko et al., 2006a). *In vitro*, SMC subunit MukB forms clamps on DNA and MukB clamps further interact with each other to form a scaffold on DNA, thereby controlling the DNA structure (Cui et al., 2008; Petrushenko et al., 2010).

MukF is the kleisin subunit which recruits MukE to MukB. MukF forms complex with MukE, and the MukEF complex can further form a complex with MukB (Petrushenko et al., 2006b). MukEF also modulates the assembly of MukBEF macromolecular structure (Woo et al., 2009). MukEF disrupts MukB-DNA interactions *in vitro* (Petrushenko et al., 2006b). Therefore, MukEF regulates the interaction between MukB and DNA. Since these activities are mainly contributed by

MukF, the role of MukE has long been unclear.

MukB forms clusters at the quarter positions along the cell length. The MukB cluster can be observed when MukB is tagged with GFP. MukEF is required for the assembly of MukB clusters (Ohsumi et al., 2001). The quarter position also is the new home of replicated DNA. These data suggest that *in vivo*, MukEF helps MukB to form a scaffold at the quarter positions of the cell length. According to this model, this MukBEF scaffold, “a condensin factory”, controls the global architecture of the chromosome.

To determine how the MukB cluster is formed, the subcellular localization of MukB and MukE was investigated. We found that MukE-GFP also formed foci at the quarter positions of the cell length but not in cells that lack MukB. Therefore the condensin factory is formed by MukBEF complex, not its individual subunits. Overproduction of MukEF could disrupt MukE foci. Also MukB foci were disrupted by overproduced MukEF. Thus, the condensin factory only can accommodate a limited number of each subunit of MukBEF.

Then the function of MukE was further studied using random mutagenesis. Eight loss-of-function MukE point mutants were constructed. Mutations L54P and L47P P67C resulted in protein misfolding and $MukE^{G96W}$ was expressed at a reduced level. All other mutants had similar expression levels as the wild type MukE. All loss-of-function MukE mutants were unable to form the quarter position foci. Focal localization of MukB was also disrupted by mutations in MukE. Therefore, the condensin factory was disrupted by all of our loss-of-function MukE mutants. These data suggest that MukBEF foci formation is essential for its function.

Five mutant MukEFs (R140C, G188E, P69T, G96W and S141P) were purified using Ni^{2+}-chelate and gel filtration chromatography. Mutation G96W disrupted MukEF complex. Other four mutant MukEF complexes were stable. They were purified and their biochemical activities were studied. All four mutants were able to form MukBEF complexes *in vitro*. These four purified mutant MukEFs inhibited the DNA binding activities of MukB as efficiently as the wild type MukEF.

Lastly, we found that four (R140C, G188E, P69T and S141P) out of six tested mutants formed MukBEF complex inside the cell. These four MukE mutants have the ability to form MukBEF complexes *in vivo* and *in vitro* and they can regulate the interaction between MukB and DNA as efficiently as wild type MukEF. In contrast, all of our loss-of-function MukE mutants are unable to form MukBEF clusters. Therefore, MukBEF complex formation is not sufficient for the MukBEF cluster formation. Binding with DNA is not sufficient for MukBEF cluster formation either. These results suggest that MukE helps MukBEF to form clusters at the quarter positions. Maybe there is an extra-chromosomal factor that is also involved in MukBEF cluster formation.

A new member of the bacterial condensins is discussed in the end. In bacteria, two families of condensins were identified before this study, MukBEF and SMC_ScpAB complexes. Only MukBEF or SMC_ScpAB was found in a given species. Using sequence analysis, we identified a third family of condensins, MksBEF (MukBEF-like SMC proteins), which is broadly present in diverse bacteria. MksBEF often coexists with another condensin. The physiological function of MksBEF protein was studied in *Pseudomonas aeruginosa* strain PAO1, which encodes SMC_ScpAB

and MksBEF complexes. Inactivation of either SMC or MksB led to anucleate cell formation. Increased frequency of anucleate cells was observed when both *smc* and *mksB* genes were knocked out. Moreover, MksBEF can complement anucleate cell formation in SMC-deficient cells. Thus, both MksBEF and SMC contribute to chromosome partitioning in *Pseudomonas aeruginosa*. Several specialized condensins might be involved in organization of bacterial chromosomes.

Chapter 1 Introduction

1.1 Chromosome Organization

Despite differences in the cellular organization of eukarya, bacteria and archaea, all organisms rely on DNA molecules, chromosomes, to store and replicate genetic information. The huge chromosome molecules must be carefully packaged to fit into the cells. Moreover, replication and segregation of chromosomes to daughter cells must be precisely controlled and coordinated during the cell cycle. Any failure in chromosome condensation and segregation may result in genomic instability, chromosome breaks, missegregation, and finally lead to developmental diseases and cancer (Koshland and Strunnikov, 1996; Strunnikov, 2010).

In eukaryotes, the DNA molecule of each chromatid is folded 10,000 to 20,000 times to form a rod-shaped structure during mitosis and the total compaction is achieved in several independent successive stages. First, DNA wraps around histone octamer in a left-handed pattern to form 11 nm nucleosomes with a small stretch of "linker" DNA that runs between nucleosomes, forming the "beads on a string'' structure (Luger et al., 1997; Robinson et al., 2006). Nucleosomes further form a spiral with six to eight nucleosomes per turn. This structure is known as the "30 nm chromatin fibers" (Robinson et al., 2006). The 11 nm nucleosomes and 30 nm chromatin fibers each contributes 6 to 7 folds compaction to chromatin structure. Chromatin fibers are further compacted into the chromatin structure. Various factors, including DNA methylation, histone modifications, histone variants and other proteins, such as SMC (structural maintenance of chromosome) proteins are involved in establishing the higher-order chromatin structure (Li and Reinberg, 2011). But the

packaging of chromosome beyond 30-nm fibers is not well understood yet.

In prokaryotes, the chromosome is normally compacted ~1000-fold into a nucleoid (Holmes and Cozzarelli, 2000). The nucleoid is organized into ~400 independent supercoiled ~10 kb domains (Deng et al., 2005; Postow et al., 2004). Negative supercoiling plays a crucial role in chromosomal compaction, but it is not sufficient to provide the 1000~fold compaction (Sherratt, 2003). A range of nucleoid-associated proteins (NAPs) like HU (heat-unstable), H-NS (histone-like nucleoid-structuring), IHF (integration host factor), FIS (factor for inversion stimulation) and Dps (DNA-binding protein from starved cells) are involved in chromosome organization in bacteria (Reyes-Lamothe et al., 2008; Zimmerman, 2006). It has been believed that NAPs may contribute to nucleoid structure and gene regulation simultaneously (Dillon and Dorman, 2010). Other nucleoid associated proteins, such as the SMC (structural maintenance of chromosome) protein complex also facilitate chromosome organization. The molecular nature of mechanism for chromosome compaction remains elusive.

1.2 SMC proteins

As the major chromosome organizers, structural maintenance of chromosome (SMC) proteins are ubiquitous and play diverse roles in higher-order chromosome dynamics in organisms ranging from bacteria to human (Hirano, 2005; Jessberger et al., 1998; Nasmyth and Haering, 2005). The various chromosome functions and unique structures of SMC proteins have attracted great attention since they were discovered. Six major SMC proteins (SMC1-6) were found in all examined eukaryotic cells. They form heterodimers in specific combinations. The SMC1 and

SMC3 form a dimer at the core of the cohesin complex that mediates sister-chromatid cohesion (Haering and Nasmyth, 2003). SMC2 and SMC4 (XCAP-E/XCAP-C) form the core of the condensin complex and they are involved in chromosome assembly and segregation (Losada and Hirano, 2005). SMC5 and SMC6 form another heterodimer, which has been implicated to function in DNA-repair and checkpoint responses (Lehmann, 2005).

Non-SMC subunits associate with the terminal globular domains of SMC proteins. All SMC complexes include a kleisin, which binds to the terminal domains of SMC protein (Schleiffer et al., 2003). All other non-SMC proteins appear to be recruited to the complex by binding to its kleisin moiety (Figure 1.1).

1.3 Structure of SMC proteins

SMC proteins have very limited identity in their sequence but they share a common unique "V-shaped" molecular architecture (Anderson et al., 2002; Melby et al., 1998). The globular N-terminal domain containing the Walker A motif (G-X-S/T-G-X-G-K-S/T-S/T) is separated from the C-terminal domain containing the Walker B motif (h-h-h-h-D, where h is a hydrophobic residue) by the first coiled coil domain, the globular hinge domain and the second coiled coil domain (figure 1.1). The SMC monomer folds back onto itself through antiparallel coiled-coil interaction. An ABC-type ATP binding 'head' domain is formed by bringing the N-terminal and C-terminal domains together at one end and a 'hinge' domain is at the other end (Nasmyth and Haering, 2005). Two SMC monomers associate with each other at the hinge domain to form a V-shaped molecule (Anderson et al., 2002; Melby et al., 1998).

Although SMC complexes display the characteristic two-armed structure, they

adopt remarkably different confirmations. It has been observed by electron microscopy that condensin forms a lollipop-like structure (Anderson et al., 2002). The head domains of condensin bind with non-SMC subunits at one end and the coiled-coil arms are tightly juxtaposed to each other to form a rod-shaped structure (Anderson et al., 2002). In cohesin, the hinge domains and the head domains are closed at both ends with coiled-coil arms wide open in the middle. The N- and C-terminal domains of the kleisin subunit SCC1 bind to the head domains of SMC3 and SMC1 respectively, to form a tripartite ring-like structure(Anderson et al., 2002; Haering et al., 2002).

1.4 Cohesin

Cohesin is the SMC protein complex which holds the sister chromatids together. Cohesin complex contains four subunits: two SMC subunits SMC1 and SMC3, a kleisin Mcd1/SCC1/RAD21 and the fourth subunit SCC3/SA. In budding yeast cohesin is normally loaded onto chromosomes shortly before initiation of DNA

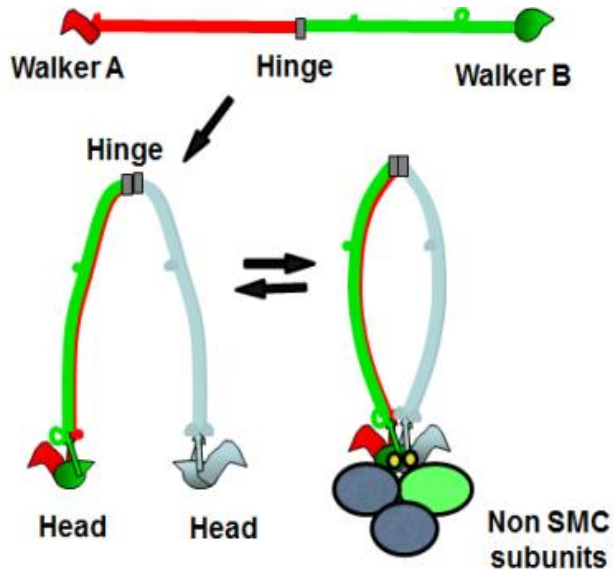

Figure. 1.1 The SMC protein structure.

(A) Secondary structure of SMC monomer. A long coiled coil that is interrupted by a central globular connects the globular N-terminal domain C-terminal domain. (B) Two SMC molecules dimerize to form antiparallel coiled coils, that are intramolecular. Each head domain consists of the terminal domains from the same protamer. (C) Non-SMC (green) binds to the head domain to from holoenzyme.

replication (Guacci et al., 1997; Michaelis et al., 1997). Cohesin complexes continue to bind until the anaphase onset. Cohesin binds chromosomes at high density around the centromere region and at lower density around chromosome arms (Blat and Kleckner, 1999; Glynn et al., 2004; Laloraya et al., 2000). The chromosome-bound cohesins become cohesive to tether sister chromatids together during S phase. This process is regulated by an evolutionarily conserved protein Eco1 (Milutinovich et al., 2007; Noble et al., 2006; Skibbens et al., 1999; Toth et al., 1999). Disassociation of cohesins from the chromosomal arms begins during prophase, and only a small fraction of cohesins remains on the sister chromatids by metaphase (Losada et al., 2000; Sumara et al., 2000; Waizenegger et al., 2000). The pericentric cohesin is preserved around the centromere to keep single-rod appearance of sister chromatids. At the onset of anaphase, the kleisin Mcd1 is cleaved by separase, resulting in complete dissolution of cohesion (Uhlmann et al., 1999).

In addition to chromosome cohesion, cohesin is also involved in other events. For example, cohesin also loaded to the sites of double strand break (DSB) to promote efficient DNA repair (Unal et al., 2004; Unal et al., 2007).

In vitro, the cohesin complex from HeLa cells is able to bind directly to dsDNA and form large protein-DNA aggregates. Cohesin also stimulates intermolecular catenation of circular DNA molecules in the presence of topoisomerase-2 (Losada and Hirano, 2001).

1.5 Condensin

Condensin complex plays a central role in chromosome assembly and segregation. It contains five subunits, the SMC2-SMC4 (XCAP-E/XCAP-C)

heterodimer and three non-SMC proteins, XCAP-D2, -G and –H (Hirano and Mitchison, 1994). XCAP-H is the kleisin subunit. During early mitosis, condensin binds to chromosomes and compacts sister chromatids into largely separate linear rod-shaped structure (Hirano and Mitchison, 1994). Condensin was first found during the process of assembly of mitotic chromosomes from sperm chromatin using unfertilized Xenopus eggs extract. It was found that these extracts can convert highly compacted sperm chromatins to rod-shaped chromatids and the protein associated with these artificial chromatids is condensin (Hirano et al., 1997).

Xenopus laevis condensin I purified from mitotic extracts can introduce positive supercoil into relaxed circular DNA in the presence of topoisomerase-1 (Kimura and Hirano, 1997). A similar activity was also observed with the condensin from *Caenorhabditis elegans* embryos (Hagstrom et al., 2002). This result indicated that condensin caused compensatory negative supercoils, which were removed by topoisomerase-1. Condensin complex is capable of producing positive three-noded knots in a nicked circular DNA in the presence of topoisomerase-2 (Kimura et al., 1999). SMC2/SMC4 from yeast has been reported to have a similar activity (Stray and Lindsley, 2003). This activity indicates that condensin is able to organize two supercoils into an ordered solenoidal form. These activities of condensin shed light on its mechanism.

1.6 Bacterial SMC proteins

Three families of SMC complexes have been found in bacteria and they are MukBEF, SMC_ScpAB and MksBEF complexes. The first complex, MukBEF was found in enterobacteria (Ezaki et al., 1991; Yamanaka et al., 1996) and certain other

γ-subdivision proteobacteria (Hiraga et al., 2000). All three subunits of MukBEF are encoded in the same operon in the order of *mukF-mukE-mukB* (Yamanaka et al., 1996). Another SMC complex, SMC-ScpAB has been found in many other bacteria and archaebacteria (Mascarenhas et al., 2002; Soppa et al., 2002) and it bears high degree of similarity to eukaryotic condensins and cohesins (Cobbe and Heck, 2004). SMC is encoded apart from its regulatory subunits ScpA and ScpB (Mascarenhas et al., 2002; Soppa et al., 2002). Although they share very low sequence identity, MukB and SMC form the same structure as eukaryotic condensin and cohesin and play a similar role inside cells. Inactivation of any subunit of MukBEF complex or SMC_ScpAB leads to severe defects in chromosome segregation and condensation, including temperature-sensitive growth, chromosome decondensation and cutting, and anucleate cell formation (Britton et al., 1998b; Jensen and Shapiro, 1999b; Niki et al., 1991; Yamanaka et al., 1996).

1.7 MksBEF is discovered in diverse bacteria.

Before this study, it was widely believed that bacteria only encode one SMC complex, MukBEF or SMC_ScpAB complex, to organize their chromosome. During the process of homology searches to each subunit of MukBEF, distant relatives of MukBEF are found beyond its previously recognized set of host species (Petrushenko et al., 2011). Although sequence homology was barely detectable, the new protein had the same operon organization and predicted secondary structure as MukBEF, including its many telltale features. Divergently, however, the new protein contains a markedly shorter coiled-coli region than that in MukB and other SMC proteins. To acknowledge these similarities and differences, this new family protein was named

MksBEF (Muk-like SMCs). Further homology searches revealed that MksBEF is broadly present in diverse bacteria, is highly divergent on the sequence level and often coexists with SMC-ScpAB or MukBEF and, sometimes, another MksBEF. Thus, several condensins might be involved in chromosome organization in bacteria.

1.8 MukBEF is a bacterial condensin in *E. coli*.

MukBEF is the only SMC complex involved in chromosome organization in *E.coli*. In the process of searching for segregation mutants in E. coli, a so-called "mukaku" form (anucleate cells) was described by Hiraga and co-workers (1989) and later by Niki and co-workers (Niki et al., 1991; Yamanaka et al., 1996). All subunits of MukBEF complex are encoded in the same operon together with an unrelated gene *smtA*, which encodes an S-adenosylmethionine-dependent methyl transferase.

MukB, MukF and MukE form a complex. In the MukBEF complex, the MukB subunit belongs to the SMC superfamily, and MukF is the kleisin subunit (Fennell-Fezzie et al., 2005; Woo et al., 2009). The MukB homodimer has the characteristic V-shaped structure and MukF links MukE and the head domains of MukB. MukE by itself cannot associate with MukB (Petrushenko et al., 2006b; Yamazoe et al., 1999).

MukEF can form different complexes with MukB. Oligomeric form of MukBEF complexes has also been found. MukEF complex is always composed of four MukEs and two MukFs (Petrushenko et al., 2006b). MukEF can form a complex with MukB in the saturated composition, $B_2(E_2F)_2$ (in the presence of Mg^{2+} ion), or the half-saturated composition, $B_2(E_2F)$ (in the absence of Mg^{2+}) (Petrushenko et al., 2006b). Addition of ATP induces the detachment of one $MukE_2F$ unit from $MukB_2(E_2F)_2$ complex, resulting formation of $MukB_2(E_2F)$ (Woo et al., 2009). MukBEF complex

also can form more complicated macromolecular structures. Rosette-shaped oligomeric structures was observed in solution of MukBEF using electron microscopy (Matoba et al., 2005). MukEF also can modulate the assembly of MukBEF macromolecular structure (Woo et al., 2009).

The nucleoids isolated from the MukB-deficient cells are more de-condensed (Weitao et al., 1999). The temperature sensitive lethality of MukB mutant can be suppressed by deletion of topoisomerase-1 (Sawitzke and Austin, 2000). Deletion in topoisomerase-1 causes increase of negative supercoiling in DNA due to unstrained activity of DNA gyrase. These results suggest that MukB mutant can be suppressed by increased negative supercoiling. Therefore, MukB may control the size of the chromosome by introducing supercoiling into DNA.

MukB also can reshape DNA *in vitro*. It can introduce right-handed knotting into relaxed circular DNA in the presence of topoisomerase-2 and left-handed supercoiling into DNA in the presence of topoisomerase-1 (Petrushenko et al., 2006a).

Another activity of MukB, the DNA bridging activity, has also been observed *in vitro*. When magnetic tweezers approach was used to investigate association between MukB and DNA, it has been found that MukB forms clusters on DNA and that MukB clusters interact with each other to bring distance DNA fragments together (Cui et al., 2008). This activity of MukB was also observed using another DNA bridging assay (Petrushenko et al., 2010). This study revealed that MukB can efficiently bring two DNA fragments together. This reaction begins with the formation of a stable MukB-DNA complex and then another protein-free DNA is captured by this complex. These results indicate that MukB forms clusters first and MukB clusters further form a

scaffold to organize DNA by binding with different segments of chromosome.

The role of MukEF remains unclear. Each subunit of the MukBEF complex is needed in cell division (Niki et al., 1991; Yamanaka et al., 1996). Defects caused inactivation of any subunit cannot be relieved by overproduction of the other two subunits (Wang et al., 2006). Overproduced MukBEF is a better condensin than MukB *in vivo* (Wang et al., 2006). In contrast, MukEF is not required for the interaction between MukB and DNA *in vitro*. Instead, MukEF inhibits the DNA reshaping activities of MukB (Cui et al., 2008; Petrushenko et al., 2010; Petrushenko et al., 2006b). These results suggest that MukEF regulates the interaction between MukB and DNA.

MukB-GFP forms distinct fluorescent foci at the quarter positions of the cells. When either *mukE* or *mukF* gene is disrupted, MukB-GFP is evenly distributed throughout the cell (Ohsumi et al., 2001). This result indicates that MukEF is required for MukB foci formation inside the cell. Foci formation is a common feature of bacterial SMC proteins inside the cell (Mascarenhas et al., 2002; Ohsumi et al., 2001). During DNA replication, newly replicated DNA was segregated to the quarter positions of the cell length first. Therefore, MukEF may help MukB to form a scaffold, “a condensin factory”, at the quarter positions of the cell to control the global architecture of the chromosome.

Here, we show that the protein cluster is formed by MukBEF complex, not its individual subunits. We further introduced mutations into MukE and studied the activities of MukE mutants. Our data show that MukBEF complex formation is not sufficient for MukBEF cluster formation. Binding with DNA is not sufficient for

MukBEF cluster either.

Chapter 2 Methods

2.1 Random mutagenesis of *mukE* gene.

Random mutagenesis of *mukE* gene was performed using GeneMorph II Random Mugagenesis Kit (Stratagene). First, the 1 kb DNA fragment containing *mukE* was synthesized by PCR using plasmid pBB14 (constructed in Dr. Rybenkov's lab) as a template, the forward primer PSEQ1 (5' AACAGCTGGCGGCGATCATC3') and the reverse primer PSEQ2 (5' CGTATGTTGCATCACCTTCA3'). pBB14 contains *mukF* and *mukE-gfp* gene under the endogenous P_{muk} promoter (Figure 4.2). The following PCR program was used: initial denaturation at 94 ºC for 2 min, 25 cycles of denaturation at 94 ºC for 30 seconds, annealing at 55 ºC for 30 seconds and elongation at 72 ºC for 1 min and 45 seconds, and the final elongation at 72 ºC for 3 min. The PCR product was purified using QIAquick PCR Purification Kit and then used as a template for random mutagenesis of *mukE* gene. The error-prone PCR was performed at the following conditions: (i) initial denaturation at 94 ºC for 2 min, (ii) 1 cycle of denaturation at 94 ºC for 30 seconds, annealing at 55 ºC for 30 seconds, elongation at 72 ºC for 1 min and 45 seconds for 1 cycles, and (iii) final elongation at 72 C for 3 min. The mutant *mukE* gene was then introduced into the plasmid pBB14 using restriction enzymes AleI and ApaLI, resulting in the pBB14 library. Then the constructed pBB14 library containing mutant *mukE* was transformed into the Δ*mukE* stain AZ5450 (Yamanaka et al., 1996). The colonies from the transformation were transferred to another fresh plate using replica plating and were grown at 37 ºC. The GFP function was further

checked in colonies which could grow at 23 ºC but not at 37 ºC. The colonies, which had similar intensity of GFP signal to that of the wild type MukE-GFP in strain AZ5450 (pBB14-wt), were further purified and sequenced. 9 mutants were analyzed in this study. Location of the mutations is shown in Figure 4.1 and Table 4.1.

2.2 Construction of Plasmids and strains

2.2.1 Plasmid and strains used in MukBEF study

Unless noted otherwise, *E. coli* and *P. aeruginosa* cells were grown in Luria broth (LB) medium or M9 medium plus 0.4% glycerol and 0.4% Casamino Acids (Difco) under aerobic conditions at 37 °C. Bacterial growth was quantified by measuring the optical density (OD) at 600 nm on an UV-1601 UV-visible spectrophotometer (SHIMADZU).

2.2.1.1 Construction of p15sp-E02a and p15sp-B02a

Plasmid p15sp-E02a is a derivative of p15k-E02a (Figure 2.1 A) (She et al., 2007). p15k-E02a contains MukE-GFP cassette downstream of the P_{muk} promoter (nucleotides [nt] 972226 to 972759 of the *E. coli* MG 1655 strain chromosome) and a kanamycin resistance gene, which are flanked by a *lacY* fragment (nt 362184 to nt 361950) on the upstream and a *lacA* fragment (nt 361032 to nt 360876) on the downstream sides. Within the fusion protein, GFP is linked to the C terminus of MukE via peptide H_9G_2A.

To construct p15sp-E02a (Figure 2.1 B), the kanamycin resistance gene in p15k-E02a was replaced by the Ω interposon containing the spectinomycin resistance gene *aadA* (Prentki et al., 1991). The *aadA* gene was amplified from plasmid pNN6029 (Prentki et al., 1991) by PCR using primers smxbaIF

(5'TGTAAAACGACGGCCAGTGC3') and smbglIIR (5'GGGAGATCTGCTATGACCATGATTACG3'). The BglII restriction site is underlined in primer smbglIIR. The purified PCR fragment was treated with XbaI and BglII and then used to replace kanamycin resistance gene in p15k-E02a to make p15sp-E02a. The plasmid p15sp-E02a was confirmed using restriction digestion with SwaI and SpeI.

Following initial screening, mutant *mukE* genes were transferred from pBB14 plasmid to p15sp-E02a using restriction enzymes NsiI and SpeI to construct plasmid p15sp-E02a containing mutant *mukE* gene. For mutant R34S Y74C, only Y74C was transferred from pBB14 to p15sp-E02a plasmid because the restriction site used for cloning was downstream from R34 (Figure 2.1 C).

Plasmid p15sp-B02a was constructed using plasmids p15sp-E02a and pBB15k-TnPB1, which contains *mukB-gfp* fusion gene under the control of the endogenous P_{muk} promoter (Figure 2.1 D). The NdeI fragment of p15sp-E02a was replaced with the NdeI fragment of pBB15k-TnPB1 which contains the entire *mukB* gene and 239 base pairs of the 5' end of the green florescence protein gene. p15sp-B02a contains the same elements, except that *mukB* gene replaces *mukE*.

2.2.1.2 Cloning of p15sp-E03a

Plasmid p15sp-E03a is a derivative of p15sp-E02a, in which the *mukE-gfp* fusion gene is replaced with *mukE* gene (Figure 2.1 E). *mukE* was amplified by PCR using p15sp-E02a as a template (Figure 2.1 C). The primers were as follows: oBEF79: 5'CGGTGGAGAAAGCAT**ATG**ATTACG3', (with the NdeI restriction site underlined and the translation initiation codon in bold) and oBEF80: 5'

GCAGTGTACA**TTA**TTCTTCCTCTCCGCTATC3', (with a BsrGI restriction site underlined and a translation termination codon in bold). The PCR fragment was treated with NdeI and BsrGI and then inserted into p15sp-E02a between the same restriction sites. The plasmid was confirmed by restriction mapping using restriction enzymes NsiI and PvuI.

The mutant MukE p15sp-E03a plasmids were constructed for S141P, G96W, G188E, R140C, Y74C and P69T.

2.2.1.3 Construction of plasmid pBB41

Plasmid pBB41 (Figure 2.1 G), which was constructed in Dr. Rybenkov's lab, was used to perform in-frame replacement of *mukB* gene with *mukB-gfp*. It contains the *mukB-gfp* fusion gene, followed by the chloramphenicol resistant gene (*cat*) and the *mukB* downstream gene *ycbB*. Within the fusion protein, GFP is linked to the C terminus of MukB via peptide $H_{12}G_2A$.

2.2.1.4 Construction of *E.coli* strains

The *lacYA::mukE-gfp-spc* strain OU110 was constructed by integrating the MukE-GFP cassette into the *lac* locus of MG1655. The MukE-GFP cassette was excised from the plasmid p15sp-E02a using SwaI restriction enzyme, gel purified, and integrated into the chromosome of MG1655 using a lambda Red recombination system (Datsenko and Wanner, 2000). Briefly, MG1655 cells carrying a Red helper plasmid pKD46 were grown at 30ºC in 20 ml of SOB medium supplemented with 100 µg/ml ampicillin and 0.2% L-arabinose. When OD_{600} reached 0.6, the cells were harvested, washed 3 times with ice-cold 10% glycerol in the water and then concentrated 100-fold in 10% glycerol. 25 µl of cells and 1 µl of DNA (between 10

ng and 100 ng) were mixed and transferred to an ice cold 0.1 cm electroporation cuvette (Genesee Scientific, 40-100). After a 1.8 KV electrical shock using a Cell-Porator (GIBCO/BRL), the cell mixture was re-suspended in 1 ml SOC medium and incubated at 37ºC for 2 hours. 0.5 ml of cells was spread onto LB agar plates containing 100 μg/ml spectinomycin. Mutants were streaked on LB agar plate without antibiotic and grown at 42ºC to eliminate temperature sensitive helper plasmid pKD46. All constructions were confirmed by PCR analysis of the recombined regions.

The mutated *mukE* OU110 strains (OU110-L47P, OU110-54P R67C, OU110-P69T, OU110-E70K, OU110-Y74C, OU110-G96W, OU110-R140C, OU110-S141P and OU110-G188E) were constructed using the same procedure. Mutant *mukE* OU111 (*mukE::kan lacYA::mukE-gfp-spc*) strains (OU111-L47P, OU111-54PR67C, OU111-P69T, OU111-E70K, OU111-Y74C, OU111-G96W, OU111-R140C, OU111-S141P and OU111-G188E) were constructed using P1 *vir* transduction of *mukE:: kan* fragment from the *E.coli* Δ*mukE* strain AZ5450 into OU110 strains.

Strain OU115 (*lacYA::mukB-gfp-spc*) was constructed by integration of MukB-GFP cassette from p15sp-B02a into MG1655 strain using the same method as for construction of mutant OU110 strains. P1*vir* transduction of the Δ*mukB::kan* fragment of OU101 (She et al., 2007) into OU110 and OU115 produced strains OU112 (Δ*mukB::kan lacYA::mukE-gfp-spc*) and OU116 (Δ*mukB::kan lacYA:: mukB-gfp-spc*), respectively.

Strain OU119 (*mukB::mukB-gfp-spc*) was constructed by integrating the HpaI fragment of pBB41 (Figure 2.1 G) into MG1655 strain using a lambda Red recombination system (Datsenko and Wanner, 2000). Strain OU120 (*lacYA::mukE-spc*) was constructed by integration of mutant *mukE* from p15sp-E03a (Figure 2.1 E) into *lac* locus of MG1655 strain using the same method as for construction of OU119. Strain OU126 (*mukE::kan mukB::mukB-gfp lacYA::mukE-spc*) strains (OU126-Y74C, OU126-G96W, OU126-R140C, OU126-S141P and OU126-G188E) were constructed by P1 *vir* transduction of the *mukE::kan* fragment from AZ5450 followed by transduction of the *lacYA::mukE-spc* fragment from OU120 into OU119.

2.2.1.5 Construction of mutant pBB08 plasmids

Mutant pBB08 plasmids (pBB08-S141P, pBB08-G96W, pBB08-G188E, pBB08-R140C, pBB08-Y74C and pBB08-P69T) were constructed by replacing the wild type *mukE* with mutant *mukE* (Figure 2.1 F). Mutant *mukEs* were amplified by PCR using mutant pBB14 plasmids as a template. The primers were as follows: oBEF85: 5' GGCGATCATCGAAGAACAACTTGC3', oBEF86: 5'CGATTCTAGA**CTA**GTGATGGTGGTGATGGTGGTG3' with an XbaI restriction site underlined and a translation termination codon in bold. The PCR fragment was treated with BsrGI and XbaI and then inserted into pBB08 between the same restriction sites. The plasmid was confirmed with AseI and AgeI double restriction digestion and sequencing of the replaced mutant *mukE*.

2.2.2 Plasmids and strains used in MksBEF study

The strains and plasmids used in this study are summarized in Table S2. The Pseudomonas aeruginosa strains MPAO1 and PW8890 (*PA4686::ISphoA/hah*) were

obtained from the University of Washington Genome Center (Jacobs et al., 2003) and single colony purified by plating on LB. The strain UCBPP-PA14 (Lee et al., 2006) was a gift of Dr. Ausubel. MPAO1 contains a 1 kb deletion that spans PA4684 and PA4685 (Dotsch et al., 2009) and was used as a Δ*mksEF* strain. PAO1-Lac (*lacI*$^{q+}$ Δ*(lacZ)M15*$^{+}$ *tetA*$^{+}$ *tetR*$^{+}$) was obtained from ATCC and was used as a wild type PAO1. Plasmids pUCP22, pSP856 and pEX18Ap were a gift of Dr. Schweizer. Plasmid pYM101 was a gift of Dr. Morita (Morita et al., 2010). Phage F116 was a gift of Dr. Lomovskaya. Cells were grown in LB or M9 plus 0.4% glucose at 37°C supplemented, when appropriate, with 20 µg/ml tetracycline, 20 µg/ml kanamycin or 100 µg/ml gentamicin. For all experiments, overnight cell culture was diluted into the fresh medium, and cells were further grown for several doubling times. DNA transformation was done as described earlier (Choi et al., 2006).

2.2.2.1 Construction of pUCP_MksB and pUCP_SMC

pUCP_MksB (Figure 2.2 A), which encodes PaMksB-His8 under the control of an arabinose-inducible promoter, was constructed by subcloning XbaI-SphI fragment from pNPA_MksB into the pUCP22 shuttle plasmid (West et al., 1994). The gene encoding PaSMC (PA1527) was amplified using PCR from the genome of UCBPP-PA14 and inserted between HindIII and XbaI sites of pUCP22 yielding plasmid pUCP_SMC (Figure 2.2 B). pUCP_MksB and pUCP_SMC were able to complement the phenotype of appropriate condensin-deficient strains in the absence of any inducer.

2.2.2.2 Construction of pEX_ΔSMC plamid, OP101 and OP102 strains.

pEX_ΔSMC was constructed by subcloning gentamicin- resistance gene flanked

by two FRT sites (Flp recognition sequences) from plasmid pSP856 (Hoang et al., 1998) between two 0.5 kb DNA fragments that flank the *smc* gene and then inserting the cassette between Kpn I and Hind III sites of the conjugal vector pEX18Ap (Hoang et al., 1998) (Figure 2.2 C). pEX_ΔSMC was then transformed into the E. coli strain SM10, and the Δ*smc::Gm* fragment transferred, via conjugation followed by sucrose counter-selection, into PAO1-Lac and MPAO1 as previously described (Hoang et al., 1998). The success of the replacement was confirmed by PCR analysis of the genome of the resulting OP101 and OP102 strains.

2.2.2.3 Construction of pEX_LacI_Mks and OP106 strain

pEX_LacI_Mks (Figure 2.2 D) was constructed by subcloning the following four fragments between KpnI and HindIII sites of plasmid pEX18Ap: (i) the 0.5 kb fragment upstream from the *mks* promoter (nucleotides -634 to -138 relative to the start of *mksF*), (ii) the FRT-flanked gentamicin resistance cassette, (iii) the 1300bp fragment of pYM101 plasmid that containing the *lacI*^{q} gene and the T7 early promoter $P_{T7(A1/04/03)}$, and (iv) the first 503 bp of *mksF*. PAO1-Lac cells were then transformed with the pEX_LacI_Mks plasmid as previously described (Choi et al., 2006) and plated on LB containing 30 μg/ml gentamicin and 5 mM IPTG. Because the plasmid does not carry a *P. aeruginosa* origin of replication, only cells that integrated gentamicin resistance gene via homologous recombination are expected to form colonies. PCR analysis of the five resulting colonies identified one clone that underwent a double-crossover recombination event at the *mks* promoter, yielding OP104 strain, which encodes IPTG-controlled MksBEF.

The gentamicin resistance gene was removed from OP105 cells by transforming

the cells with pFLP2 plasmid, which encodes Flp recombinase, followed by sucrose counter-selection to remove the plasmid (Hoang et al., 1998). Δ*smc::Gm*^{R} locus was then transferred into the resulting unmarked OP105 strain from OP102 via phage F116 transduction, yielding a conditional condensin-deficient double mutant OP106. For all strains, success of the gene replacement procedures was confirmed by PCR analysis of the affected regions.

2.3 Fluorescence microscopy

2.3.1 Live cell fluorescence microscopy

Fluorescence microscopy was done as described earlier (She et al., 2007). Cells were grown in M9 medium containing 0.4% casamino acid (Difco). Where appropriate, 100 μg/ml spectinomycin was added. Cell aliquots (OD_{600} values between 0.6 and 0.8) were supplemented with 10 μM Hoechst 33342, the incubation was continued for 15 min, and 300 μl of cell suspension was applied to a poly-L-lysine-coated coverslip. Following a 5-min incubation, excess cell culture was removed and the coverslips were rinsed six times in phosphate-buffered saline (PBS), placed on top of 15 μl of 5 μM Hoechst 33342 in PBS, spotted onto a microscope slide, and observed using an Olympus BX-50 microscope equipped with a BX-FLA fluorescent attachment. Photographs were taken using an Insight charge-coupled-device camera (Hitschfel Instruments). Image overlays and color adjustment were done using Adobe Photoshop software. Subcellular localization of the fluorescent foci was quantified using the program Nucleus.

2.3.2 Fixed cell fluorescence microscopy

300 μl cells at OD_{600} of 0.8 were fixed in 70% ice cold ethanol, incubated on ice

for 10 min, rinsed with PBS (phosphate buffered saline), deposited onto polylysine-coated microscope slides, stained with 100 nM DAPI and 1x SyproOrange and observed by fluorescence microscopy. As described earlier (Wang et al., 2006), this procedure ensures even staining of protein (SyproOrange) and DNA (DAPI) and facilitates thereby reliable detection of anucleate cells. To visualize MksB-overproducing cells, PAO1 cells harboring pUCP_MksB plasmid were grown in M9 containing 0.4% glycerol up to OD_{600} of 0.2, supplemented with 0.5% L-arabinose and further incubated for 6 h. Chloramphenicol-arrested PAO1 cells were collected 1 h after the addition of the drug to 100 μg/ml (approximately 3x MIC) to the culture (OD_{600} of 0.4) that was grown at 37 °C in M9 medium supplemented with 0.4% glucose.

2.4 Determination of protein expression levels

The expression levels of MukE, MukF and MukB were measured using quantitative immunoblotting. OU111 strains were grown in LB medium at room temperature up to OD_{600} of 0.6. The cells were cooled down in the ice cold water bath for 10 min. 10 ml cell culture was subject to centrifugation at 4000 rpm for 10 min at 4°C and washed once with TN buffer (20 mM Tris-Cl, pH 8.0, 150 mM NaCl). After the supernatant was removed, the pellet was re-suspended in the TN buffer at 10 OD/ml final concentration. 0.1 OD cells were loaded onto a SDS-PAGE gel for electrophoreses next to serially diluted purified MukEF and MukB. After being transferred to polyvinylidene fluoride (PVDF) membrane, each subunit of MukBEF was visualized by immunodetection using antibodies raised against each subunit and quantified by ImageQuant.

2.5 Purification of MukB

DH5α cells harboring pBBEF10 were inoculated into 30 ml LB medium with 100 μg/ml ampicillin and incubated at 37 °C overnight. The overnight cell culture was then diluted into 3 liters of fresh pre-warmed LB medium at 37°C supplemented with 100 μg/ml ampicillin. When OD_{600} reached 0.6, L-arabinose was added to the cell culture to the final concentration of 0.1%. After 3 hours of induction, cells were harvested by centrifugation at 4,000 rpm (Beckman Coulter JLA-8.1000 Rotor) at 4 °C for 25 min and washed once with ice cold TN buffer (20 mM Tris-Cl, pH 8.0; 150 mM NaCl). 50 ml TN buffer was used for 1 liter cell culture. The cell suspension was subjected to centrifugation at 4,000 rpm (Eppendorf A-4-26 Rotor) for 12 min and then the pellet was frozen at -80 °C. The cells were thawed and re-suspended in 60 ml buffer A (20 mM HEPES, pH 7.7; 300 mM NaCl; 20 mM Imidazole; 1 mM PMSF, and 20 ml buffer A for 1 liter cell culture). The cell suspension was passed 3 times through a French Press at 800 psi. The cell lysate was clarified by centrifugation at 18,000 rpm for 25 min at 4 °C (Beckman Coulter JA-20 Rotor).

The clarified lysate was loaded onto a nickel-charged 15 ml self-packed His-Bind column (Novagen Cat.No. 69670-4) equilibrated in Buffer A (20 mM HEPES, pH 7.7; 300 mM NaCl; 20 mM Imidazole; 1 mM PMSF). The column was washed with 10 column volumes of Buffer A and 6 volumes of Buffer C (20 mM HEPES, pH 7.7; 235 mM NaCl; 120 mM Imidazole; 1 mM PMSF), and then eluted with 6 column volumes of Buffer B (20 mm HEPES, pH 7.7, 50 mm NaCl, 400 mm imidazole, 1 mm PMSF). 2 mM EDTA and 1 mM DTT were added to the eluted protein. The protein was further purified on a 15 ml heparin-agarose (Sigma) column (Heparin I). After the protein was loaded, the column was washed with 6 volumes of Buffer 1 (20

mM HEPES, pH 7.7, 5% glycerol, 2 mM EDTA, 1 mM DTT, 1 mM PMSF) plus 50 mM NaCl and 400 mM imidazole, then with 4 volumes of Buffer 1 plus 50 mM NaCl. The protein was eluted with a 10 volume gradient of 50 mM to 750 mM NaCl in Buffer 1. The peak fractions were pooled, concentrated by dialysis against 20% polyethylene glycol, MW 20,000 in Buffer 1 plus 200 mM NaCl, further dialyzed against 20 mM HEPES, 200 mM NaCl, 2 mM EDTA, 1 mM DTT, 50% glycerol, and stored at –20 °C (Figure 2.3).

MukB was further purified using a 1-ml HiTrap heparin column (Amersham Biosciences) (Heparin II) (Figure 2.4). 1 mg MukB was diluted 10 times to reduce NaCl concentration from 200 mM to 50 mM and glycerol concentration from 50% to 5%. The protein was loaded onto the column and washed with 5 volumes of Buffer 1 plus 50 mM NaCl. Then the protein was eluted with a 10 volume gradient of 50 mM to 750 mM NaCl in Buffer 1. The fractions from the high and low salt peaks were pooled separately, dialyzed against 20 mM HEPES, 200 mM NaCl, 2 mM EDTA, 1 mM DTT, 20% glycerol, and kept on ice for up to 2 weeks.

2.6 Purification of MukEF

The plasmid pBB08 carries *mukEF* gene with a nine histidine tag at the C-terminus of *mukE*. The Δ*mukEF* strain OU102 (Wang et al., 2006) was used to bear the plasmid to avoid contamination from the endogenous MukEF. The mutant MukEF protein was purified using Ni^{2+}-NTA chromatography as described in Section 2.5. The eluted MukEF fraction was then concentrated by dialysis agaisnt 20 mM HEPES, pH 7.8; 200 mM NaCl; 2 mM EDTA; 5% glycerol; 20% PEG; 1 mM DTT; 1 mM PMSF to decrease the volume from 45 ml to about 1 ml. For further purification, 1 ml of

concentrated MukEF was applied to 25 ml HR Sephacryl S-300 gel filtration column at the flow rate of 60 µl/min. Elution buffer (20 mM HEPES, pH 7.8; 200 mM NaCl; 2 mM EDTA; 1 mM DTT; 5% glycerol; 1 mM PMSF) was applied at the flow rate of 150 µl/min. 900 µl fractions were collected and analyzed by SDS-PAGE (Figure 2.5). The three most concentrated and purest fractions were pooled, dialyzed against 20 mM HEPES, pH 7.8; 200 mM NaCl; 2 mM EDTA; 1 mM DTT; 50% glycerol; 1 mM PMSF, and kept at -20 °C for further use.

2.7 *In vitro* Reconstitution of MukB and mutant MukEF

Reconstitution was done as described before (Petrushenko et al., 2006b). $MukE_2F$ mutants and $MukB_2$ (5 µg) were mixed at 2 to 1 molar ratio. After 20 min incubation on ice, reconstitution buffer (20 mM HEPES, 200 mM NaCl, 20% glycerol, 2 mM $MgCl_2$, 1 mM DTT) was added to the reaction mixture to the final volume of 40 µl and further incubated for 20 min at room temperature. The sample was applied to a 1 ml Sephacryl S-300 gel filtration column. The column was packed using a BD 1 ml syringe (Becton, Dickinson and Company). The protein mixture was eluted with 20 mM HEPES, 40 mM NaCl, 5% glycerol, 2 mM $MgCl_2$ and 1 mM DTT . Each drop was collected separately as one fraction. The volume of one drop was ranging from 30 µl to 35 µl depending on the column. Each set of experiments was done using the same column within 24 hours. Fraction 1 was collected from the first drop after the sample was loaded onto the column.

2.8 Gel shift assay

The gel shift assay was performed as previously described (Petrushenko et al., 2006b). 10 ng of supercoiled plasmid pBR322 was incubated with 0.1 µg MukB

proteins in the Reaction buffer (20 mM HEPES, 40 mM NaCl, 7% glycerol, 1 mM DTT, 2 mM $MgCl_2$) in the final volume of 9 µl at 37 °C for 30 min. To ensure the 2 to 1 molar ratio of $MukE_2F$ to MukB, 0.13 µg of MukEF in 1 µl volume was added and the sample was further incubated for the indicated amount of time at 37 °C. The reaction was stopped by chilling it on ice for 10 min. The sample was subjected to electrophoresis in 0.7% agarose gel containing 89 mM Tris-borate at 4 V/cm for 4 hours at 4 °C. The running buffer (89 mM Tris-borate) was circulated in the electrophoresis box using peristaltic pumping system to reduce the heat effect. The gel then was stained in 89 mM Tris-borate containing 1 X SYBR-Gold (SYBR® Gold Nucleic Acid Gel Stain, Invitrogen) for 30 min on shaker at room temperature.

2.9 DNA relaxation assay

DNA relaxation assay was performed as previously described (Petrushenko et al., 2006b). 1 µg MukB was mixed with MukEF at the indicated molar ratio, and the mixture was kept on ice for 20 min. Then the reaction buffer was adjusted to 20 mM HEPES, 40 mM NaCl, 7% glycerol, 1 mM DTT and 2 mM $MgCl_2$ (10 µl in total volume) and incubated at 37 °C for 30 min. Then 10 ng (2 µl) supercoiled plasmid pBR322 was added to MukBEF and further incubated at 37 °C for 10 min. 35 fmol (1µl) *E.coli* Topoisomerase I was added and incubated for 5 min at 37 °C. Reactions were quenched by adding 4.33 µl Stop buffer (50 mM Tris-HCl, 0.5% SDS, 20mM EDTA, 200mM NaCl, 0.5 mg/ml proteinase K) followed by 40 min incubation at 50 °C. The samples were subjected to electrophoresis in 0.8% agarose gel in 1X TAE buffer at 4 V/cm at room temperature for 3 hours. The gel then was stained in 1X TAE buffer containing 1 X SYBR-Gold (SYBR® Gold Nucleic Acid Gel Stain,

Invitrogen) for 30 min on a shaker at room temperature.

2.10 Sedimentation rate analysis of mutant MukEF protein

30 µg of mutant MukEF was mixed with 30 µg each of thyroglobulin (19.2 S, 8.6 nm), catalase (11.2 S, 5.3 nm), apoferritin (17.6 S, 6.2 nm), catalase (11.2 S, 5.1 nm), alcohol dehydrogenase (7.3 S, 4.6 nm), bovine serum albumin (4.3 S, 3.6 nm) and carbonic anhydrase (2.8 S, 2.0 nm) in reconstitution buffer. The protein mixture was loaded on top of 10% to 40% sucrose gradient prepared in reconstitution buffer (except that glycerol concentration was 10%) and centrifuged at 55,000 rpm for 12 h at 4ºC in TLS 55 rotor (Beckman). The proteins in collected fractions were resolved by SDS-PAGE, visualized by Coomassie Blue staining, and quantified using densitometry. The standard error of the method was determined by the volume of fractions and it should be the sedimentation rate corresponding to the smallest fraction. The standard error can be calculated using the equation: 0.5*(S of Catalase – S of Carbonic Anhydrase)/(peak fraction of Catalase – peak fraction of Carbonic Anhydrase).

2.11 Stokes radius analysis of mutant MukEF protein

30 µg of mutant MukEF was mixed with 30 µg each of thyroglobulin (19.2 S, 8.6 nm), catalase (11.2 S, 5.3 nm), apoferritin (17.6 S, 6.2 nm), catalase (11.2 S, 5.1 nm), alcohol dehydrogenase (7.3 S, 4.6 nm), bovine serum albumin (4.3 S, 3.6 nm) and carbonic anhydrase (2.8 S, 2.0 nm) in reconstitution buffer. The protein mixture was kept at room temperature for 20 min and loaded onto a 2 ml Sephacryl S300 column (10 mm X 200 mm, catalog # 737-1091, Bio-Rad) . The same reconstitution buffer (Section 2.9) was used to elute protein from the column at flow rate of 0.167

ml/min. The eluent was collected at 2 drops per fraction (about 110 µl). The proteins in collected fractions were resolved by SDS-PAGE, visualized by Coomassie Blue staining, and quantified using densitometry.

2.12 Isolation of MukBEF from the cell

This procedure was adapted from the protocol for nucleoid isolation as described earlier (She et al., 2007). OU111 strains were grown in 150 ml LB medium at room temperature to an OD_{600} of 0.8, chilled by swirling the flask in the ice-cold water bath for 10 min, concentrated by centrifugation and washed once with TNS buffer (20% sucrose, 10 mM TrisCl, 100 mM NaCl). Then the cells were resuspended in 0.75 ml TNS buffer and treated with 0.1 ml TELyz buffer (35 mM TrisCl, 85 mM EDTA, 0.4 mg/ml lysozyme) for 1 min on ice. Following lysozyme treatment, the cells were immediately lysed by gently mixing the suspension with 0.25 ml BDE buffer (1% Brij58, 0.4% deoxycholate, 10 mM EDTA) followed by incubation at room temperature for 3 min. DNA was digested by adding 10 µl of 20 mg/ml DNaseI and 2 mM $MgCl_2$ for 5 min on ice. The reaction was stopped by adding 2 mM EDTA. 0.6 ml cell lysate was mixed with 200 µg each of the protein size markers (apoferritin (17.6 S, 6.2 nm), catalase (11.2 S, 5.3 nm), alcohol dehydrogenase (7.3 S, 4.6 nm), bovine serum albumin (4.3 S, 3.6 nm)) and loaded onto a 10 ml of 15% to 60% sucrose gradient in 10 mM Tris-HCl pH 7.8, 200 mM NaCl, 2 mM EDTA, 1 mM dithiothreitol, 1 mM PMSF. The protein complexes were separated by centrifugation at 38,000 rpm at 4 °C for 30 hours using a Beckman Ti-70 rotor. After centrifugation, about 20 fractions were collected from the bottom. Each fraction was subjected to Western blotting against anti-MukB, anti-MukE or anti-MukF antibody, as

appropriate, to determine the location of each subunit of MukBEF complex. The sedimentation rate of each subunit was determined from the comparison with the protein size marker.

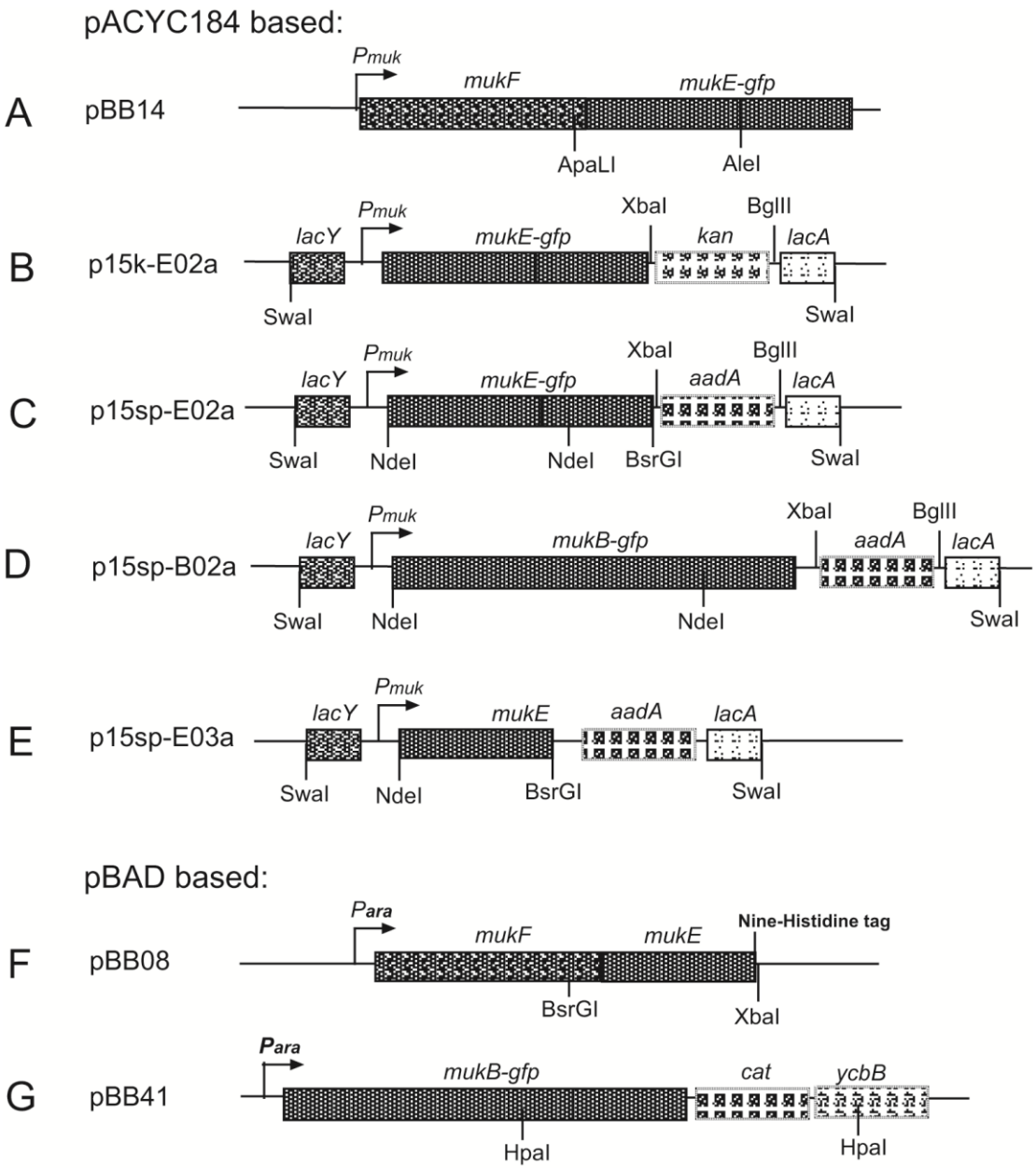

Figure 2.1 Schematic representations of fragments of plasmids used in MukBEF study.

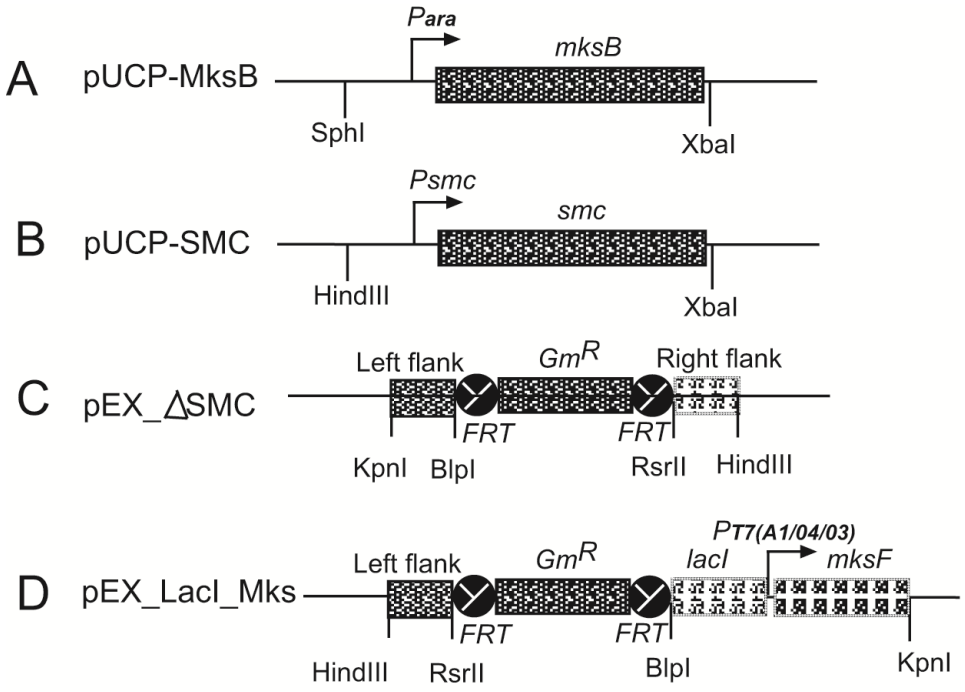

Figure 2.2 Schematic representations of fragments of plasmids used in MksBEF study.

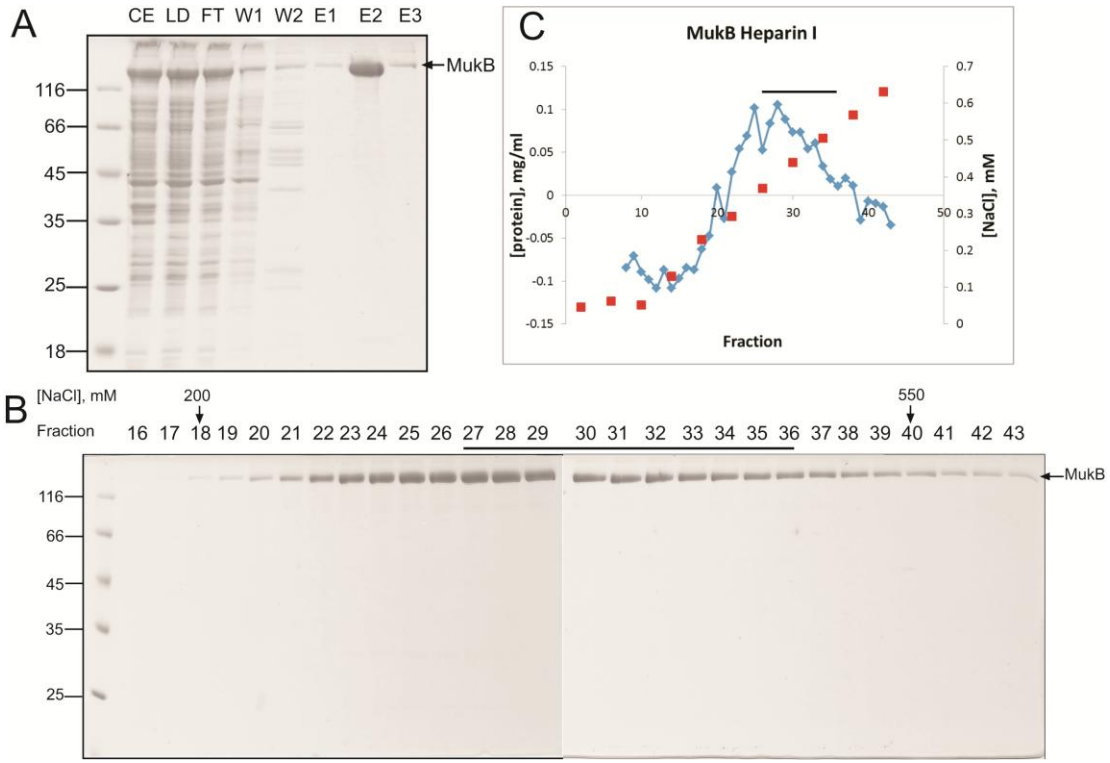

Figure 2.3 Purification of MukB on Ni^{2+}chelate column and Heparin I column.

(A) SDS-PAGE gel that analyzes Ni^{2+} chelate column fractions. CE: cell extract; LD: loading; FT: flow-through; W1: washed by Buffer A; W2: washed by Buffer C; E1: eluted by 8 ml Buffer B; E2: eluted by 45 ml Buffer B; E3: eluted by 22 ml Buffer B. (B) SDS-PAGE gel that analyzes Heparin I fractions. Fractions 16 to 43 are shown. Fractions 27 to 36 (indicated by black bar) were pooled together as the high salt fraction. (C) Protein profiles following elution from the Heparin I column. Protein concentrations were determined by a Bradford assay.

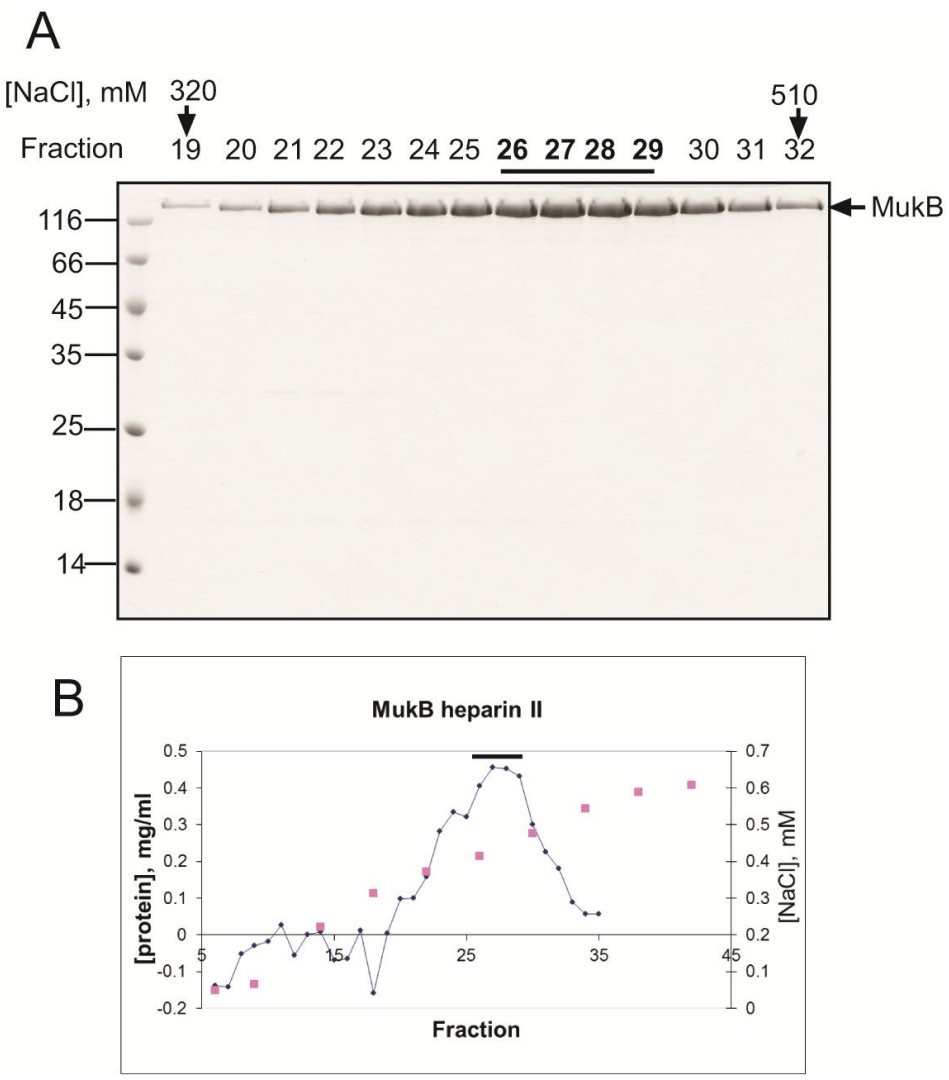

Figure 2.4 Purification of MukB on Heparin II.

(A) SDS-PAGE gel that analyzes Heparin II fractions. Fractions 19 to 32 are shown. Fractions 26 to 29 (indicated by black bar) were pooled together as the high salt fraction. All purification steps were performed at 4°C and each fraction was about 220 µl. (B) Protein profiles following elution from the Heparin II column. Protein concentrations were determined by a Bradford assay.

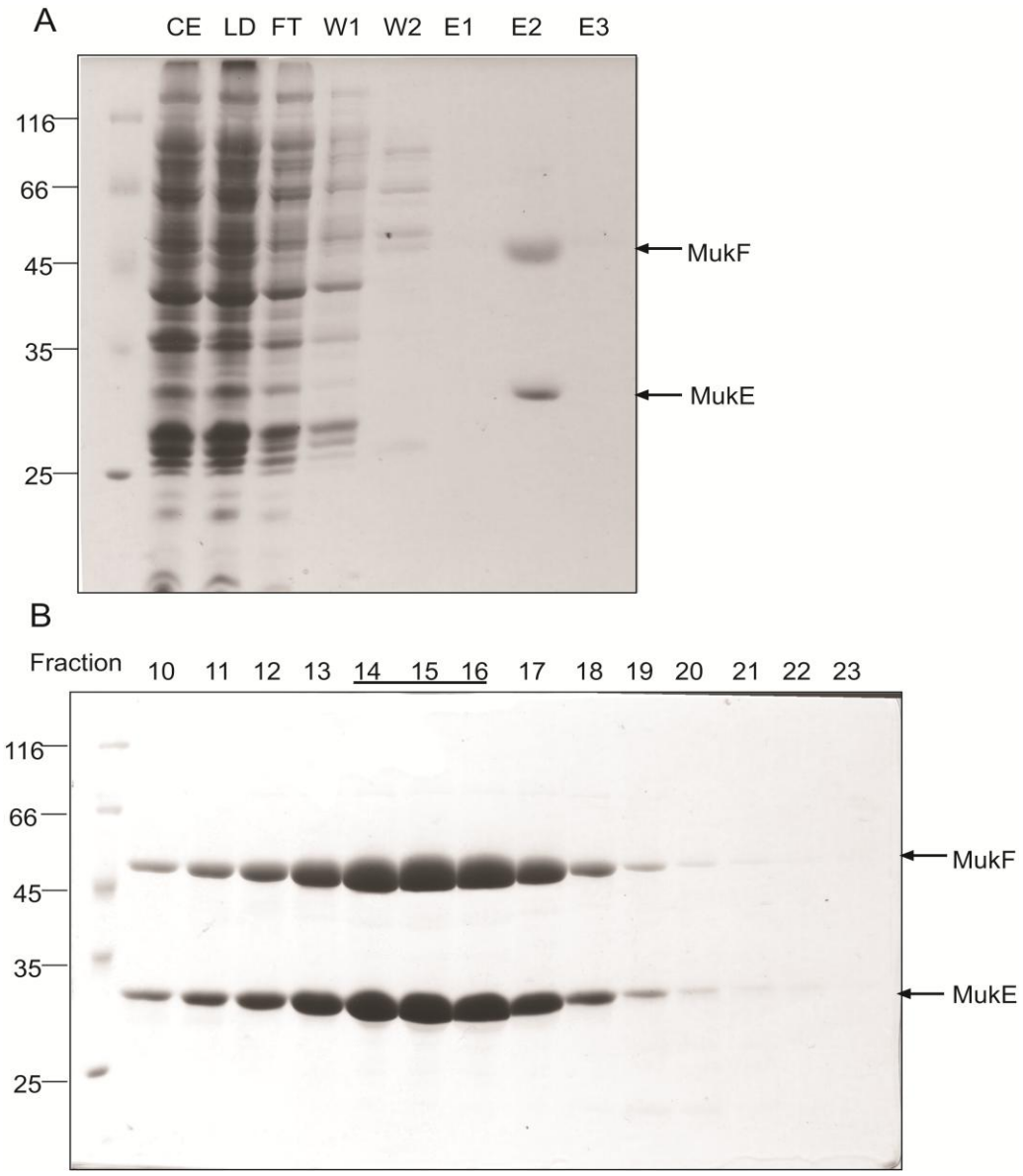

Figure 2.5 Purification of mutant MukES141PF.

(A) SDS-PAGE gel that analyzes Ni^{2+} chelate column purification fractions of $MukE^{S141P}F$. CE: cell extract; LD: loading; FT: flow-through; W1: washed by Buffer A; W2: washed by Buffer C; E1: eluted by 8 ml Buffer B; E2: eluted by 45 ml Buffer B; E3: eluted by 22 ml Buffer B. (B) SDS-PAGE gel that analyzes S300 sephacryl column purification profile of $MukE^{S141P}F$. Each fraction was 1 ml and fractions 10 to 23 were shown. Fractions 14 to 16 were pooled together and concentrated.

Chapter 3 MukBEF complex forms quarter position foci.

This chapter is adapted from (She et al., 2007).

Introduction

MukB forms distinct clusters along the length of the cell at about the one-quarter and three-quarter positions (den Blaauwen et al., 2001; Ohsumi et al., 2001). No clusters were detected in cells deficient in MukE or MukF (Ohsumi et al., 2001). The SMC protein from *Bacillus subtilis* was also shown to form distinct foci together with its cognate non-SMC subunits ScpA and ScpB (Lindow et al., 2002; Volkov et al., 2003). Thus, formation of clusters by SMC complexes appears to be a common phenomenon in bacteria. It was proposed, therefore, that bacterial SMCs drive chromosome segregation by condensing the newly replicated DNA towards its new home at the quarter positions (Graumann, 2001). Here, we propose that MukEF helps MukB to form a condensin factory at the quarter positions of cell length to organize the global structure of the chromosome. The foci formation of MukBEF is investigated first. We also investigated the relationship between the copy number of each subunit of MukBEF and foci formation.

3.1 MukE-GFP forms foci at the quarter positions but not in the absence of MukB.

First, MukEF localization was examined in the *lacYA::mukE-gfp-spt* strain OU110, which produces endogenous MukE and a C-terminal GFP fusion of MukE from an ectopic location. As judged by quantitative immunoblotting, OU110 produces about 600 copies of MukE-GFP per cell in addition to 300 copies of endogenous MukE (Figure 3.1 A).

MukE-GFP formed well-defined fluorescent clusters (Figure 3.1 A). The MukE-GFP foci were smaller than the nucleoids, indicating that these represent distinct structures and are not the result of random association of MukBEF with DNA. Similar to MukB-GFP, MukE-GFP foci were located at the quarter positions inside the cell (Figure 3.1 B).

We next examined if MukEF can form clusters in the absence of MukB. MukE-GFP was evenly distributed throughout the Δ*mukB::kan lacYA::mukE-gfp* OU112 cells (Figure 3.1 A). This was not due to the lower cultivation temperature required for OU112 cells. The distributions of MukE-GFP in OU110 cells were identical at 37°C and at 23°C (Figure 3.1 B and C). Thus, MukE-GFP forms clusters inside the cell but only in the presence of MukB.

We found no clusters of MukE-GFP in OU110 cells harboring the MukEF-encoding pBB08 plasmid (Figure 3.1 A). Similarly, MukE-GFP was evenly distributed after mild overproduction of MukF (data not shown). Only at a high level of overproduction of MukEF did we observe MukE-GFP clusters (Figure 3.1 A). These, however, were often located at the poles of the cell, virtually never colocalized with nucleoids (less than 6% of cells), and resembled protein aggregates by their stark appearance. We conclude that the protein clusters at the quarter positions can accommodate only a limited number of MukE proteins.

3.2 Elevated levels of MukEF displace MukB-GFP from the quarter foci.

MukB-GFP forms foci at the quarter positions in the presence but not in the absence of MukEF (Ohsumi et al., 2001). To further explore this relationship, we examined the effect of MukEF on the formation of MukB foci.

Subcellular localization of MukB-GFP was investigated using strain OU116, which lacks endogenous MukB but produces a C-terminal GFP fusion of MukB from an ectopic location (Section 2.2.5). In this strain, MukB-GFP is produced at about the same level as the untagged protein, 600 and 400 copies per cell, respectively (Figure 3.2 C). In agreement with previous data (Ohsumi et al., 2001), MukB-GFP formed clear foci in the middle of short cells or at the quarter positions of the longer cells (Figure 3.2 A and B). Similar foci, albeit with somewhat stronger background, were observed in the *mukB*$^{+}$ *mukB-gfp* OU115 strain (data not shown).

Overproduction of MukEF interfered with localization of MukB-GFP. Although MukB-GFP clusters could still be detected at mild overproduction levels of MukEF, most of the fluorescence was distributed throughout the cell and could be found even in the DNA-free sections of the cell (Figure 3.2 A, arrowheads). Following induction of MukEF, MukB-GFP was found in clusters away from DNA (Figure 3.2 A). Most of the induced cells (82%) contained internal foci in addition to the bright spots at the cell poles. The majority of these were located next to or at the tip of the nucleoids (Figure 3.2 A, double arrows). Only 8% of examined cells contained MukB-GFP foci that could have colocalized with DNA. No such alternative clusters were found upon overproduction of SmtA or TopA (data not shown). Although fluorescence from across the cell was somewhat increased in these cases, at least 60% of cells contained MukB-GFP foci at expected locales. It appears, therefore, that MukB-GFP was recruited to MukEF aggregates via its specific interactions with the kleisin, which indicates, in turn, that the protein was folded correctly. We conclude, therefore, that overproduced MukEF precludes MukB from binding the chromosome.

Conclusion

We found that MukE forms the same kind of foci at the quarter positions along the cell length as MukB. MuE foci can be disrupted by inactivation of MukB or overproduction of MukEF. Overproduction of MukEF also precluded formation of MukB foci. Therefore, we conclude that the protein cluster is formed by MukBEF, not its individual subunits. Also, MukBEF cluster at the quarter positions can accommodate only a limited number of proteins. These data indicates that MukEF mediates the assembly of MukBEF into a macromolecular structure at the quarter positions.

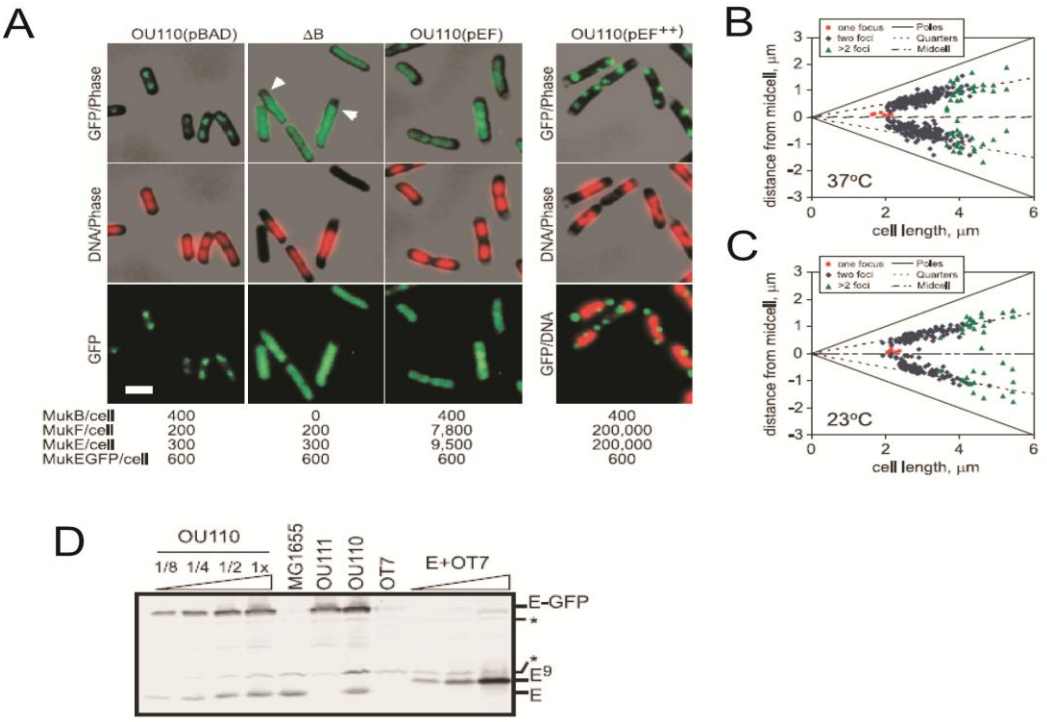

Figure 3.1 Subcellular localization of MukE-GFP.

(A) Fluorescence micrographs of OU110 or OU112 (ΔB) cells harboring the vector (pBAD) or pBB08 (pEF) or induced to overproduce MukEF (pEF^{++}). OU110 cells were grown in LB medium at 37℃; OU112 cells were grown at 23℃. The copy number of Muk proteins is shown beneath the micrographs. Arrowheads point to the GFP signal in the DNA-free sections of the cell. Size bar, 2 μm. (B and C) Subcellular localization of MukE-GFP clusters in OU110 cells grown in LB medium at 37℃ (B) or 23℃ (C). GFP fluorescence is shown in green, DNA is in red, and phase contrast is in gray. (D) Immunoblot analysis of MukE-GFP content in OU110 cells. Diluted as indicated, 0.1 OD unit of OU110, MG1655, OT7, and the OU110-derived Δ*mukE mukE-gfp* OU111 cells was analyzed along with 17 fmol, 70 fmol, and 340 fmol of purified MukE-His9. The copy numbers of MukE-GFP and MukE were estimated as 600 and 250, respectively, in agreement with the earlier estimate of

340 ± 100 MukE copies per cell (Petrushenko et al., 2006b). An asterisk marks the major cross-reacting bands. E, MukE; E^9, MukE-His9.

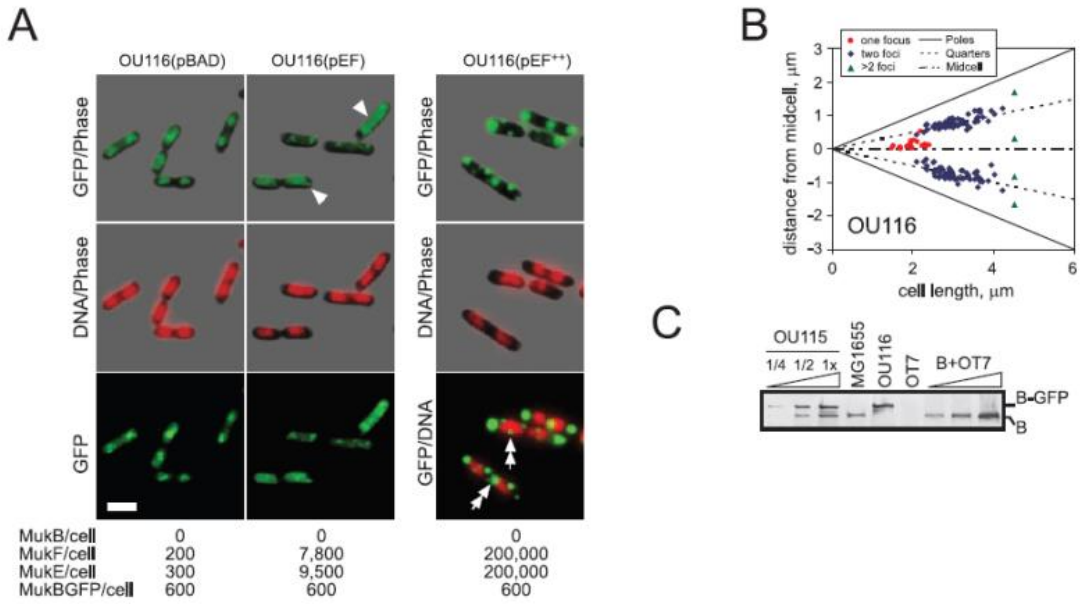

Figure 3.2 Subcellular localization of MukB-GFP.

(A) Fluorescence micrographs of OU116 (Δ*mukB mukB-gfp*) cells harboring pBAD, pBB08 (pEF), or induced pBB08 (pEF^{++}) plasmids grown in LB medium at 37 ℃. Arrowheads point to MukB-GFP fluorescence in the DNA-free sections of the cell. Double arrows indicate foci in the vicinity of the nucleoids. Size bar, 2 μm. (B) Subcellular localization of MukB-GFP clusters in OU116 cells grown in LB at 37 ℃. (C) Immunoblot analysis of MukB-GFP content in OU116 and its parental *mukB*$^+$*mukB-gfp* OU115 strain. Loads are 0.025, 0.05, and 0.1 OD units of OU115 cells and 0.1 OD units of MG1655, OU116, and Δ*mukBEF* OT7 cells. Purified MukB (B+OT7) in amounts of 30 fmol, 90 fmol, and 300 fmol is supplemented with 0.1 OD unit of OT7 cells. The copy number of MukB-GFP and MukB was estimated as 600 and 400 per cell, respectively. B, MukB.

Chapter 4 Mutational analysis of bacterial condensin MukBEF

Introduction

In the previous chapter, we found that MukBEF forms cluster at the one-quarter and three-quarter positions along the cell length and that the protein cluster is formed by MukBEF, not its individual subunits. These data support the view that MukBEF forms a macromolecular structure on the chromosome. To further study the function of MukE, a series of MukE mutants was constructed using random mutagenesis. First, we investigated how mutations in MukE influence the subcellular localization of MukBEF. Then, the biochemical activities of MukE mutants were studied. Finally, we explored the MukBEF complex formation inside the cell.

4.1 Construction of random loss-of-function mutants of MukE

This part of experiment was done by Dr. Elena Mordukhova. A series of MukE mutants was constructed using error-prone PCR. Then the mutant *mukE* library was subcloned into the plasmid pBB14 which encodes MukF and GFP tagged MukE under the control of arabinose inducible promoter. The mutant pBB14 was screened by selection of the colonies that could not complement the temperature sensitive phenotype of the Δ*mukE* strain AZ5450. To weed out misfolding mutants, the cells were examined by fluorescence microscopy. Only cells with a clear GFP fluorescence were analyzed further. Then the mutants were sequenced, which revealed 9 point mutations.

We found that four mutants contain the same point mutation D195G together with other one or two point mutations. $MukE^{D195G}$, which contains only the D195G mutation, did not show any temperature sensitivity. We conclude, therefore that the

observed phenotypes of the double mutants were caused by the second mutations. The details about the mutations are summarized in Figure 4.1 and Table 4.1.

Table 4.1 Nucleotide and amino acid substitutions in mutant *mukE* gene.

Variant	Substitution in nucleotide sequence	Substitution in amino acid sequence
21	2 C → T T→C	No S141P
125	2 C → T G→ T A → G	No G96W D195G
126	2 C → T T→C C→T A → G	No L47P R67C D195G
136	2 C → T G→A	No G188E
139	2 C → T C → T	No R140C
147	2 C→ T T → C A→ G	No L54P D195G
152	2 C→ T G→ A	No E70K
157	2 C→ T C→ A A→ G	No R34S* Y74C
160	2 C→ T C → A A→ G	No P69T D195G

Asterisk indicates that R34S was eliminated from this mutant prior to subsequent analysis.

4.2 Protein expression and colony formation.

The 9 generated mutant *mukE*s were transferred into the plasmid p15sp-E02a from pBB14 and then integrated into the *lac* locus of *E.coli* MG1655 strain using a lambda Red recombination system (Datsenko and Wanner, 2000), resulting in OU110

(*lacYA::mukE-gfp-spc*) strains. Then the endogenous *mukE* was disrupted using P1 *vir* transduction of *mukE::kan* from Δ*mukE* strain AZ5450, yielding a series of OU111 (*mukE::kan lacYA::mukE-gfp-spc*) strains.

The protein expression level for each MukE mutant was measured in OU111 strain using immunoblotting as described in the Methods Section. In OU111 strain, the endogenous *mukE* is disrupted by *kan,* and *mukE-gfp* is expressed from an ectopic location within *lacYA* locus (She et al., 2007). In this strain, the copy number of MukE-GFP is about 600 per cell, which is similar to that of MukE-GFP in OU110 strain (Figure 4.2 and Table 4.2).

Two mutants, L54P and L47P R67C were expressed at a very low level, about 10 copies per cell, suggesting defects in protein folding. In addition, G96W was expressed at a reduced level, 100 per cell. The copy number of other mutants was similar to that of the wild type MukE-GFP (Figure 4.2 and Table 4.2).

The mutations of MukE were examined in the crystal structure of MukBEF complex (Woo et al., 2009). This structure contains a MukB dimer, one MukF monomer and a MukE dimer (Figure 4.1). MukB structure contains only its N-terminal and C- terminal head domains connected by a short linker sequence in between, which replaced the coil-coils and the hinge domain. Therefore, this MukB is designated as MukBhd. MukF is composed of four sequential domains: the N-terminal winged helix domain (WHD) (residues 1-120), the four-helix bundle (residues 121-291), the middle linker peptide (residues 292-354) and the C-terminal WHD (residues 355-440). MukE consists of the N-terminal WHD and the C-terminal WHD. Two MukEs interact with each other via their N-terminal WHDs to form a

homodimer, and their C-terminal WHDs are facing apart (Figure 4.1A). MukBhd homodimer and MukE homodimer are linked together by MukF. The C-terminal WHD of MukF binds with the first dimerized MukBhd. The long flexible middle region of MukF binds with the second MukBhd and continues to interact with MukE homodimer by crossing between the N-terminal and C-terminal WHDs of both MukEs. Besides the middle flexible linker region of MukF, the C-WHD of one MukE monomer also interact the four-helix bundle of MukF.

Leucine-54 and leucine-47 are located at the α4-helix of the N-terminal WHD (Figure 4.1 A and B). In both case, a hydrophobic residue leucine is replaced by a proline, which is the only cyclic amino acid and often serves as a conformational constraint. Probably the structure of N- terminal domain is changed by these two MukE mutations, resulting in protein misfolding. It is not surprising then that these two mutants showed very low protein expression levels (Figure 4.2 and Table 4.2). Glycine-96 is located at the interface between the C- terminal WHD of MukE and the four-helix bundle of MukF (Figure 4.1). When a glycine with its small side chain is changed to tryptophan with a large indole side chain, the interaction between MukE and MukF is probably affected, resulting in an unstable MukEF complex. Free $MukE^{G96W}$ is easy to be degraded; therefore OU111-G96W only had reduced level of MukE (Figure 4.2).

We next measured the colony forming units (CFU) for all OU111 mutants (Figure 4.2 and Table 4.2). All of our loss-of-function *mukE* mutants were initially selected because they could not grow at 37 ºC. It is necessary to determine the temperature sensitivity in a quantitative way and therefore the CFU of all mutants

was examined in OU111 strain. Except for the mutant Y74C, the CFU of all other mutants is at least 3 orders of magnitude lower than that of the wild type strain. Although Y74C was isolated together with another point mutation, R34S, only Y74C was transferred from pBB14 into p15sp-E02a and then integrated into OU111 strain thanks to the restriction site chosen during cloning. Apparently Y74C is a viable mutation.

The CFU of OU111-S141P is two orders of magnitude lower than that of the other mutants. Apparently, expression of $MukE^{S141P}$ from OU111 is toxic to the cell.

Table 4.2 Mutant MukE copy number in OU111 strain, CFU of mutant OU111 stains and sedimentation rate of purified mutant MukEF.

Mutant	MukE-GFP copy number per cell	CFU at 37 ºC	CFU at room temperature	Sedimentation rate (S)[a]
Wild type				7.5
Wild type	830±245	2.6×10^8	2.7×10^8	7.7±0.4
L47PR67C	11±8	3.4×10^4	5.4×10^7	ND
L54P	11±7	1.3×10^5	4.5×10^7	ND
P69T	430±300	4.5×10^5	6.0×10^7	7.6±0.4
E70K	800±300	4.6×10^4	6.4×10^7	ND
G96W	160±75	2.3×10^5	4.0×10^7	ND
R140C	880±480	1.1×10^5	3.9×10^7	7.8±0.4
S141P	880±450	300	5.4×10^7	7.6±0.4
G188E	860±370	2.1×10^5	4.1×10^7	7.9±0.4
Y74C	400±100	$2.1X10^8$	2.1×10^8	7.3±0.4

[a] 7.5 S is the sedimentation rate of MukEF from (Petrushenko et al., 2006b);

ND, not determined.

4.3 Mutant MukEs do not form foci at the quarter positions of the cell length.

We next examined formation of MukBEF foci in the mutant strains. MukBEF forms clear foci at the quarter positions along the cell length when MukB or MukE is tagged with a fluorescent protein (Danilova et al., 2007; Ohsumi et al., 2001; Shin et al., 2009). Focal localization is one of the most pronounced *in vivo* activities of MukBEF complex. Foci formation of MukBEF can be disrupted by inactivation of any subunit of this complex (Ohsumi et al., 2001; She et al., 2007), overproduction of MukEF (Chapter 3) and mutations in MukF (Shin et al., 2009). In these experiments, we used the OU111 strain which contains the wild type *mukB* and *mukF* in their endogenous loci and either the wild type or mutant *mukE* fused with the *gfp* gene under the control of P_{muk} promoter in the *lacYA* locus. Since mutant *mukE* strains cannot grow at 37 °C, all OU111 strains were grown in M9 medium at room temperature.

In agreement with previous studies (She et al., 2007), the wild type MukE-GFP formed foci at the quarter positions along the longitudinal axis of the cell (Figure 4.3). The viable Y74C mutant also localized to the quarter positions. 29% (58/200) cells in P69T and 20% (33/168) cells in E70K contain strange foci, but this kind of foci does not coincide with DNA. All other mutants were evenly distributed across the cell. OU111-L47P R67C and OU111-L54P showed very weak GFP signal. All other mutants have similar intensity of fluorescence to that of OU111-wt. This intensity of GFP signal is related to the protein expression level and was consistent with the results of the measurements of the protein expression level (Section 4.2). Therefore,

except for OU111-L47PR67C and OU111-L54P, the observed loss of GFP foci in all other mutants is not cause by low protein expression.

4.4 Mutations in MukE disrupt focal localization of MukB.

We next determined whether or not MukB is able to form foci in strains with mutant MukE. Localization of MukB-GFP was examined in OU126 strain. This strain encodes the wild type *mukF*, and *mukB- gfp* under the endogenous P_{muk} promoter and *mukE* with its endogenous promoter at the *lacYA* locus. In these experiments, cells were grown in M9 medium at room temperature. In the OU126-wt strain, MukB-GFP formed foci at the quarter positions along the cell length as we expected (Figure 4.4). MukB-GPF also showed similar localization pattern in OU126-Y74C. In the other mutant OU126 strains, MukB-GFP was only evenly distributed throughout the cell. Because we did not observed MukE and MukB foci in all unviable *mukE* mutant strains, we concluded that all of our loss-of-function MukE mutants disrupted the foci formation of MukBEF complex (Figure 4.4).

4.5 Some MukE mutants are able to join MukBEF foci.

Next, we determined if MukE mutants are able to join the existing MukBEF foci. To this end, MukE-GFP localization was studied in OU110 strain. This strain contains the wild type *mukBEF* operon and the mutant *mukE-gfp* fusion gene under the endogenous P_{muk} promoter at the *lacYA* locus. This strain contains all three wild type subunits of MukBEF and exhibits the wild type phenotype even in the presence of inactive MukE-GFP. In OU110-wt, which contains the wild type *mukE-gfp* gene at the lacYA locus, MukE form foci at the quarter position of the cell length (She et al., 2007). If a mutant MukE has the ability to interact with any component of MukBEF

clusters, this mutant should also show high intensity GFP signal at the quarter positions of the cell. Otherwise, GFP would be evenly distributed across the cell.

In this experiment, cells were grown in M9 medium supplemented with 0.4% Casamino Acids at 30°C. In OU110-R140C, OU110-S141P, OU110-G188E and OU110-Y74C strains, MukE-GFP joined the foci already formed by MukBEF complex as observed in OU110-wt strain. 14% cells in OU110-P69T and 5% cells in OU110-E70K formed foci at the quarter position and this kind of foci is much diffused. The others showed even distributed GFP signal (Figure 4.5).

Based on the *in vivo* localization of MukE and MukB, we conclude that all loss-of-function mutants disrupt formation of the MukBEF foci. Four out of eight mutants: R140C, S141P, G188E and Y74C are able to join the existing MukBEF foci.

Based on the *in vivo* phenotypes of MukE mutants (Figure 4.5), we classified them into four groups. Group I mutants include P69T, E70K and G96W. These mutants cannot form or join MukBEF foci. Group II mutants, which include R140C, S141P and G188E, cannot form foci, but are able to join pre-existing MukBEF foci. Y74C is a Group III mutant, which forms MukBEF foci and also is able to join MukBEF foci. This mutant is also viable. Group IV mutants, which showed very low GFP signal, include L47P R67C and L54P. This group of mutant proteins is apparently misfolded and degraded inside the cell.

4.6 Mutant G96W is unable to form MukEF complex.

Next, we examined biochemical activities of the mutant MukE proteins. First, mutant MukEF proteins were purified. Six mutant MukEs ($MukE^{P69T}$, $MukE^{S141P}$, $MukE^{G96W}$, $MukE^{R140C}$, $MukE^{G188E}$ and $MukE^{Y74C}$) from the first 3 groups were

introduced into the plasmid pBB08. This plasmid contains *mukF* and *mukE* genes under the control of arabinose inducible promoter. In this plasmid, *mukE* gene encodes nine histidine residues at its 3' end. The constructed pBB08 plasmids were introduced into the Δ*mukEF E.coli* strain OU102 (Wang et al., 2006) to avoid possible contamination from the wild type MukEF during protein purification. The proteins were then purified using Ni-chelate chromatography. Five of the proteins, mutants and $MukE^{P69T}$ from Group I, $MukE^{R140C}$, $MukE^{S141P}$ and $MukE^{G188E}$ from Group II and $MukE^{Y74C}$ from Group III formed a stable complex with MukF that eluted as a single peak from the Ni^{2+}- and gel filtration columns (Figure 4.7).

The sixth mutant, $MukE^{G96W}$, eluted alone, without MukF from the first Ni^{2+}-column (Figure 4.8). For this mutant, both MukE and MukF proteins were expressed well during induction. However, only half of the MukF remained soluble after cell lysis, and virtually none of it was retained with MukE during chromatography. We conclude that the mutation G96W disrupts the interaction between MukE and MukF. The other selected MukE mutants formed a complex with MukF and were purified as a MukEF complex (Figure 4.8).

4.7 Mutant MukEF proteins form a complex with MukB in vitro.

Previous experiments established that MukB and MukEF form two different complexes depending on reconstitution conditions (Petrushenko et al., 2006b). When reconstituted in the buffer containing 40 mM NaCl and 2 mM $MgCl_2$, MukB and MukEF form a complex $MukB_2(MukE_2F)_2$. When MukB and MukEF were reconstituted in the buffer containing 200 mM NaCl and 2 mM EDTA, $MukB_2(MukE_2F)$ was produced. We employed both conditions to evaluate the

assembly of MukBEF by mutant MukE.

The mutant proteins were examined in this experiment including S141P, P69T, R140C, G188E and Y74C. The experiment was done at room temperature. $MukE_2F$ and $MukB_2$ were mixed at 2:1 ratio and the protein mixture was loaded onto a 1 ml gel filtration column. When the protein was reconstituted in 40 mM NaCl and 2 mM $MgCl_2$ buffer, the peak of MukEF was co-eluted with the peak of MukB. Only half of the MukEF co-eluted with MukB when the 200 mM NaCl and 2 mM EDTA buffer was used. All mutant proteins in this experiment behaved very similar to the wild type MukEF (Figure 4.9). They formed $MukB_2(MukE_2F)_2$ when reconstitution was done in the presence of 2 mM $MgCl_2$, and $MukB_2(MukE_2F)$ complex in buffer containing 200 mM NaCl and 2 mM EDTA. Therefore, we conclude that all the selected mutants are able to form a complex with MukB.

4.8 Mutations in MukE do not affect inhibition by MukEF of DNA binding activity of MukB.

Previous studies showed that MukEF inhibits the interaction between MukB and DNA. When MukEF was added to pre-assembled MukB-DNA complex, gradual disassembly of MukB-DNA complex could be observed (Petrushenko et al., 2006b). Here, we determined if the same holds true for the mutant MukEF. The complex between DNA and MukB was formed by incubation for 30 min at 37 °C. Then the mutant MukEF was added and incubation continued. The reactions were stopped after various times by chilling them on ice for 10 min and analyzed by gel electrophoresis. When wild type MukEF was used, more and more MukB was released from DNA-MukB complex when we increased incubation time with MukEF. All five purified

mutant MukEFs also disrupted the MukB-DNA complex as the wild type protein in this assay (Figure 4.10).

We next examined the effects of MukEF on MukB-DNA interaction using another coupled assay. Previous studies showed that MukB can protect supercoiled DNA from relaxation by topoisomerase I and that MukEF can inhibit this activity of MukB (Petrushenko et al., 2006b). Here, we determined if the mutant MukEFs also de-stimulate the interaction between DNA and MukB. In this experiment, MukB and MukEF were mixed at various ratios and incubated for 30 min at 37 °C to form MukBEF complex. DNA was added to reconstituted MukBEF complex and further incubated for 10 min at 37 °C. In this reaction, only MukB and not MukBEF can form a complex with DNA. The *E.coli* topoisomerase I was then added and incubated for 5 min at 37 °C to allow relaxation of supercoiled DNA. For wild type MukEF, when the ratio between $MukE_2F$ and $MukB_2$ was 2:1, we observed complete DNA relaxation. For mutant G188E, DNA was completely relaxed at the ratio of 1:1 between $MukE_2F$ and $MukB_2$. All other mutants can completely liberate DNA from MukB at the same molar ratio of $MukE_2F$ to $MukB_2$ as for the wild type MukEF (Figure 4.11). We concluded that these mutations in MukE do not affect inhibition of the DNA binding activity of MukB by MukEF.

4.9 Mutations did not affect sedimentation rate of purified MukEF proteins.

We next evaluated the size of mutant MukEFs using sucrose gradient centrifugation. We measured sedimentation rate of mutant MukEF proteins using 10% to 40% sucrose gradient and ultra-centrifugation. The sedimentation rate of the wild type MukEF was 7.7 S ± 0.4 S, which is very close to the 7.5 S determined in

the previous study (Petrushenko et al., 2006b). The sedimentation rate of all mutant MukEFs are also very close to wild type MukEF (Figure 4.12 and Table 4.2). When the difference of sedimentation rates between wild type and mutant is compared with the standard error of the method, the method we used here to measure the sedimentation rate also has error and the standard error of the method is 0.4 S. Therefore, the difference between the sedimentation rates of all mutant MukEFs and that of previous determined wild type MukEF is less than or equal to the standard error of the method. We conclude that all purified mutant MukEFs have similar sedimentation rate as the wild type MukEF and therefore, our mutations did not change the shape of MukEF complex.

4.10 Mutant MukEFs form complex with MukB in vivo

Last, we examined the MukBEF complex formation inside the cell. Cells were disrupted by treatment with mild detergents at low salt condition as described in (She et al., 2007) with some modifications. This procedure was used to isolate *E.coli* chromosome (Murphy and Zimmerman, 1997) and prevents dissociation of many proteins, including MukBEF complex, from DNA. Once cells were lysed by detergents, DNA was digested using DNase I to release DNA associated proteins. The whole cell extract was then loaded onto sucrose gradient and protein complexes were separated by ultra-centrifugation and then fractions were collected from the bottom. Peaks for each subunit were determined using SDS-PAGE and western blotting.

For the wild type MG1655 strain, MukB eluted as two peaks at 7.7 S and 11.87 S. The second, 11.87 S peak migrated with the MukEF peak. Therefore, the second MukB peak was formed by MukBEF complex and the first MukB peak represents

free MukB. The MukB peak from MukBEF complex is much smaller than the first free MukB peak (Figure 4.13).

For the OU111-wt strain, which encodes the wild type MukE-GFP at the *lacYA* locus, MukB also formed two peaks with the first peak at 7.7 S and the second peak with 12.5 S, respectively. The second MukB peak coincides with the MukEF peak. Therefore, OU111-wt strain also contains two populations of MukB, the free MukB and MukBEF complex (Figure 4.13).

In both strains, the difference of the sedimentation rate for free MukB between MG1655 and OU111-wt is less than the standard error of the method. The sedimentation rate of MukBEF complex from OU111-wt is 25% greater than that for MG1655 strain. If the MukBEF complex formed in OU111 strains is the saturated $MukB_2(E\text{-}GFP_2F)_2$, the contribution of GFP to the total molecular weight of MukBEF complex is 20%. If the half-saturated MukBEF complex $MukB_2(E\text{-}GFP_2F)$ is formed, the contribution of GFP to the total molecular weight of MukBEF complex is 13%. Therefore, we can conclude that GFP does not affect the sedimentation rate of MukBEF complex much.

The MukBEF peak from OU111 strain is higher than that from MG1655, which means there are more MukB involved in MukBEF complex formation in OU111 strain. Probably the increased amount of MukE in OU111 strains disturbs the equilibrium between free MukB and MukBEF complex. As a result, more MukB is involved in MukBEF complex formation. Another possibility is that the GFP tagged MukBEF complex is not as active as the endogenous MukBEF, therefore the cell needs more MukB(E-GFP)F to fulfill its function.

We next examined MukBEF complex formation in mutant *mukE* OU111 strains. In four *mukE* mutant stains (OU111-S141P, OU111-P69T, OU111-R140C and OU111-G188E), we observed results similar to those for OU111-wt. There are two peaks for MukB, 7.5 S and 12.1 S in all these strains. Therefore we conclude that these mutant MukEFs form a complex with MukB. We also observed a small peak or a shoulder on the left side of the MukF peak which does not overlap with MukE peak in these four mutant OU111 strains. This extra MukF peak was not observed in the OU111-wt strain. This peak could indicate that MukBEF is unstable in mutant OU111 strains. We conclude that mutant OU111 strains form MukBEF complex, but the mutant MukBEF complexes are not as stable as that from OU111-WT (Figure 4.14).

Table 4.3 The sedimentation rates of MukB and MukBEF from MG1655 strain and OU111 strains

Mutant	MukBEF peak (S)	MukBpeak (S)	BEF/B
MG1655	11.87	7.7	0.45
OU111-WT	12.5	7.8	0.765
P69T	12.1	7.9	1.05
S141P	12.6	8,2	1.16
R140C	12.3	7.9	0.857
G188E	12.0	8.2	1.09

For OU111-G96W, only MukE-GFP and MukB peaks were observed and they were well separated from each other. This result is consistent with our previous finding of $MukE^{G96W}F$ dissociation during Ni^{2+}- chelate chromatography (Section 4.6). Because in OU111-G96W strain, $MukE^{G96W}$-GFP and MukF cannot form a

stable complex and the free MukF is easily degraded inside cell, MukE^{G96W}-GFP and MukB could not form complex with each other and they only form separate peaks.

For the viable OU111-Y74C strain, we did not observed MukBE^{Y74C}F complex. Only MukF comigrated with MukB, but not MukE-GFP. Apparently MukBE^{Y74C}F complex is unstable and MukE-GFP is released from the complex during centrifugation. This mutant will be further discussed in the next section.

4.11 Mutant MukBE^{Y74C}F is unstable.

During initial screening, we isolated a non-viable double mutant MukE$^{R34S\ Y74C}$. Only Y74C was transferred into the plasmid p15sp-E02a (Section 2.2 and Figure 2.1 B) and then subsequently integrated into the chromosome of the OU111 strain. We found that OU111-Y74C had similar CFU to OU111-wt at room temperature and 37 ºC. Therefore, OU111-Y74C strain is viable. Then the dominance of MukE^{Y74C} was examined by introducing other mutant MukEs or the wild type MukE into the OU111-Y74C. The CFU of these OU111-Y74C strains carrying another mutant or the wild type MukE on a plasmid was measured. We found that OU111-Y74C containing plasmid p15sp-E02a-R140C was not viable at 37 ºC and OU111-Y74C with the plasmid p15sp-E02a-wt was viable (Figure 4.15 A). Probably MukBE^{Y74C}F is unstable and the other mutant MukE or wild type MukE can compete with MukE^{Y74C} to form MukBEF complex inside cell. Once the other loss-of-function mutant MukE^{R140C} is introduced, it replaces MukE^{Y74C} to form a stable loss-of-function MukBE^{R140C}F complex resulting in the nonviable phenotype.

This idea was further confirmed in the *in vitro* experiments. Although mutant MukE^{Y74C}F could be purified (Section 4.6) and form a MukBE^{Y74C}F complex

(Section 4.7), both MukE^{Y74C}F and MukBE^{Y74C}F were unstable. First, we examined the stability of MukEF. When all purified MukEF mutants and the wild type MukEF were resolved by non-denaturing gel, only MukE^{Y74C}F fell apart into MukE and MukF and the other mutants and wild type MukEF complex remained intact at these conditions (Figure 4.15 B).

Then, we examined whether MukBE^{Y74C}F complex is stable. MukB$_2$(E$_2$F)$_2$ complex was reconstituted first as described at Section 2.7 and then the complex was loaded onto 15% to 60% sucrose gradient. After centrifugation, the fractions were collected from the bottom and then resolved by SDS-PAGE. For the wild type MukB$_2$(E$_2$F)$_2$, The peaks of three subunits co-migrated with each other. For MukB$_2$(E$^{Y74C}_2$F)$_2$, the peak of MukE^{Y74C} stayed at the lower sucrose density fractions compared to the peaks of MukB and MukF (Figure 4.15 C). Therefore, we conclude that MukE^{Y74C}F and MukBE^{Y74C}F complex are unstable.

Conclusion

We constructed a series of loss-of-function MukE mutants using random mutagenesis. All of these mutants disrupted the MukBEF clusters at the one-quarter and three-quarter positions of the cell length. Therefore cluster formation is essential function of MukBEF. Then five mutants were purified. Except for G96W, all other four mutants are able to form MukBEF complex and they also inhibit the interaction between MukB and DNA as efficiently as wild type MukEF. These four mutants also form MukBEF in vivo. Therefore, MukBEF complex formation is not sufficient for MukBEF cluster formation. Binding with DNA is not sufficient for MukBEF cluster formation either. We propose that MukEF forms complex with MukB first and then

MukE guides MukBEF to form clusters at the quarter position of the cell length. Maybe other factors are also involved in MukBEF macromolecular structure formation.

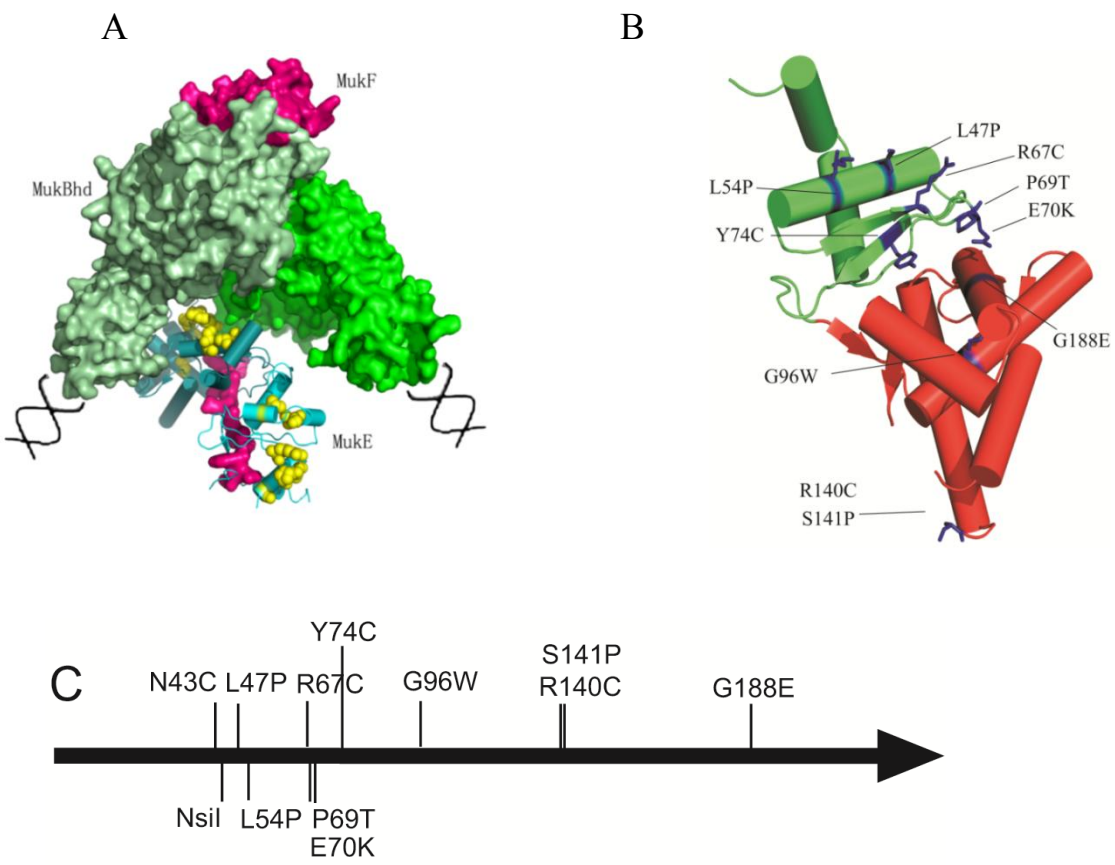

Figure 4.1 The crystal structure MukBEF complex and MukE.

(A) The crystral structure of MukBEF adapted from (Woo et al., 2009). PDB code is 3EUJ. The structure shows a dimer of MukB head domain, MukF monomer and two MukEs. MukB and MukF structure are shown in surface, MukE in cartoon and point mutation of MukE in balls and sticks. (B) MukE monomer structure adapted from (Woo et al., 2009); PDB code is 3EUH. The secondary structural elements in the N- and the C-terminal portions of MukE structure are colored in green and red, respectively. Mutations are shown in blue and labeled. (C) Mutations are shown in MukE primary sequence and the position of restriction site for NsiI which was used for transferring mutations from pBB14 to p15sp-E02a is also shown.

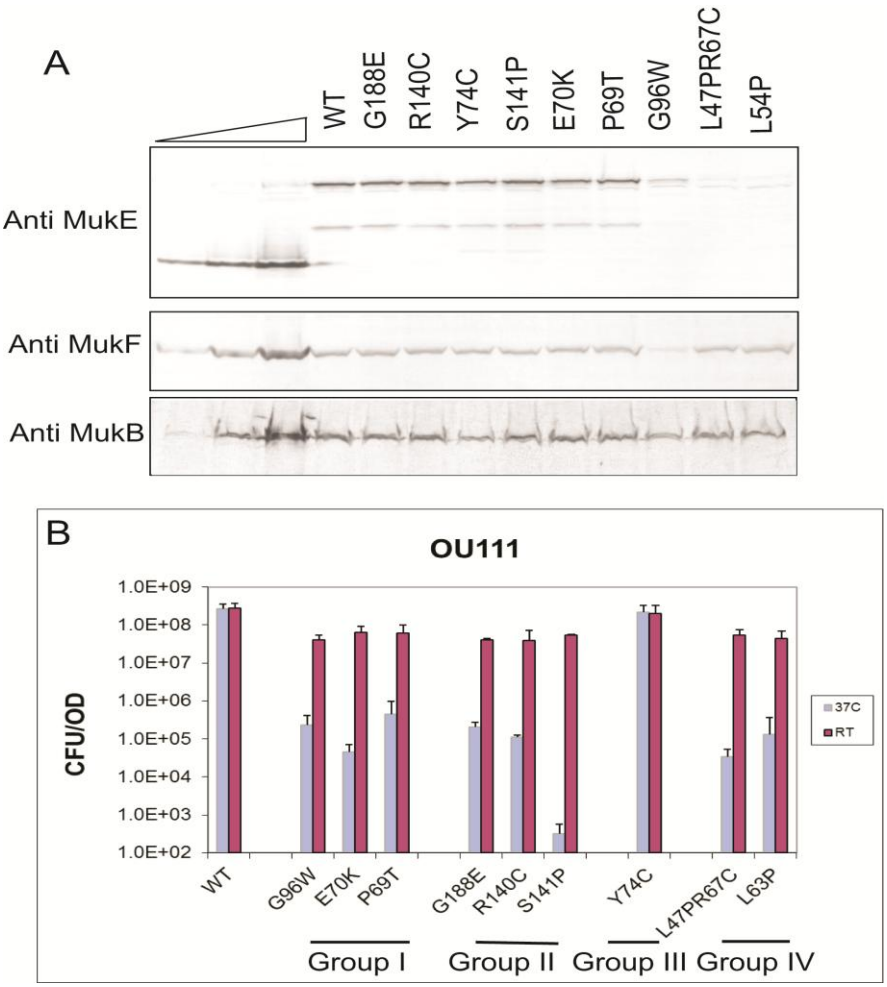

Figure 4.2 Protein expression level and CFU of OU111 strains.

(A) MukBEF expression level in OU111 stains. OU111 strains were grown at room temperature in LB medium to OD_{600} of 0.6. Cells were chilled in ice cold water for 10 min, washed and concentrated in TN buffer. 0.1 OD of boiled cells was loaded along with the serially diluted purified MukBEF onto SDS-PAGE gel. The lanes with calibration mixture contain 30 fmol, 90 fmol and 300 fmol of MukB, 10 fmol, 40 foml and 200 fmol of MukF, and 20 fmol, 80 fmol and 400 fmol of MukE. Each subunit was detected by corresponding anti-MukE, anti-MukF and anti-MukB separately (B) CFU of mutant OU111 strains. Exponential stage cells were diluted appropriately and spread on LB agar plates containing 100 μg/ml spectinomycin. The

number of colonies was counted after incubation for 24 hours (37 °C) or 2 days (the room temperature). Error bars indicate standard deviation from at least three experiments.

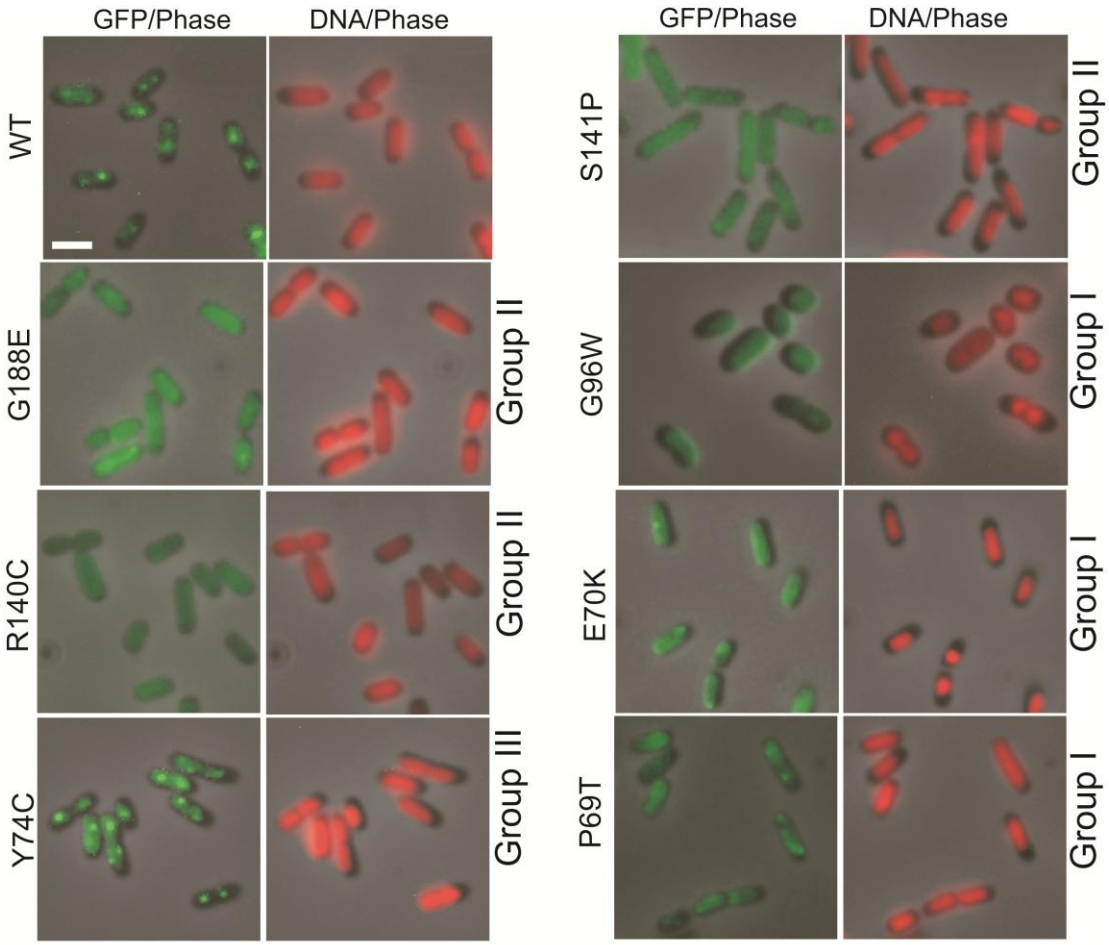

Figure 4.3 Fluorescence micrographs of MukE mutants in OU111 (Δ*mukE::kan lacYA::mukE*-gfp*) strains.

Cells were grown in M9CA + glycerol medium at room temperature. Pictures were taken when cells reached exponential stage (OD_{600} of 0.6 to 0.8). GFP fluorescence is shown in green, DNA is in red, and phase contrast is in gray. Size bar, 2 μm.

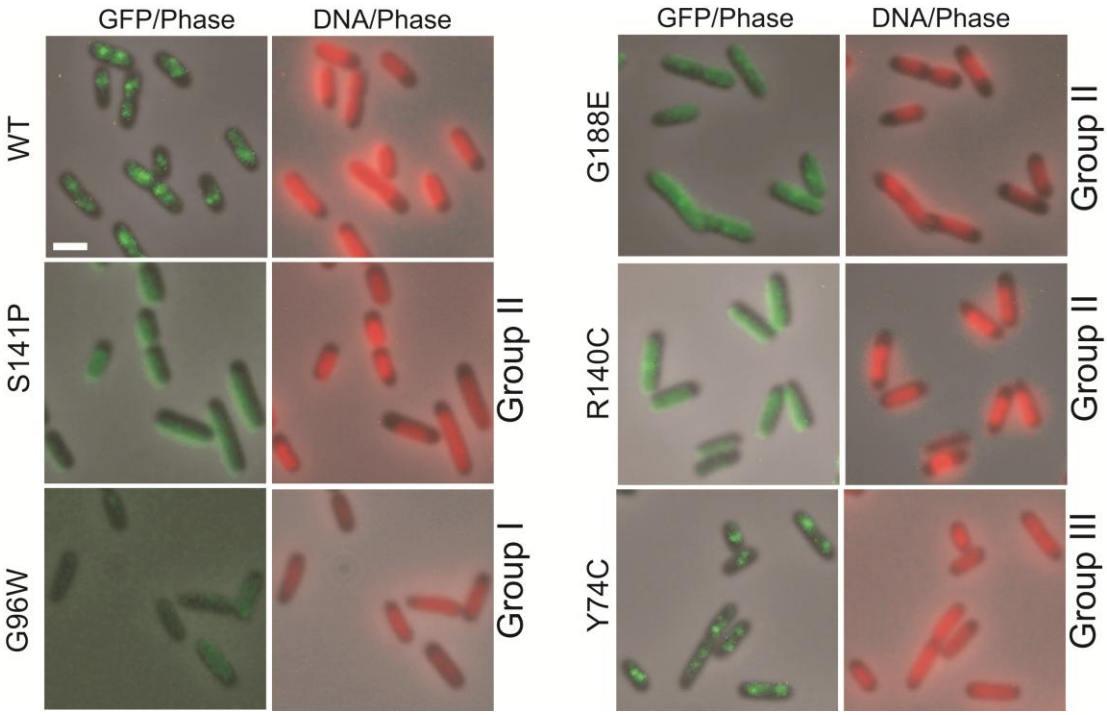

Figure 4.4 Fluorescence micrographs of MukE mutants in OU126 (*mukB::mukB-gfp* Δ*mukE::kan lacYA::mukE) strains.**

Cells were grown in M9CA + glycerol medium at room temperature. Pictures were taken when cells reached exponential stage (OD_{600} of 0.6 to 0.8). GFP fluorescence is shown in green, DNA is in red, and phase contrast is in gray. Size bar, 2 μm.

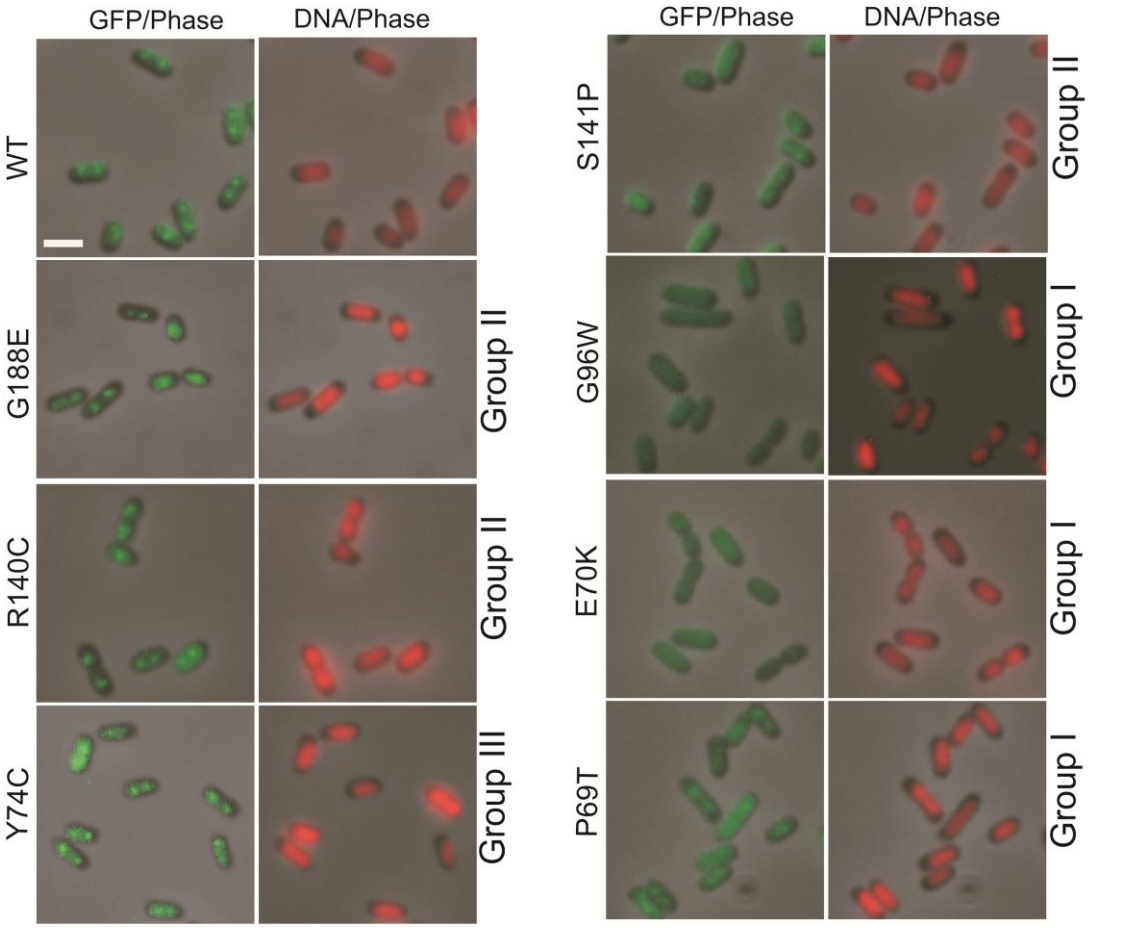

Figure 4.5 Fluorescence micrographs of MukE mutants in OU110 (*lacYA::mukE*-gfp*) strains.

Cells were grown in M9CA + glycerol medium at 30°C. Pictures were taken when cell reached exponential stage. GFP fluorescence is shown in green, DNA is in red, and phase contrast is in gray. Size bar, 2 μm.

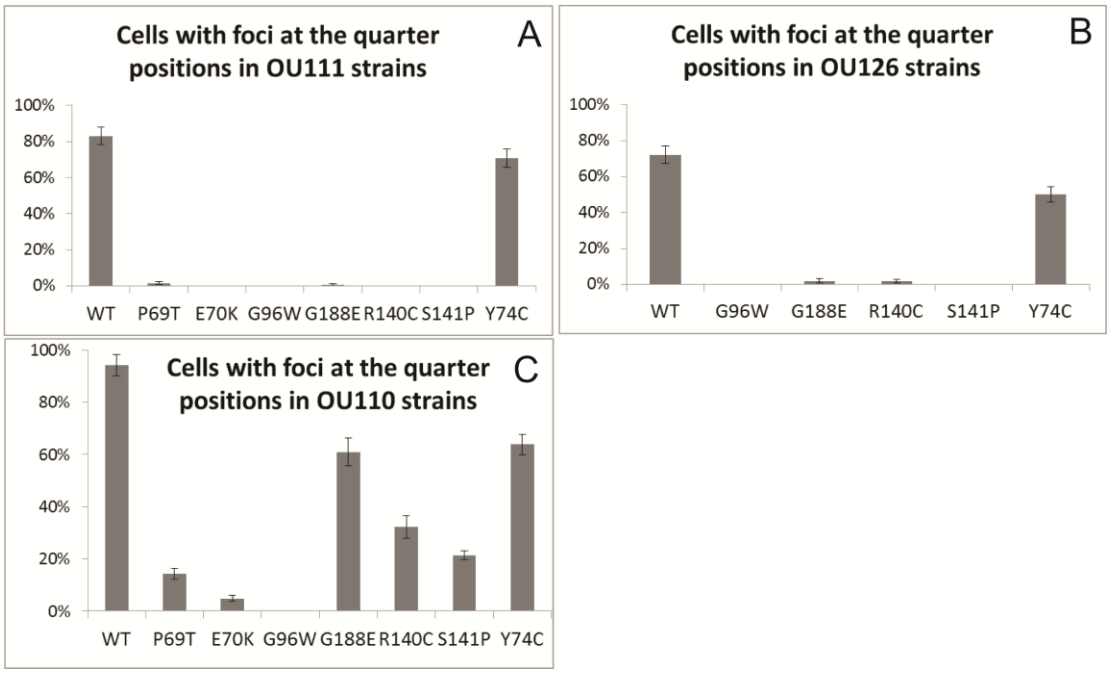

Figure 4.6 Frequencies of cells with foci at the quarter position.

Percentage of cells with foci at the quarter positions in (A) OU111 (Δ*mukE::kan lacYA::mukE*-gfp*) strains, (B) OU126 (*mukB::mukB-gfp* Δ*mukE::kan lacYA::mukE**) strains and (C) OU110 (*lacYA::mukE*-gfp*) strains. Error bar represents the standard error of the methods.

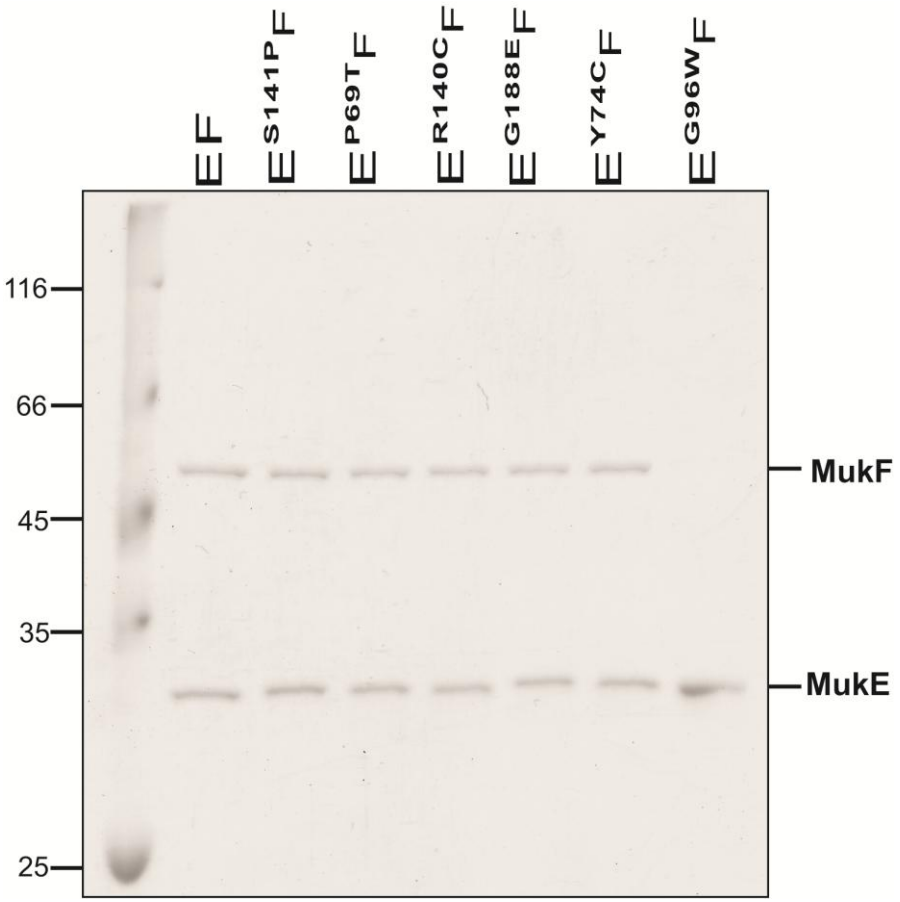

Figure 4.7 Purified MukEF Mutants.

SDS-PAGE gel that analyzes purified MukEF mutants. Expect for $MukE^{G96W}$, the other five MukEF mutants form stable MukEF complexes and were purified. Purified proteins were resolved by SDS-PAGE and visualized by Coomassie Blue staining.

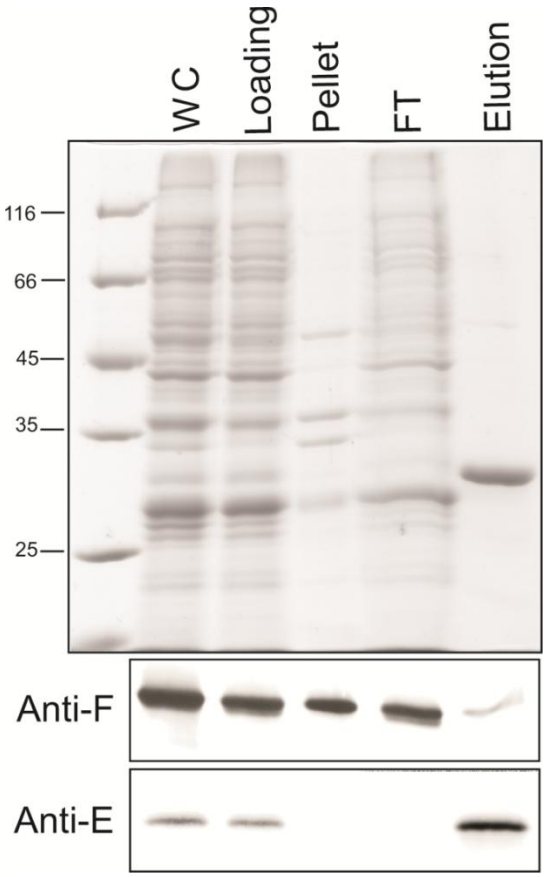

Figure 4.8 Purification of Mutant MukE^{G96W}F.

Fraction eluted from a Ni^{2+}-chelate column examined by SDS-PAGE gel (top panel), western blotting using antibody against MukF (middle panel) or MukE (bottom panel). 10 μg total protein from cell extract was loaded in lane WC and cell extract was separated into the Loading and Pellet fractions by centrifugation at 18,000 rpm for 25 min and analyzed in lane Loading and Pellet respectively. Loading fraction was separated as the flow through (FT) and Elution fraction after Ni^{2+}-chelate column. The amount of protein loaded at each fraction was determined by measuring protein concentrations using a Bradford assay.

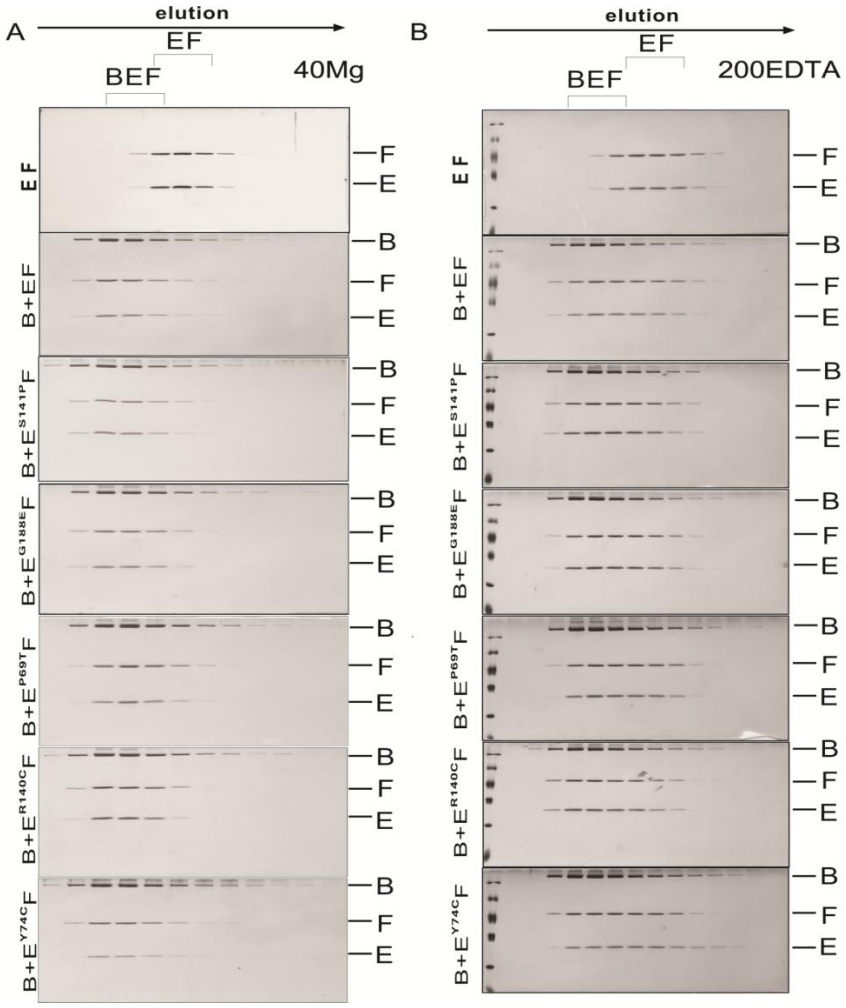

Figure 4.9 Sephacryl S300 analysis of reconstituted MukBEF.

$MukE_2F$ (3.19 µg) and MukB (5 µg) were mixed in 30 µl of reconstitution buffer at 2:1 ratio at room temperature for 20 min. The protein mixture was resolved by gel filtration through a 1 ml Sephacryl S300 column equilibrated in the buffer containing 40 mM NaCl, 2 mM $MgCl_2$ (A) or 200 mM NaCl, 2 mM EDTA (B). MukB and MukBEF migrated with similar mobilities close to the void volume of the column. Eluted proteins were resolved by SDS-PAGE and visualized by silver staining. Positions of MukB (B), MukF (F), and the His-tagged MukE (E) are indicated on the right.

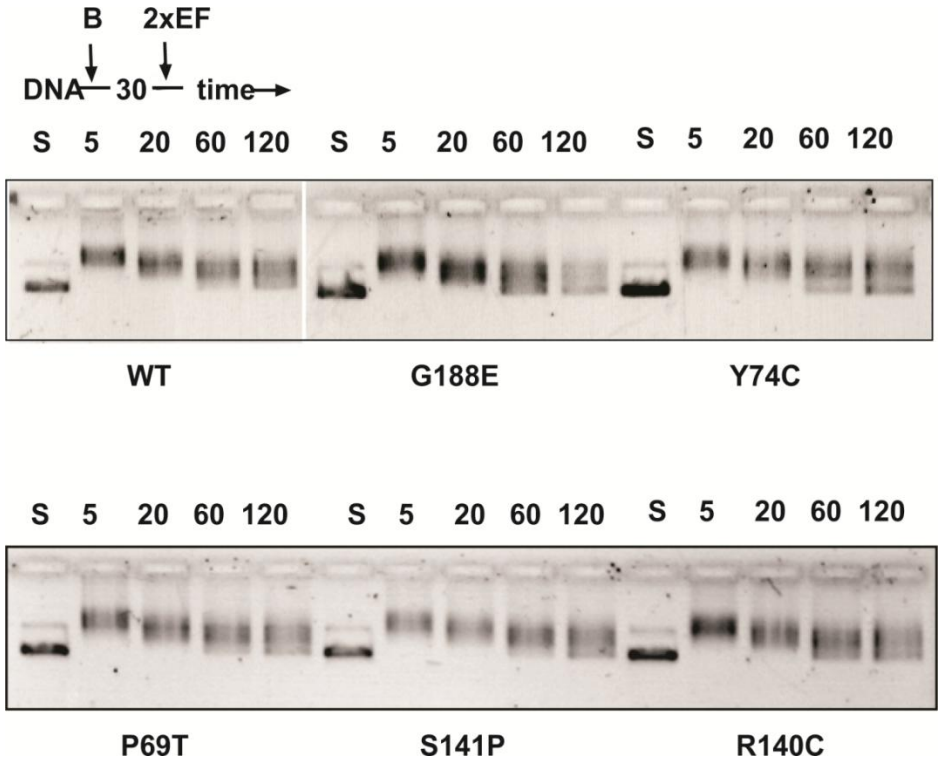

Figure 4.10 Time course of DNA displacement by MukEF.

3.5 fmol of supercoiled pBR322 DNA was incubated with 0.3 pmol $MukB_2$ with 2 mM MgATP for 30 min at 37°C. The reactions were then supplemented with 0.3 pmol $MukE_4F_2$ after the indicated times, chilled on ice for 10 minutes and analyzed by gel electrophoresis. S, DNA substrate.

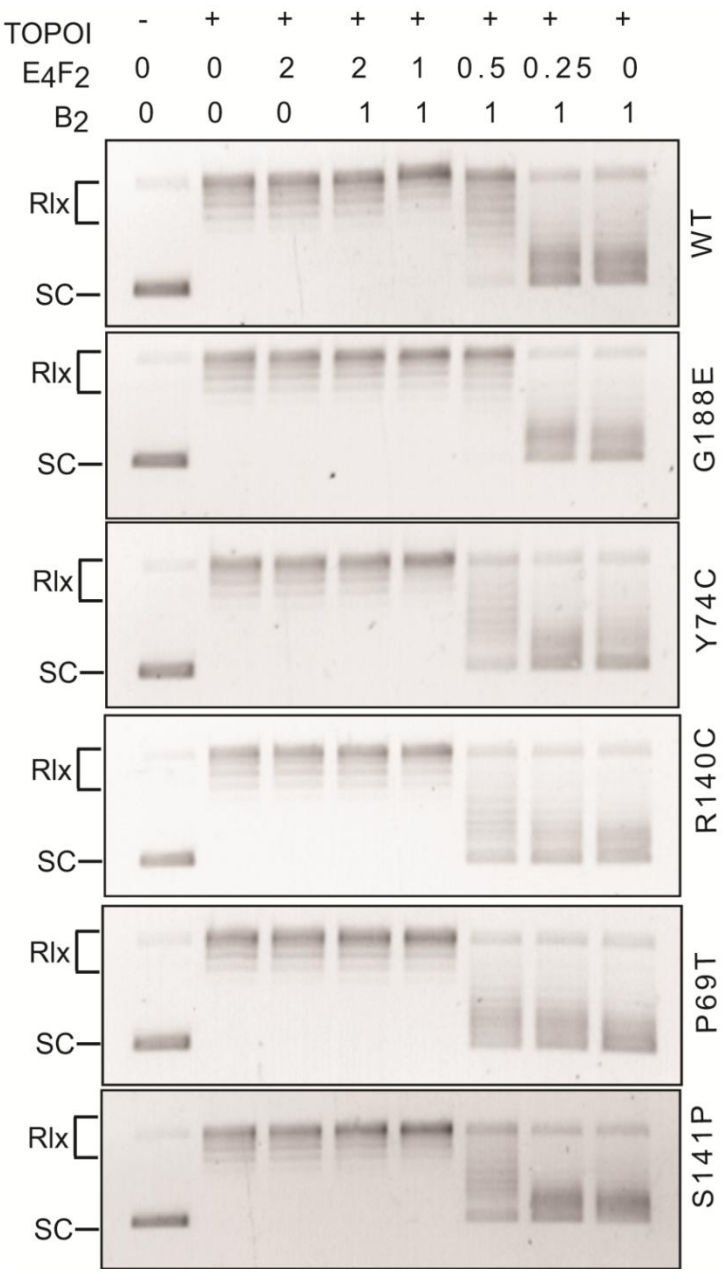

Figure 4.11 DNA relaxation assay.

10 ng (3.5 fmol) of supercoiled pBR322 DNA was incubated with preassembled MukBEF complex for 10 min at 37°C. The reaction mixtures were treated with 35 fmol topoisomerase 1 for 5 min at 37°C. The reactions were quenched, deproteinized, and resolved by agarose gel electrophoresis.

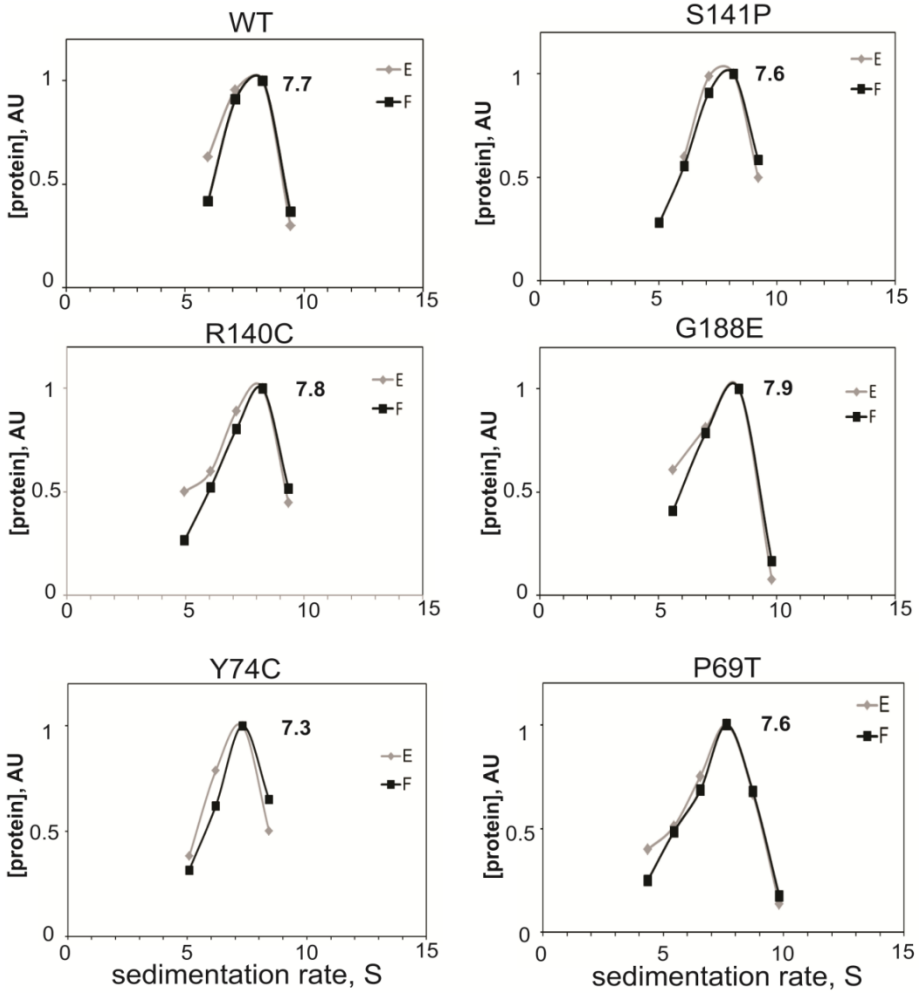

Figure 4.12 Sedimentation analyses of MukEF mutant proteins.

MukEF mutant proteins were mixed with the protein size markers (apoferritin (17.6 S, 6.2 nm), catalase (11.2 S, 5.3 nm), alcohol dehydrogenase (7.3 S, 4.6 nm), bovine serum albumin (4.3 S, 3.6 nm)) and loaded onto 10% to 40% sucrose gradient in the buffer containing 40 mM NaCl and 2 mM $MgCl_2$. After proteins were resolved by centrifugation, the amount of each protein in collected fractions was determined using densitometric analysis of Coomassie-stained SDS-PAGE gels. Protein concentrations were further normalized to the highest level found for a given protein across the gradient. Normalized concentrations of MukF and MukE are plotted against the values of sedimentation coefficient corresponding to each fraction.

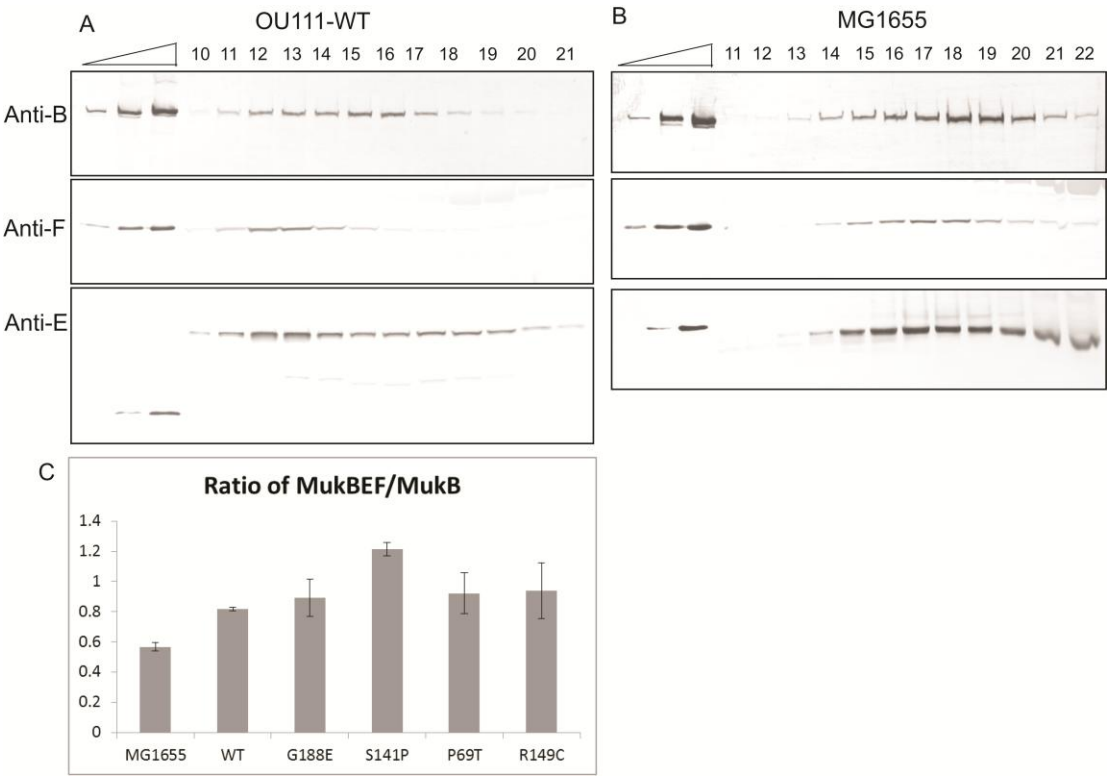

Figure 4.13 Copurification of MukEF mutants with MukB.

OU111-WT (A) and MG1655 (B) cells were grown in 150 ml LB medium at room temperature to an OD_{600} of 0.8, chilled by swirling the flask in the ice-cold water bath, and concentrated by centrifugation. Following lysozyme treatment, cells were lysed in 1 ml of Brij 58-deoxycholate mixture at room temperature. The nucleoid was further digested with DNase I (Sigma-Aldrich). After the reaction was terminated by adding EDTA, 0.6 ml cell lysate was mixed with the protein size markers (apoferritin (17.6 S, 6.2 nm), catalase (11.2 S, 5.3 nm), alcohol dehydrogenase (7.3 S, 4.6 nm), bovine serum albumin (4.3 S, 3.6 nm)), and loaded onto a 15% to 60% sucrose gradient in 10 mM Tris-HCl pH7.8, 200 mM NaCl, 2 mM EDTA, 1 mM dithiothreitol, 1 mM PMSF. The protein complexes were separated by centrifugation at 38,000 rpm for 30 hours using a Beckman Ti-70 rotor. After centrifugation, about

20 aliquot fractions were collected from the bottom. Each fraction was subject to western blotting against anti-MukB, anti-MukE and anti-MukF antibody to determine the location of each subunit of MukBEF complex. Sedimentation rate of each fraction was determined from the mobility of the protein size marker. (C) The histogram shows the ratio of MukB in MukBEF complex to free MukB in OU111 strains and MG1655 strain. The western blotting results were quantified using ImgaeQuant and graphed as the amount of protein versus the sedimentation rate. Then the graphs were fitted to a double Gaussian distribution curve. The amount of protein was chosen as the height of these two peaks, which corresponds to MukBEF complex and free MukB.

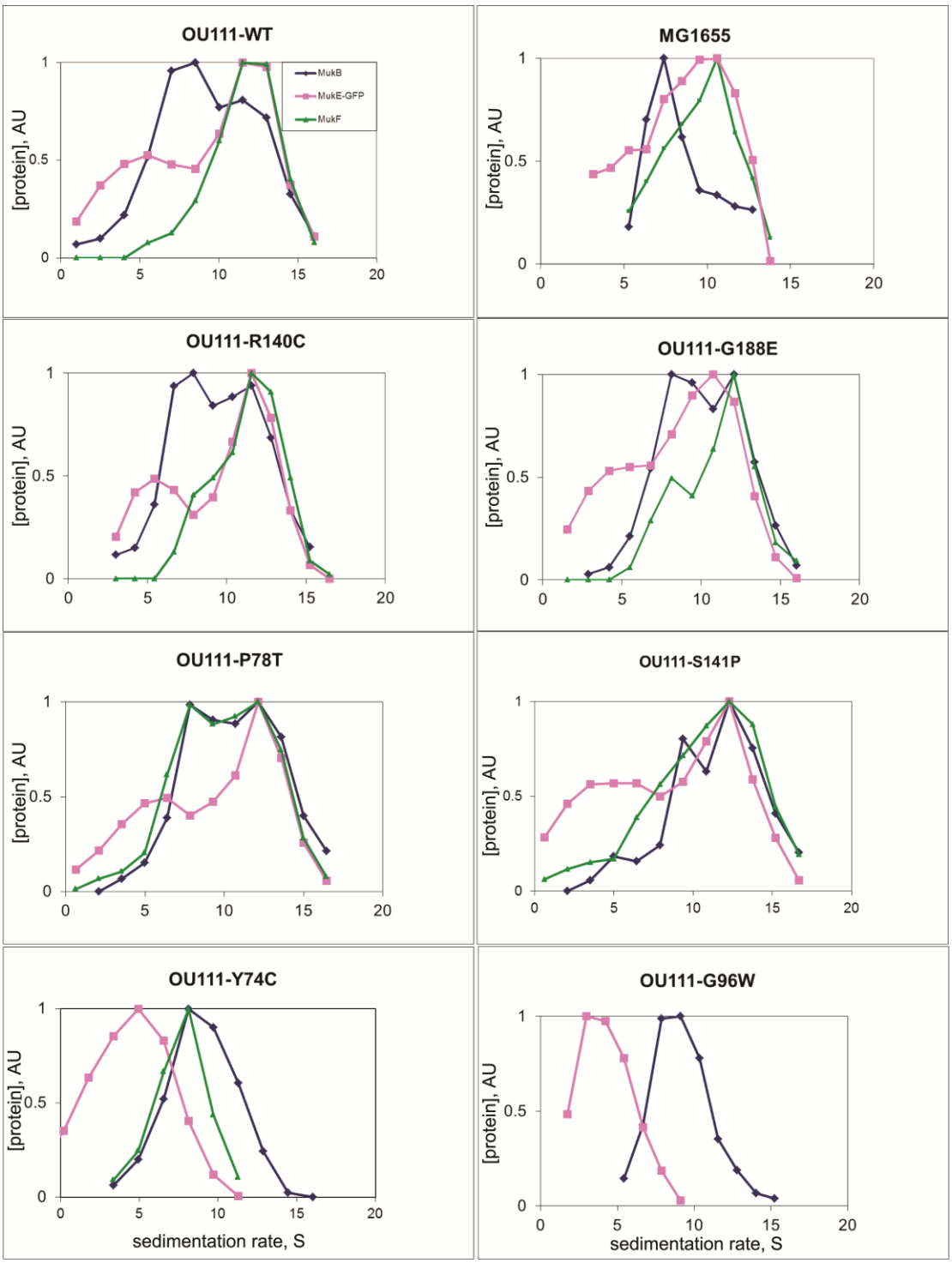

Figure 4.14 Summary of copurification of MukBEF complex in vivo.

The western blotting results for each subunit shown in Figure 4.13 were quantified using ImgaeQuant and graphed as the amount of protein versus the sedimentation rate determined by protein size markers.

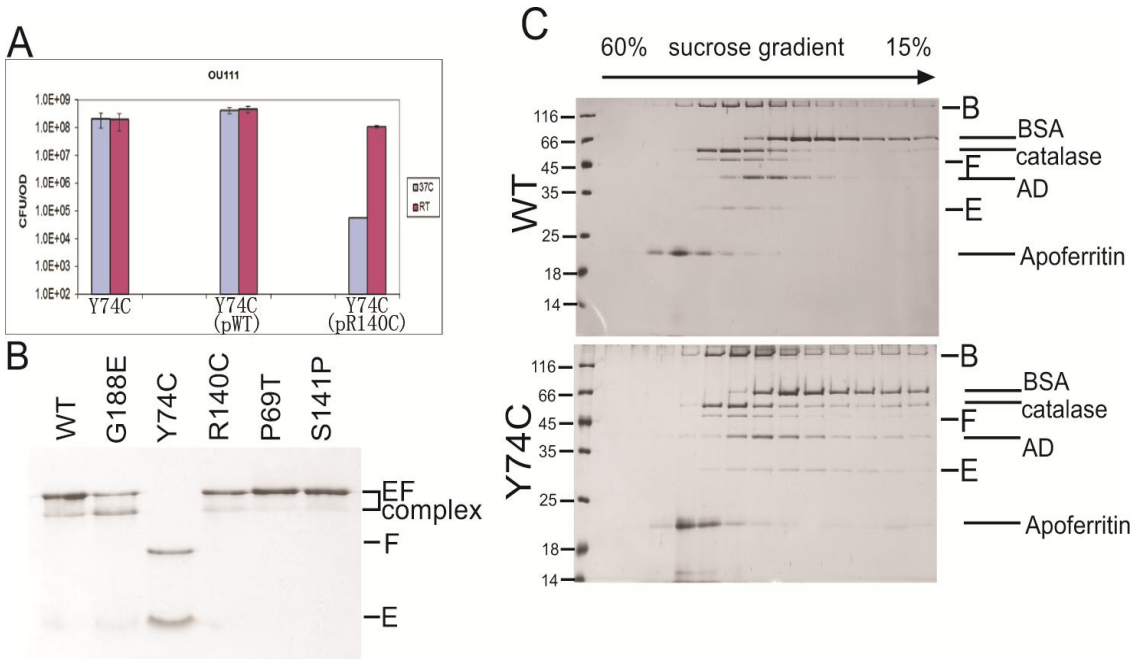

Figure 4.15 Mutant MukE^{Y74C}F and pre-assembled MukBE^{Y74C}F are unstable.

(A) CFU of OU111-Y74C, OU111-Y74C with plasmid p15sp-E02a-WT (Y74C(pWT)) and OU111-Y74C with plasmid p15sp-E02a-R140C (Y74C(pR140C)). (B) Purified MukEF proteins were resolved through 4% to 16% non-denaturing polyacrylamide gel. (C) MukBEF complexes were assembled using the same condition as in Figure 4.13. MukBEF complexes were loaded onto a 15% to 60% sucrose gradient with protein markers. After 30 hours centrifugation at 38,000 rpm for 30 hours in a Beckman TLS-55 rotor, about 14 aliquot fractions were collected from the bottom, resolved by SDS-PAGE and visualized by silver staining.

Chapter 5 A new family of bacterial condensin

This chapter is adapted from (Petrushenko et al., 2011).

Introduction

In this chapter, the newly discovered bacterial condensin MksBEF will be discussed. MksBEF has the same operon organization and predicted secondary structure as MukBEF, including its many telltale features. However, MksB contains a markedly shorter coiled-coli region than that in MukB and other SMC proteins. Further homology searches revealed that MksBEF is broadly present in diverse bacteria, is highly divergent on the sequence level and often coexists with SMC-ScpAB or MukBEF and, sometimes, another MksBEF.

The function of MksBEF was studied in *Pseudomonas Aeruginosa*, which encodes MksBEF in addition to previous identified SMC_ScpAB complex. *P. aeruginosa* is an opportunistic human pathogen and it has unique ability to thrive and survive in a great variety of habitats. Previous DNA microarray studies of *P. aeruginosa* revealed that these two proteins are expressed in a growth conditions dependent manner (Waite et al., 2006), and, therefore, contribute to metabolism of this bacterium. In particular, both MksBEF and SMC were upregulated during exponential phase but were ultimately assigned to different clusters, suggesting that both proteins are needed in growing cells but are differentially regulated.

5.1 Pseudomonas aeruginosa MksB contributes to chromosome partitioning.

PAO1 strain of *P. aeruginosa* encodes the conventional SMC-ScpAB condensin (proteins PA1527, PA3197 and PA3198) and MksBEF complex (proteins PA4684, PA4685 and PA4686). To gain insight into the physiological function of MksBEF, we

took advantage of the transposon disruption library available at the University of Washington Genome Center (Jacobs et al., 2003). Strain PW8890 from this collection harbors transposon IS*phoA/hah* insertion at the hinge region of MksB (*mksB::ISphoA/hah*), which presumably inactivates it.

Examination of PW8890 using fluorescence microscopy revealed increased frequency of anucleate cells (1.2%; 11 out of 937) in cultures grown in M9 at 37 °C (Figure 5.1 A) but not in LB and not in strains harboring plasmid-encoded MksB (Figure 5.1 C). These data indicate that MksB functions in chromosome maintenance and that the demand for its activity varies depending on growth conditions. In contrast, Δ*smc* mutants of PAO1 (Figure 5.1 A) produced 2.5% anucleate cells both in LB and M9 (15 out of 626 cells in LB and 28 out of 1189 in M9; Figure 5.1 C). For both mutants, production of anucleate cells could be suppressed by a plasmid-borne *mksB* or *smc* (Figure 5.1 C), as appropriate, but not by the vector alone (data not shown).

Unlike with the *E. coli* MukBEF, condensin-deficient *P. aeruginosa* cells did not increase in size or formed filaments, which could be masking possible chromosome compaction defects. However, overproduction of MksB resulted in marked chromosome condensation (Figure 5.1 B). No such condensation was detected in cells arrested with chloramphenicol (Figure 5.1 B) or those harboring the vector alone (data not shown). Similar condensation of the *E. coli* chromosome was observed earlier upon overproduction of MukB (Wang et al., 2006) and H-NS (Spurio et al., 1992) but not of MukEF or topoisomerase I (Wang et al., 2006). Thus, the found chromosome condensation reflects the activity of the overproduced protein. This

result further supports the notion that MksB might be controlling the chromosome size by bringing distant DNA segments together.

The observed frequencies of anucleate cells are lower than those found for condensin mutants of E. coli and Bacillus subtilis (Britton et al., 1998a; Niki et al., 1991; Wang et al., 2006), but exceed the 0.1% reported for the condensin-deficient *Caulobacter crescentus* (Jensen and Shapiro, 1999a). In further discord with other condensins, neither the *mksB* nor Δ*smc* strains were deficient in colony formation at 23°C or 37°C, and MksEF-deficient cells failed to produce anucleate cells either in LB or M9 (data not shown). Such discrepancies could be explained by high frequency of compensatory mutations that could be masking effects of missing condensins. Alternatively, MksBEF and SMC could be playing partially redundant functions. In tentative support of the latter notion, we found that the frequency of conjugal transfer of Δ*smc::Gm*^{R} into PW8890 was more than three orders of magnitude lower than into the wild type PAO1 strain (data not shown).

We next constructed a conditionally condensin-deficient strain using gene-replacement procedures that minimize accumulation of compensatory mutations (see Section 2.2). The resulting OP106 strain (*LacI*^{q}*-P*$_{T7}$*-mksFEB* Δ*smc::Gm*) lacks *smc* gene and expresses MksBEF from a tightly controlled IPTG-inducible promoter $P_{T7(A1/04/03)}$ (Lanzer and Bujard, 1988). When overnight OP106 cells, grown in LB in the presence of IPTG, were transferred into the fresh medium without IPTG, formation of anucleate cells could be observed (Figure 5.1 D, E). As before, the frequency of anucleate cells was relatively low but could be increased if cells were diluted again into the fresh medium and allowed to grow further. After 16 h of

continuous growth (compared to 6 h in the “regular” experiment), 5.7% cells displayed severe chromosome partitioning defects (Figure 5.1 D). Such defects, however, failed to develop in the presence of IPTG (Figure 5.1 D, E). In contrast, IPTG had only minimal effect on anucleate cell formation in the Δ*smc::Gm* OP103 cells, which produce MksBEF from its endogenous promoter (Figure 5.1 E). We conclude therefore that MksBEF, similar to SMC, functions in chromosome partitioning. Curiously, induction of MksBEF in the presence of SMC resulted in a small increase in the frequency of anucleate cells (Figure. 5E), indicating that the functions of the two condensins overlap only partially and that their balanced production is essential for faithful chromosome segregation.

Conclusion

In *P. aeruginosa*, Inactivation of both MksBEF and SMC leads to increased frequencies of anucleate cells. MksBEF can complement anucleate cell formation in SMC-deficient cells. Therefore we conclude both proteins are involved in bacterial chromosome organization.

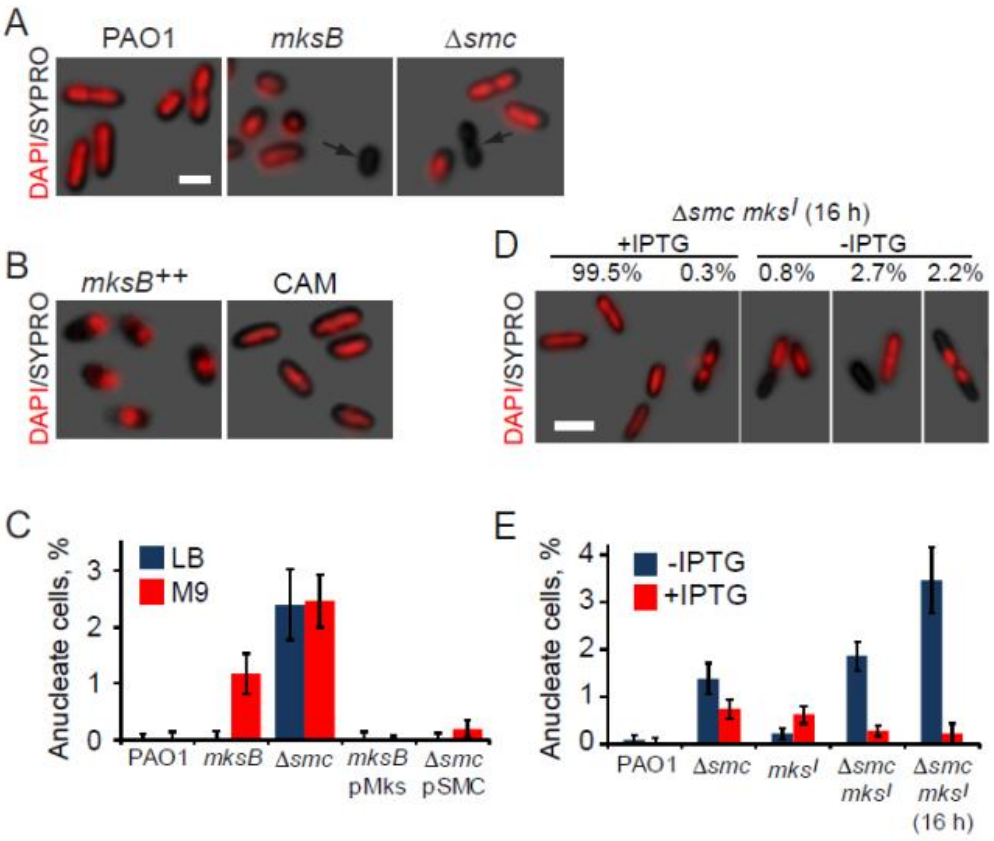

Figure 5.1 Chromosome packing defects in condensin-deficient P. aeruginosa.

(A) Fluorescence micrographs of fixed *mksB*-deficient PW8890 cells, Δ*smc::Gm* mutants and the parental PAO1-Lac (PAO1) cells. Anucleate cells (arrows) were found among PW8890 and Δ*smc* but not PAO1 cells. Size bar, 1 µm. (B) Arabinose-induced overproduction of MksB (*mksB*$^{++}$) induces chromosome condensation, whereas no chromosome condensation is observed when cell growth and protein synthesis are arrested by treatment with 100 µg/ml chloramphenicol (CAM). (C) Anucleate cell formation (±SEM) in LB and M9 medium by PAO1-Lac, *mksB* and Δ*smc* cells that harbor, when indicated, plasmids pUCP_MksB (pMks) or pUCP_SMC (pSMC). (D) Anucleate and guillotine cell formation by the P_{T7}-*mksFEB* Δ*smc* OP106 cells (Δ*smc mks*^{I}) exponentially grown in LB for 16 h in the presence or absence of 5 mM IPTG. (E) Anucleate cell formation (OD_{600} of 0.6) for cells grown in LB for 6 h or, where indicated, for 16 h either in the presence or absence of 5 mM IPTG. Tested were the parental PAO1-Lac, the Δ*smc* OP103, the P_{T7}-*mksFEB* OP105 (*mks*^{I}) and the P_{T7}-*mksFEB* Δ*smc* OP106 cells.

Chapter 6 Discussion

Since their discovery, SMC proteins have grabbed great attention because of their diverse functions in chromosome organization and their unique structure. Although extensive studies of SMC proteins have been done, there remains a lively debate about the mechanism of SMC protein. SMC proteins are involved in almost all aspects of chromosome organization. The mechanism of SMC protein is very complicated. At the same time, we are also dealing with the biggest molecules, the chromosome, inside the cell. Organization of the chromosome is also a very complicated process.

MukBEF is the SMC protein in *E.coli*. All three subunits of this complex are required for cell growth at 37 ºC. Inactivation of any subunit causes the same phenotypes, including temperature sensitive growth, chromosome decondensation and cutting and anucleate cell formation.

The mechanism of MukBEF remains elusive. MukB has the ability to form a scaffold to organize DNA *in vitro*. Why do bacteria need MukEF? Is MukEF only used to regulate the interaction between DNA and MukB as found *in vitro*? Or does MukEF have other functions inside the cell?

MukEF modulates the assembly of MukBEF macromolecular structure *in vitro*. MukEF also regulate the interaction between MukB and DNA *in vitro*. MukEF helps MukB to form protein clusters at the quarter positions of the cells.

Bacterial proteins are localized at specific positions inside the cell according to their functions (Shapiro et al., 2009). Foci formation at the quarter position of the cell length is a common feature of SMC proteins in bacteria (Jensen and Shapiro, 2003;

Mascarenhas et al., 2002; Mascarenhas et al., 2005; Ohsumi et al., 2001). In *E.coli*, MukB forms protein clusters and the MukB clusters are always located on the nucleoid, which is consistent with its function in chromosome organization. MukB cluster formation depends on MukEF. Also MukB clusters are formed at the quarter positions of the cell length. The quarter position of the cell length is usually considered as the new home of newly replicated DNA. Further studies showed that MukB foci also colocalize with *oriC* (Danilova et al., 2007). Topoisomerase-1 mutant *topA* causes the increase in negative supercoiling inside the cell and can suppress the temperature sensitivity of *mukB* mutant, but cannot suppress the abnormal positioning of chromosomal loci (Danilova et al., 2007). This indicates that MukB clusters not only introduce supercoiling to condense chromosome, but also organize the global structure of chromosome. Therefore, these data suggest that MukEF helps MukB to form a scaffold at the quarter positions to organize the chromosome structure. First, we studied the localization of this complex. Then to further elucidate the function of MukEF, we introduced mutations into MukE to disrupt the function of this protein, and then we characterized the activities of MukE mutants.

6.1 Protein foci are formed by MukBEF complex, not its individual subunits.

Formation of protein clusters by MukB-GFP and MukE-GFP is dependent on the presence of the complementary subunits. It has been shown that MukEF was also required for stable association of MukB with the chromosome. Conversely, no MukE or MukF comigrated with the nucleoids from Δ*mukB* cells (She et al., 2007). Thus, stable binding to the chromosome is a property of the complex between MukB and MukEF. Protein foci are also formed by MukBEF complex, not its individual

subunits. These data indicate that formation of MukBEF foci and stable association with chromosome could be mechanistically related.

It is noteworthy that elevated levels of MukEF displaced MukB from the chromosome. This effect was observed (Figure 3.1 A) at both high and low levels of protein overproduction. Overproduced MukF, which links MukB and MukE within the complex, was also disruptive to the formation of MukBEF clusters, although its effects were less pronounced at the uninduced levels than the effect of MukEF (data not shown). In contrast, the clusters were not notably affected by mild overproduction of MukE (data not shown). The result is in accord with *in vitro* reconstitution studies, which demonstrated that the two MukBs at the core of MukBEF have different affinities to MukEF and that saturating binding of MukEF to MukB disrupts MukB-DNA complex (Petrushenko et al., 2006b). Apparently, the overproduced MukEF is able to bind the low-affinity site on MukB and thereby displace the protein from DNA.

The functional significance of this effect is unclear. It may indicate that the association of MukBEF with the chromosome is dynamic and that MukEF helps remove MukB from DNA. Even if true, this cannot be the sole function of MukEF. This explanation is inconsistent with the stimulatory effects of MukEF on the binding of MukB to the chromosome (She et al., 2007) or the finding that MukBEF is a better condensin than MukB (Wang et al., 2006). It seems more likely that MukEF mediates the assembly of MukBEF into a macromolecular structure, as was proposed in the electron microscopy study (Matoba et al., 2005).

6.2 MukBEF complex formation is not sufficient for MukBEF clusters formation.

The function of MukEF was further investigated by random mutagenesis. Random mutagenesis has been a powerful tool in studies of the protein function. Nine MukE mutants were constructed. Each mutant contains between one and three amino acid substitutions (Table 4.1). Overall the mutations are distributed throughout the entire *mukE* gene, although there are two hot spots (Fig4.1 B and C, Table 4.1). Only two mutants out of nine led to protein misfolding. Overall our random mutagenesis strategy was successful.

First, we investigated the in vivo activities of *mukE* mutants. All mutant MukEs could not form foci at the quarter positions of the cell length. The focal localization of MukB was also disrupted by all mutations in MukE. Therefore, all MukE mutants disrupted MukBEF cluster. Then four mutant MukEFs (P69T, S141P, R140C and G188E) were purified and these mutant MukEFs could form complex with MukB *in vitro*. These purified mutant MukEFs showed similar effect as the wild type MukEF to inhibit the MukB-DNA complex formation also. At last we showed that mutant MukEFs also form complex with MukB in vivo. Therefore, MukE mutants form MukBEF complex *in vivo* and *in vitro*, only MukBEF cluster formation is destroyed. Because all of our loss-of-function MukE mutants disrupted MukBEF clusters, we conclude that protein cluster formation is the critical step for the function of MukBEF.

The protein cluster formed by MukBEF could be “the condensin factory” that controls the overall structure of the chromosome. Since MukB is able to control the

organization of the chromosome, the function of MukEF is to help MukB to form this condensin factory.

MukBEF complexes can be formed in different compositions. *In vitro* studies showed that they can form either saturated complex $MukB_2(E_2F)_2$ or half-saturated complex $MukB_2(E_2F)$ depending on reconstitution buffers (Petrushenko et al., 2006b). ATP Binding can release one E_2F from $MukB_2(E_2F)_2$ complex and result in $MukB_2(E_2F)$ formation (Woo et al., 2009). We found that *in vitro* mutant MukEFs are also form two different MukBEF complexes as wild type MukEF (Petrushenko et al., 2006b). These results indicate that our MukEF mutants did not affect the interaction between MukEF and MukB.

In MG1655 strain, two kinds of MukB population was observed inside the cell and only a very small amount of MukB is found in MukBEF complex. The first kind of MukB is the MukBEF protein clusters, which control the global architecture of the chromosome. The second kind of MukB could exist as free MukB or MukBEF complex. Based on our results, the second type of MukB probably exists as free MukB. Since in our *in vivo* co-purification experiment, MukB exists as free MukB or MukBEF complex, we propose that the second MukB population is free MukB. Only MukEF can recruit free MukB to form protein complexes and further to form higher order macromolecular structures at the quarter positions to organize the global structure of the chromosome.

During the process of transferring mutations from pBB14 plasmid to p15sp-E02a plasmid, only one point mutation Y74C in the mutant R34S Y74C was kept and this mutant turned out to be viable. This mutant did not disrupt MukBEF foci

formation, and therefore it supports our conclusion that MukBEF foci formation is its essential function. This mutant aroused our great interest also because it only can form very weak MukEF and MukBEF complex. Because tyrosine 74 is located at the interface between the N-terminal WHD and the C-terminal WHD of MukE, the interaction between these two domains could be affected and the overall structure was probably changed. As a result, this mutant Y74C cannot form a stable MukBE^{Y74C}F complex. When MukE^{G188E} was transferred into the OU111-Y74C strain using a plasmid, the stable loss-of-function MukBE^{G188E}F complex was formed, resulting in temperature sensitive growth. Also there are several experiments which can prove mutant MukE^{Y74C} forms MukBEF complex. First, we observed MukE^{Y74C} forms quarter position foci, same as MukB focal localization in strain OU111-Y74C. Second, MukE^{Y74C}F was purified and MukBE^{Y74C}F was also reconstituted *in vitro*. These data indicate that mutant MukE Y74C forms MukBEF complex *in vivo* and *in vitro*.

We first showed that the clusters are formed by MukBEF complex, not individual subunits. Then our results further showed that foci formation by MukBEF is its essential function and that complex between MukEF and MukB is not sufficient protein cluster formation. Binding with DNA is not sufficient for protein cluster formation either. Based on our experiment results, we propose that MukB can form two kinds of structure. First is free MukB and second is MukBEF cluster. These two kinds of MukBEF structure could coexist inside the cell. MukEF can help MukB to form the clusters at the quarter positions of the cell length, which are observed as MukBEF foci inside cell by fluorescence microscopy. All of our loss-of-function

MukE mutants disrupted MukBEF foci. Four mutants out of five did not affect MukBEF complex formation *in vivo* and *in vitro*. They also regulate the interaction between MukB and DNA as efficiently as wild type MukEF. Therefore binding with DNA is not sufficient for MukBEF cluster formation either. These data suggest that MukE helps MukBEF complex to form cluster at the quarter positions. There is maybe an extra-chromosomal factor that is involved in "condensin factory" formation.

Two MukE mutants R140C and S141P may be involved in the interaction between MukE and the extra-chromosomal factor. These two mutations are located on a flexible loop at the C-terminal WHD and they face the opposite direction of MukB. These two mutants could not affect the MukE structure and they are not involved in interaction with MukF or MukB either. Therefore these two mutants could disrupt the interaction between MukE and other unidentified factor. If the extra-chromosomal factor exists, arginine 140 and serine 141 could be the good candidate of its binding sites.

6.3 The Pseudomonas aeruginosa MksBEF

A new family of condensins, MksBEF (MukBEF-like SMC proteins), was identified using sequence analysis, and this MksBEF complex is broadly present in diverse bacteria. We characterized MksBEF function by inactivation of this protein in *Pseudomonas aeruginosa*. Functional assessment revealed that the *Pseudomonas aeruginosa* MksB acts as a condensin. PaMksB demonstrated the key activities expected of condensins including ATP modulated DNA binding and condensation in vitro (Petrushenko et al., 2011) and in vivo (Figure 5.1 B). Taken together with the

increased frequency of anucleate cells in the MksB-deficient strain (Figure 5.1), the synergistic effects of mutations in *smc* and *mksB* and the ability of MksBEF to complement anucleate cell formation in SMC-deficient cells (Figure 5.1 D, E), these data strongly argue that the protein, similar to other condensins, plays a role in chromosome organization and segregation.

6.4 Possible functions of Mks proteins

Our finding of a new family of condensins raises interesting questions about the function of these proteins. It is tempting to propose that, similar to their eukaryotic counterparts, MksBEF, MukBEF and SMC-ScpAB play distinct roles in global packing of bacterial chromosome. Perhaps one of these families acts as a prokaryotic counterpart of eukaryotic cohesins and establishes bridges between sister chromosomes. Alternatively, each of these systems could be optimized for its own set of physiological conditions and, therefore, having all three proteins would benefit environmentally growing and pathogenic bacteria but not necessarily laboratory strains. The latter idea is tentatively supported by the finding that chromosome packing defects in *mksB* and *smc* mutants of P. aeruginosa differ depending on growth conditions (Figure 5.1 C). This interpretation naturally explains why MksBEF subfamilies cut across bacterial subdivisions and appear to correlate with the occupied niche of a bacterium rather than its phylum or why the archetypal strains of *E. coli* and *Bacillus subtilis* do not encode any MksBEFs. MksBEFs could conceivably be spread from one bacterium to another via horizontal gene transfer or, perhaps, retained because additional adaptive advantage to a given niche. Alternatively, of course, each of these systems could have evolved independently, and

their occurrence in specific bacteria reflects little but random selection.

This study reveals that the role of condensins in chromosome maintenance is even more versatile than we previously thought. Other families of condensins, perhaps with novel functions, might emerge in future explorations of genomes. Unraveling the roles of these proteins will likely offer clues to the biogenesis and evolutionary origins of the chromatin structure and will undoubtfully enhance our ability to manipulate chromosomes on the global scale.

Appendices

Table S1. Bacterial strains and plasmids used in MukBEF study

	Relevant genotype or description	**Source or reference**
E.coli strains		
MG1655	Wild type strain	
OT7	PB103 with Δ*mukBEF::Kan*	(Yamazoe et al., 1999)
OU101	MG1655 with Δ*mukB::Kan*	(She et al., 2007)
OU102	MG1655 with Δ*mukEF::Kan*	(Wang et al., 2006)
AZ5450	Yk1100 with Δ*mukE::Kan*	(Yamanaka et al., 1996)
OU110	MG1655 with *lacYA::mukE-gfp-spc*	(She et al., 2007)
OU111	MG1655 with Δ*mukEF::Kan lacYA::mukE-gfp-spc*	(She et al., 2007)
OU115	MG1655 with *lacYA::mukB-gfp-spc*	(She et al., 2007)
OU116	MG1655 with Δ*mukB::Kan lacYA::mukB-gfp-spc*	(She et al., 2007)
OU119	MG1655 with Δ*mukB::mukB-gfp*	This study
OU120	MG1655 with *lacYA::mukE-spc*	This study
OU126	MG1655 with Δ*mukE::Kan* Δ*mukB::mukB-gfp lacYA::mukE-spc*	This study
Plasmids		
pBB14	Derivative of pACYC184, P_{muk}-*mukF-mukE-gfp*	Constructed at Rybenkov's lab
p15k-E02a	Kan^R, Derivative of pACYC184, P_{muk}-*mukE-gfp*, used for integration of mukE-gfp into *lacYA*	Constructed at Rybenkov's lab

P15sp-E02a	Spc^R, Derivative of pACYC184, P_{muk}-*mukE-gfp*, used for integration of *mukE-gfp* into *lacYA*	(She et al., 2007)
P15sp-E03a	Spc^R, Derivative of pACYC184, P_{muk}-*mukE*, used for integration of mukE into *lacYA*	This study
pBB41	Cm^R, Derivative of pACYC184, P_{muk}-*mukB-gfp*, used for in-frame *mukB-gfp* replacement	Constructed at Rybenkov's lab
PBB15k-TnpB1	Kan^R, Derivative of pACYC184, P_{muk}-*mukB-gfp*,	Constructed at Rybenkov's lab
pBB08	Ap^R, P_{BAD}-*mukF-mukE*	(Wang et al., 2006)
pBB10	Ap^R, P_{BAD}-*mukB*	(Wang et al., 2006)

Table S2. Bacterial strains and plasmids in MksBEF study

	Relevant genotype or description	**Source or reference**
P. aeruginosa strains		
PAO1-Lac	$lacI^{q+}$ Δ*(lacZ)M15*$^+$ *tetA*$^+$ *tetR*$^+$	ATCC
MPAO1	PAO1 with 1 kb deletion at *mksEF*, used as a Δ*mksEF* strain	(Jacobs et al., 2003)
PW8890	PAO1 with *PA4686::ISphoA/hah*, used as a *mksB* strain	(Jacobs et al., 2003)
UCBPP-PA14	a highly virulent strain, used to clone *mksB* gene	(Lee et al., 2006)
OP101	PAO1-Lac with Δ*smc*:: Gm^R *FRT*	This study
OP102	MPAO1 with Δ*smc*:: Gm^R *FRT*	This study
OP103	PAO1-Lac with Δ*smc*:: Gm^R *FRT,* constructed by phage transduction	This study
OP104	PAO1-Lac with $LacI^q$-P_{T7}-*mksFEB* Gm^R *FRT*	This study
OP105	PAO1-L ac with unmarked $LacI^q$-P_{T7}-*mksFEB*	This study
OP106	PAO1-L ac with $LacI^q$-P_{T7}-*mksFEB* Δ*smc::GmR FRT*	This study
Plasmids		
pUCP22	Ap^R, shuttle plasmid	(West et al., 1994)

pUCP_MksB	pUCP22 with *mksB* inserted at MCS	This study
pUCP_SMC	pUCP22 with *smc* inserted at MCS	This study
pEX18Ap	Ap^R; $oriT^+$ $sacB^+$,gene replacement vector with MCS from pUC18	(Hoang et al., 1998)
pSP856	Ap^R, Gm^R; source of Gm^R cassette, used to construct pEX_□SMC	(Hoang et al., 1998)
pYM101	Source of $lacI^q$ gene and the T7 early promoter $P_{T7(A1/04/03)}$	(Morita et al., 2010)
pEX_□SMC	Ap^R, Gm^R; derivative of pEX18Ap, *smc* replacement vector,	This study
pNPA_MksB01	Ap^R, pBADN with *mksB-His8*, used for MksB purificaiton	This study
pET_MksEF	pET21d(+) with *mksFE-His8*, used for MukEF purification	This study
pEX_LacI_Mks	Ap^R, Gm^R; derivative of pEX18Ap, conditional in-frame mks mutant vector,	This study

Table S3. Primers used in study

Primer name	Primer sequence (5' TO 3')	reference
1-A	CCGGTTGGCTAAGACGTT	Used for determination of SwaI fragment of p15k-E02a is integrated into MG1655, reverse primer in mukE gene.
1-B	CGCTACCATTACCAGTTG	Used for determination of SwaI fragment of p15k-E02a is integrated into MG1655, forward primer in E.coli chromosome, paired with 1-A.
2-A	ATGACTTCCGATCCAGAC	Used for determination of SwaI fragment of p15k-E02a is integrated into MG1655, reverse primer in E.coli chromosome, paired with 2-B.
2-B	ACACTGGCAGAGCATTAC	Used for determination of SwaI fragment of p15k-E02a is integrated into MG1655, forward primer in Kan^R, paired with 2-A.
spMG1655 F	GCGATGAGCGAAATGTAG	Used for determination of SwaI fragment of p15sp-E02a is integrated into MG1655, forward primer in Spc^R, paired with 2-A.

PSEQ1	AACAGCTGGCGGCGATCATC	Forward primer for *mukE* gene mutagenesis.
PSEQ2	CGTATGTTGCATCACCTTCA	Reverse primer for *mukE* gene mutagenesis.
smxbaIF	TGTAAAACGACGGCCAGTGC	Forward primer for amplifying *aadA* gene from pNN6029.
smbglIIR	GGGAGATCTGCTATGACCATGATTACG	Reverse primer for amplifying *aadA* gene from pNN6029, with BglII site.
oBEF79	CGGTGGAGAAAGCAT**ATG**ATTACG	Forward primer for amplifying *mukE*, with NdeI site.
oBEF80	GCAGTGTACA**TTA**TTCTTCCTCTCCGCTATC	Reverse primer for amplifying *mukE*, with stop codon and BsrGI site.
oBEF85	GGCGATCATCGAAGAACAACTTGC	Forward primer used for amplifying MukE from pBB14, upstream of BsrGI site in mukF.
oBEF86	CGATTCTAGACTAGTGATGGTGGTGATGGTGGTG	Reverse primer used for amplifying MukE gene from pBB14, with 7 his tag, stop codon and XbaI site.
oBEF87	GGAACCGTATATTACCCTGG	Forward sequencing primer for MukEF from pBB08 in *smtA*.
oBEF88	GATGGACGAACAGCAGCAGC	Forward sequencing primer for MukEF in pBB08, in *mukF*.
oBEF90	GATGATGATGGTCGACGG	Reverse sequencing primer for MukEF in pBB08, downstream of *mukE*.
oPA11	TGCGTCGCCCGTGCCTTTGC	Up from MksF, forward primer
oPA12	AGTCCACGGCCCTGTCAGGC	Down from MksB; complement to: GCCTGACAGGGCCGTGGACT
oPA13	GAACACGCGCAACAGGAGGC	Up from MksB; forward primer

oPA14	GTATTGAGCAGGGCGAAGCGG	Down from MksE; reverse primer; complement to CCGCTTCGCCCTGCTCAATAC
oPA15	TCCCATCCATA TACCCCCGG	Up from GntR-SMC operon in PA14 or PAO1
oPA16	AGTAGTTCGCCCCCTCTCCC	Down from ZipA, reverser primer; oPA15/oPA16 5.3 kb
oPA17	CCTGGTAC CAACGTCAGTCGCGGCTCG	KpnI-LF forward primer for GntR-SMC left flank
oPA18	CTTCTTGCTTAGCTCGCCATCA GCGTTCGGC	Reverse primer for GntR-SMC left flank: LF-BlpI; (Opa17/18~0.55kb)
oPA19	CTTCTTCGGTCCGGAGGCGGTCGCATT GGC	Forward primer for RsrII-fRF; for SMC-ZipA Right Flank
oPA20	CCCAAGCTTTTCGCGGGCACTGACGC	Reverse primer for rRF-HindIII; for SMC-ZipA Right Flank
oPA21	CTTCTTGCTAAGCCGAATTAGCTTCAAA AGCGCTC	BlpI-Frt, forward primer for BlpI-Frt-GmR-Frt-RsrII, complement to: gagcgcttttgaagctaattcgGCTtAGCaagaag
oPA29	cctcctCGGTCCGACGCGAAGAACGAGGA GGC	Forward primer for RsrII-MksB right flank; from MksB
oPA30	cccaagcttAGTCCACGGCCCTGTCAGGC	Down from MksB=Opa12+HindIII; for cloning MksB right flank
oPA31	cctggtacCGAGCTGGTCTGCGATACCC	Forward primer for KpnI-MksB left flank
oPA32	cttcttGCTtAGCAAGCGGCGGATGCCGTA GCG	Reverse primer for MksB left flank; =oPA14+BlpI, complement to CGCTACGGCATCCGCCGCTT-BlpI
oPA33	cctcctCGGTCCAACGCCTGGCGCTGTTC ACC	Forward primer for RsrII-MksE right flank; from MksE (RsrII-gaa-Opa13)
oPA34	cccaagcttAAGCGGCGGATGCCGTAGCG	Reverse primer for RsrII-MksE right flank; from MksE;=Opa14+HindIII, complement to : CGCTACGGCATCCGCCGCTT-HindIII
oPA35	cctggtaccTGCGTCGCCCGTGCCTTTGC	Forward primer for KpnI-MksF left flank (KpnI-oPA11)
oPA36	cttcttGCTtAGCGGGAATCTGCCGGTCGCT GG	Reverse primer for DeltaMksEF left flank, complement to CCAGCGACCGGCAGATTCCC-BlpI

oPA37	aagaagTCTAGAGCCGAACGCTGATGGCG	XbaI forward primer for SMC gene
oPA38	aagaagAAGCTTCACTCAGGCTTCAGCCAATGC	Hind III reverse primer for SMC gene, complement to GCATTGGCTGAAGCCTGAGTGAAGCTTcttctt
oPA39	GTCCGAATTCATGCGCCTGAAGAGCATCAAGC	Forward primer used to amplify SMC gene from PAO1, GTCC-EcoRI-atgcgcctgaagagcatcaagc, from strar codon ATG
oPA40	GTCCGCATGCGCTTCCTCGATGAAGTTGCG	Reverse primer for amplifying SMC gene from PAO1, ggac-XbaI + complementary to cgcaacttcatcgaggaagc, 500bp from start codon
oPA41	GCCTGCATCGCACTCATCGG	Upstream of mksF, forward primer used to check chromosome recombination. 2673-2692
oPA42	TCTTCGTGGGAGCTTCGGGC	Downstream of mksB, reverse primes used to check recombination, complementary to GCCCGAAGCTCCCACGAAGA
oPA44	GTCCAAGCTTTCATGCGTCAGCCTCCTGTTGC	Reverse primer for amplify MksFE from PAO1,complemeant to gcaacaggaggctgacgcatga+HindIII+ GTCC
oPA46	GTCCAAGCTTTTCACGCCGGTTCGCCGGCTTCCTC	Reverse primer for amplify MksB from PAO1,complemeant to gaggaagccg gcgaaccggc gtgaa +HindIII+ GTCC
oPA47	cgagcgttgcgaacagctcaacc	Rorward primer for checking the integration of SMC into att site, paired with Pser-down
oPA48	TGCTGGGGAAGTTCACCGTGGTCG	Reverser primer used for checking the integration of SMC into att site, paired with Pser-up
Pser-up	CGAGTGGTTTAAGGCAACGGTCTTGA	
Pser-down	AGTTCGGCCTGGTGGAACAACTCG	
oPA51	cttcttCGGTCCGGCTATCACCGAAGTGTCG	Forward primer for RsrII-fRF, PA4683-MksF Rightflank, Compement to cgacacttc ggtgatagccCGGACCGaagaag
oPA52	cccAAGCTTgctcgccgggaatcttcagg	reverse primer for rRF-HindIII, for PA4683-MksF Rightflank
Blp-LacIq-T7-R	AagaagGCTtAGCTCACTGCCCGCTTTCCAGT	Forward primer for LacIq-T7 fragment, BlpI-LacIQ-T7-SMC/MksF
oPA54	cctGGTACCTGCGCCAGGGGAATCTGC	Reverse primer for LacIQ-T7-MksF,RF-kpn, Complement to GCAGATTCCCCTGGCGCAGGTACCAGG, 500 bp from strat

		codon
oPA55	cttcttCGGTCCGACACAGGGCGTTACCCC GC	Forward primer for RsrII-fRS, alkB2-SMC Rightflank, Compement to gcggggtaacgccctgtgtCGGACCGaagaag
oPA56	cccAAGCTTaccgacaggatccagccc	Reverse primer for rRF-HindIII, for alkB2-SMC Rightflank
RsrII-LacIq-T7-R	AagaagCGGtCCGTC ACT GCC CGC TTT CCA GT	Forward primer for LacIq-T7 fragment, RsrII-LacIQ-T7-SMC/MksF
oPA58	GTCCGGTACCGCTTCCTCGATGAAGTT GCG	Reverse primer for LacIQ-T7-SMC,RF-KpnI, Complement to cgcaacttcatcgaggaagcGGTACCGGAC, 500BP from start codon of SMC
oPA61	gccgaaggccaggctgaagc	Forward primer, upstream of upstream sequence of smc, used to check chromosome recombination.
oPA62	CGATCTCCTGGTCGCCGATG	Reverse primer, downstream of LacIq-T7-SMC fragment, used for checking chromosome recombination.Complement to catcggcgaccaggagatcg
oPA64	GGTCAGCTGGGCGTTGGTC	Reverse primer, downstream of LacIq-T7-MksF fragment, used for checking chromosome recombination. Complement to gaccaacgc ccagctgacc
oPA65	CAGGACCACTTCTGCGCTCG	Forward primer in bla gene of pEX18Ap, complement,4966-4947
oPA66	cctatcctgcccggctgacg	Forward primer in OriT gene of pEX18Ap,2548-2567
oPA67	GCATCGAGCTGATCTTCGAC	Forward primer used to amplify smc probe, at 236 bp from start codon
oPA68	GTTCTGCGAGTCCAGGTAGC	Reverse primer used to amplify smc probe, at 2952 bp from start codon
oPA69	AGCTCAAGCAGCTGTTCCTC	Forward primer used to amplify mksB probe, at 596 bp from start codon
oPA70	TTCTCGCCTTCCTCGTACTG	Reverse primer used to amplify mksB probe, at 2294 bp from start codon

oPA71	ATCGTCGTATCCCACTACCG	Forward primer used to amplify LacIq probe, at 259 bp from start codon
oPA72	CCGCTCACAAGTCAACACTC	Reverse primer used to amplify LacIq probe, at 1239 bp from start codon

References

Anderson, D.E., Losada, A., Erickson, H.P., and Hirano, T. (2002). Condensin and cohesin display different arm conformations with characteristic hinge angles. The Journal of cell biology *156*, 419-424.

Blat, Y., and Kleckner, N. (1999). Cohesins bind to preferential sites along yeast chromosome III, with differential regulation along arms versus the centric region. Cell *98*, 249-259.

Britton, R.A., Lin, D.C., and Grossman, A.D. (1998a). Characterization of a prokaryotic SMC protein involved in chromosome partitioning. Genes Dev *12*, 1254-1259.

Britton, R.A., Lin, D.C., and Grossman, A.D. (1998b). Characterization of a prokaryotic SMC protein involved in chromosome partitioning. Genes Dev *12*, 1254-1259.

Choi, K.H., Kumar, A., and Schweizer, H.P. (2006). A 10-min method for preparation of highly electrocompetent Pseudomonas aeruginosa cells: application for DNA fragment transfer between chromosomes and plasmid transformation. J Microbiol Methods *64*, 391-397.

Cobbe, N., and Heck, M.M. (2004). The evolution of SMC proteins: phylogenetic analysis and structural implications. Mol Biol Evol *21*, 332-347.

Cui, Y., Petrushenko, Z.M., and Rybenkov, V.V. (2008). MukB acts as a macromolecular clamp in DNA condensation. Nat Struct Mol Biol *15*, 411-418.

Danilova, O., Reyes-Lamothe, R., Pinskaya, M., Sherratt, D., and Possoz, C. (2007). MukB colocalizes with the oriC region and is required for organization of the two Escherichia coli chromosome arms into separate cell halves. Molecular microbiology *65*, 1485-1492.

Datsenko, K.A., and Wanner, B.L. (2000). One-step inactivation of chromosomal genes in Escherichia coli K-12 using PCR products. Proceedings of the National Academy of Sciences of the United States of America *97*, 6640-6645.

den Blaauwen, T., Lindqvist, A., Lowe, J., and Nanninga, N. (2001). Distribution of the Escherichia coli structural maintenance of chromosomes (SMC)-like protein MukB in the cell. Molecular microbiology *42*, 1179-1188.

Deng, S., Stein, R.A., and Higgins, N.P. (2005). Organization of supercoil domains and their reorganization by transcription. Molecular microbiology *57*, 1511-1521.

Dillon, S.C., and Dorman, C.J. (2010). Bacterial nucleoid-associated proteins, nucleoid structure and gene expression. Nat Rev Microbiol *8*, 185-195.

Dotsch, A., Pommerenke, C., Bredenbruch, F., Geffers, R., and Haussler, S. (2009). Evaluation of a microarray-hybridization based method applicable for discovery of single nucleotide polymorphisms (SNPs) in the Pseudomonas aeruginosa genome. BMC Genomics *10*, 29.

Ezaki, B., Ogura, T., Niki, H., and Hiraga, S. (1991). Partitioning of a mini-F plasmid into anucleate cells of the mukB null mutant. Journal of bacteriology *173*, 6643-6646.

Fennell-Fezzie, R., Gradia, S.D., Akey, D., and Berger, J.M. (2005). The MukF subunit of Escherichia coli condensin: architecture and functional relationship to kleisins. The EMBO journal *24*, 1921-1930.

Glynn, E.F., Megee, P.C., Yu, H.G., Mistrot, C., Unal, E., Koshland, D.E., DeRisi, J.L., and Gerton, J.L. (2004). Genome-wide mapping of the cohesin complex in the yeast Saccharomyces cerevisiae. PLoS Biol *2*, E259.

Graumann, P.L. (2001). SMC proteins in bacteria: condensation motors for chromosome segregation? Biochimie *83*, 53-59.

Guacci, V., Koshland, D., and Strunnikov, A. (1997). A direct link between sister chromatid cohesion and chromosome condensation revealed through the analysis of MCD1 in S. cerevisiae. Cell *91*, 47-57.

Haering, C.H., Lowe, J., Hochwagen, A., and Nasmyth, K. (2002). Molecular architecture of SMC proteins and the yeast cohesin complex. Molecular cell *9*, 773-788.

Haering, C.H., and Nasmyth, K. (2003). Building and breaking bridges between sister chromatids. BioEssays : news and reviews in molecular, cellular and developmental biology *25*, 1178-1191.

Hagstrom, K.A., Holmes, V.F., Cozzarelli, N.R., and Meyer, B.J. (2002). C. elegans condensin promotes mitotic chromosome architecture, centromere organization, and sister chromatid segregation during mitosis and meiosis. Genes Dev *16*, 729-742.

Hiraga, S., Ichinose, C., Onogi, T., Niki, H., and Yamazoe, M. (2000). Bidirectional migration of SeqA-bound hemimethylated DNA clusters and pairing of oriC copies in Escherichia coli. Genes to cells : devoted to molecular & cellular mechanisms *5*, 327-341.

Hirano, T. (2005). SMC proteins and chromosome mechanics: from bacteria to humans. Philos Trans R Soc Lond B Biol Sci *360*, 507-514.

Hirano, T., Kobayashi, R., and Hirano, M. (1997). Condensins, chromosome condensation protein complexes containing XCAP-C, XCAP-E and a Xenopus homolog of the Drosophila Barren protein. Cell *89*, 511-521.

Hirano, T., and Mitchison, T.J. (1994). A heterodimeric coiled-coil protein required for mitotic chromosome condensation in vitro. Cell *79*, 449-458.

Hoang, T.T., Karkhoff-Schweizer, R.R., Kutchma, A.J., and Schweizer, H.P. (1998). A broad-host-range Flp-FRT recombination system for site-specific excision of chromosomally-located DNA sequences: application for isolation of unmarked Pseudomonas aeruginosa mutants. Gene *212*, 77-86.

Holmes, V.F., and Cozzarelli, N.R. (2000). Closing the ring: links between SMC proteins and chromosome partitioning, condensation, and supercoiling. Proceedings of the National Academy of Sciences of the United States of America *97*, 1322-1324.

Jacobs, M.A., Alwood, A., Thaipisuttikul, I., Spencer, D., Haugen, E., Ernst, S., Will, O., Kaul, R., Raymond, C., Levy, R.*, et al.* (2003). Comprehensive transposon mutant library of Pseudomonas aeruginosa. Proc Natl Acad Sci U S A *100*, 14339-14344.

Jensen, R.B., and Shapiro, L. (1999a). The Caulobacter crescentus smc gene is required for cell cycle progression and chromosome segregation. Proc Natl Acad Sci U S A *96*, 10661-10666.

Jensen, R.B., and Shapiro, L. (1999b). The Caulobacter crescentus smc gene is required for cell cycle progression and chromosome segregation. Proceedings of the National Academy of Sciences of the United States of America *96*, 10661-10666.

Jensen, R.B., and Shapiro, L. (2003). Cell-cycle-regulated expression and subcellular localization of the Caulobacter crescentus SMC chromosome structural protein. Journal of bacteriology *185*, 3068-3075.

Jessberger, R., Frei, C., and Gasser, S.M. (1998). Chromosome dynamics: the SMC protein family. Current opinion in genetics & development *8*, 254-259.

Kimura, K., and Hirano, T. (1997). ATP-dependent positive supercoiling of DNA by 13S condensin: a biochemical implication for chromosome condensation. Cell *90*, 625-634.

Kimura, K., Rybenkov, V.V., Crisona, N.J., Hirano, T., and Cozzarelli, N.R. (1999). 13S condensin actively reconfigures DNA by introducing global positive writhe: implications for chromosome condensation. Cell *98*, 239-248.

Koshland, D., and Strunnikov, A. (1996). Mitotic chromosome condensation. Annual review of cell and developmental biology *12*, 305-333.

Laloraya, S., Guacci, V., and Koshland, D. (2000). Chromosomal addresses of the cohesin component Mcd1p. The Journal of cell biology *151*, 1047-1056.

Lanzer, M., and Bujard, H. (1988). Promoters largely determine the efficiency of repressor action. Proc Natl Acad Sci U S A *85*, 8973-8977.

Lee, D.G., Urbach, J.M., Wu, G., Liberati, N.T., Feinbaum, R.L., Miyata, S., Diggins, L.T., He, J., Saucier, M., Deziel, E.*, et al.* (2006). Genomic analysis reveals that Pseudomonas aeruginosa virulence is combinatorial. Genome Biol *7*, R90.

Lehmann, A.R. (2005). The role of SMC proteins in the responses to DNA damage. DNA repair *4*, 309-314.

Li, G., and Reinberg, D. (2011). Chromatin higher-order structures and gene regulation. Current opinion in genetics & development *21*, 175-186.

Lindow, J.C., Kuwano, M., Moriya, S., and Grossman, A.D. (2002). Subcellular localization of the Bacillus subtilis structural maintenance of chromosomes (SMC) protein. Molecular microbiology *46*, 997-1009.

Losada, A., and Hirano, T. (2001). Intermolecular DNA interactions stimulated by the cohesin complex in vitro: implications for sister chromatid cohesion. Curr Biol *11*, 268-272.

Losada, A., and Hirano, T. (2005). Dynamic molecular linkers of the genome: the first

decade of SMC proteins. Genes Dev *19*, 1269-1287.

Losada, A., Yokochi, T., Kobayashi, R., and Hirano, T. (2000). Identification and characterization of SA/Scc3p subunits in the Xenopus and human cohesin complexes. The Journal of cell biology *150*, 405-416.

Luger, K., Mader, A.W., Richmond, R.K., Sargent, D.F., and Richmond, T.J. (1997). Crystal structure of the nucleosome core particle at 2.8 A resolution. Nature *389*, 251-260.

Mascarenhas, J., Soppa, J., Strunnikov, A.V., and Graumann, P.L. (2002). Cell cycle-dependent localization of two novel prokaryotic chromosome segregation and condensation proteins in Bacillus subtilis that interact with SMC protein. The EMBO journal *21*, 3108-3118.

Mascarenhas, J., Volkov, A.V., Rinn, C., Schiener, J., Guckenberger, R., and Graumann, P.L. (2005). Dynamic assembly, localization and proteolysis of the Bacillus subtilis SMC complex. BMC Cell Biol *6*, 28.

Matoba, K., Yamazoe, M., Mayanagi, K., Morikawa, K., and Hiraga, S. (2005). Comparison of MukB homodimer versus MukBEF complex molecular architectures by electron microscopy reveals a higher-order multimerization. Biochemical and biophysical research communications *333*, 694-702.

Melby, T.E., Ciampaglio, C.N., Briscoe, G., and Erickson, H.P. (1998). The symmetrical structure of structural maintenance of chromosomes (SMC) and MukB proteins: long, antiparallel coiled coils, folded at a flexible hinge. The Journal of cell biology *142*, 1595-1604.

Michaelis, C., Ciosk, R., and Nasmyth, K. (1997). Cohesins: chromosomal proteins that prevent premature separation of sister chromatids. Cell *91*, 35-45.

Milutinovich, M., Unal, E., Ward, C., Skibbens, R.V., and Koshland, D. (2007). A multi-step pathway for the establishment of sister chromatid cohesion. PLoS Genet *3*, e12.

Morita, Y., Narita, S., Tomida, J., Tokuda, H., and Kawamura, Y. (2010). Application of an inducible system to engineer unmarked conditional mutants of essential genes of Pseudomonas aeruginosa. J Microbiol Methods *82*, 205-213.

Murphy, L.D., and Zimmerman, S.B. (1997). Isolation and characterization of spermidine nucleoids from Escherichia coli. Journal of structural biology *119*, 321-335.

Nasmyth, K., and Haering, C.H. (2005). The structure and function of SMC and kleisin complexes. Annu Rev Biochem *74*, 595-648.

Niki, H., Jaffe, A., Imamura, R., Ogura, T., and Hiraga, S. (1991). The new gene mukB codes for a 177 kd protein with coiled-coil domains involved in chromosome partitioning of E. coli. EMBO J *10*, 183-193.

Noble, D., Kenna, M.A., Dix, M., Skibbens, R.V., Unal, E., and Guacci, V. (2006). Intersection between the regulators of sister chromatid cohesion establishment and maintenance in budding yeast indicates a multi-step mechanism. Cell Cycle *5*, 2528-2536.

Ohsumi, K., Yamazoe, M., and Hiraga, S. (2001). Different localization of SeqA-bound nascent DNA clusters and MukF-MukE-MukB complex in Escherichia coli cells. Molecular microbiology *40*, 835-845.

Petrushenko, Z.M., Cui, Y., She, W., and Rybenkov, V.V. (2010). Mechanics of DNA bridging by bacterial condensin MukBEF in vitro and in singulo. EMBO J *29*, 1126-1135.

Petrushenko, Z.M., Lai, C.H., Rai, R., and Rybenkov, V.V. (2006a). DNA reshaping by MukB. Right-handed knotting, left-handed supercoiling. J Biol Chem *281*, 4606-4615.

Petrushenko, Z.M., Lai, C.H., and Rybenkov, V.V. (2006b). Antagonistic interactions of kleisins and DNA with bacterial Condensin MukB. J Biol Chem *281*, 34208-34217.

Petrushenko, Z.M., She, W., and Rybenkov, V.V. (2011). A new family of bacterial condensins. Molecular microbiology.

Postow, L., Hardy, C.D., Arsuaga, J., and Cozzarelli, N.R. (2004). Topological domain structure of the Escherichia coli chromosome. Genes Dev *18*, 1766-1779.

Prentki, P., Binda, A., and Epstein, A. (1991). Plasmid vectors for selecting IS1-promoted deletions in cloned DNA: sequence analysis of the omega interposon. Gene *103*, 17-23.

Reyes-Lamothe, R., Wang, X., and Sherratt, D. (2008). Escherichia coli and its

chromosome. Trends Microbiol *16*, 238-245.

Robinson, P.J., Fairall, L., Huynh, V.A., and Rhodes, D. (2006). EM measurements define the dimensions of the "30-nm" chromatin fiber: evidence for a compact, interdigitated structure. Proceedings of the National Academy of Sciences of the United States of America *103*, 6506-6511.

Sawitzke, J.A., and Austin, S. (2000). Suppression of chromosome segregation defects of Escherichia coli muk mutants by mutations in topoisomerase I. Proceedings of the National Academy of Sciences of the United States of America *97*, 1671-1676.

Schleiffer, A., Kaitna, S., Maurer-Stroh, S., Glotzer, M., Nasmyth, K., and Eisenhaber, F. (2003). Kleisins: a superfamily of bacterial and eukaryotic SMC protein partners. Molecular cell *11*, 571-575.

Shapiro, L., McAdams, H.H., and Losick, R. (2009). Why and how bacteria localize proteins. Science *326*, 1225-1228.

She, W., Wang, Q., Mordukhova, E.A., and Rybenkov, V.V. (2007). MukEF Is required for stable association of MukB with the chromosome. J Bacteriol *189*, 7062-7068.

Sherratt, D.J. (2003). Bacterial chromosome dynamics. Science *301*, 780-785.

Shin, H.C., Lim, J.H., Woo, J.S., and Oh, B.H. (2009). Focal localization of MukBEF condensin on the chromosome requires the flexible linker region of MukF. The FEBS journal *276*, 5101-5110.

Skibbens, R.V., Corson, L.B., Koshland, D., and Hieter, P. (1999). Ctf7p is essential for sister chromatid cohesion and links mitotic chromosome structure to the DNA replication machinery. Genes Dev *13*, 307-319.

Soppa, J., Kobayashi, K., Noirot-Gros, M.F., Oesterhelt, D., Ehrlich, S.D., Dervyn, E., Ogasawara, N., and Moriya, S. (2002). Discovery of two novel families of proteins that are proposed to interact with prokaryotic SMC proteins, and characterization of the Bacillus subtilis family members ScpA and ScpB. Molecular microbiology *45*, 59-71.

Spurio, R., Dürrenberger, M., Falconi, M., La Teana, A., Pon, C.L., and Gualerzi, C.O. (1992). Lethal overproduction of the E*scherichia coli* nucleoid protein H-NS: ultramicroscopic and molecular autopsy. Molecular and General Genetics *231*, 201-211.

Stray, J.E., and Lindsley, J.E. (2003). Biochemical analysis of the yeast condensin Smc2/4 complex: an ATPase that promotes knotting of circular DNA. The Journal of biological chemistry *278*, 26238-26248.

Strunnikov, A.V. (2010). One-hit wonders of genomic instability. Cell Div *5*, 15.

Sumara, I., Vorlaufer, E., Gieffers, C., Peters, B.H., and Peters, J.M. (2000). Characterization of vertebrate cohesin complexes and their regulation in prophase. The Journal of cell biology *151*, 749-762.

Toth, A., Ciosk, R., Uhlmann, F., Galova, M., Schleiffer, A., and Nasmyth, K. (1999). Yeast cohesin complex requires a conserved protein, Eco1p(Ctf7), to establish cohesion between sister chromatids during DNA replication. Genes Dev *13*, 320-333.

Uhlmann, F., Lottspeich, F., and Nasmyth, K. (1999). Sister-chromatid separation at anaphase onset is promoted by cleavage of the cohesin subunit Scc1. Nature *400*, 37-42.

Unal, E., Arbel-Eden, A., Sattler, U., Shroff, R., Lichten, M., Haber, J.E., and Koshland, D. (2004). DNA damage response pathway uses histone modification to assemble a double-strand break-specific cohesin domain. Molecular cell *16*, 991-1002.

Unal, E., Heidinger-Pauli, J.M., and Koshland, D. (2007). DNA double-strand breaks trigger genome-wide sister-chromatid cohesion through Eco1 (Ctf7). Science *317*, 245-248.

Volkov, A., Mascarenhas, J., Andrei-Selmer, C., Ulrich, H.D., and Graumann, P.L. (2003). A prokaryotic condensin/cohesin-like complex can actively compact chromosomes from a single position on the nucleoid and binds to DNA as a ring-like structure. Mol Cell Biol *23*, 5638-5650.

Waite, R.D., Paccanaro, A., Papakonstantinopoulou, A., Hurst, J.M., Saqi, M., Littler, E., and Curtis, M.A. (2006). Clustering of Pseudomonas aeruginosa transcriptomes from planktonic cultures, developing and mature biofilms reveals distinct expression profiles. BMC Genomics *7*, 162.

Waizenegger, I.C., Hauf, S., Meinke, A., and Peters, J.M. (2000). Two distinct pathways remove mammalian cohesin from chromosome arms in prophase and from centromeres in anaphase. Cell *103*, 399-410.

Wang, Q., Mordukhova, E.A., Edwards, A.L., and Rybenkov, V.V. (2006). Chromosome condensation in the absence of the non-SMC subunits of MukBEF. J Bacteriol *188*, 4431-4441.

Weitao, T., Nordstrom, K., and Dasgupta, S. (1999). Mutual suppression of mukB and seqA phenotypes might arise from their opposing influences on the Escherichia coli nucleoid structure. Molecular microbiology *34*, 157-168.

West, S.E., Schweizer, H.P., Dall, C., Sample, A.K., and Runyen-Janecky, L.J. (1994). Construction of improved Escherichia-Pseudomonas shuttle vectors derived from pUC18/19 and sequence of the region required for their replication in Pseudomonas aeruginosa. Gene *148*, 81-86.

Woo, J.S., Lim, J.H., Shin, H.C., Suh, M.K., Ku, B., Lee, K.H., Joo, K., Robinson, H., Lee, J., Park, S.Y.*, et al.* (2009). Structural studies of a bacterial condensin complex reveal ATP-dependent disruption of intersubunit interactions. Cell *136*, 85-96.

Yamanaka, K., Ogura, T., Niki, H., and Hiraga, S. (1996). Identification of two new genes, mukE and mukF, involved in chromosome partitioning in Escherichia coli. Molecular & general genetics : MGG *250*, 241-251.

Yamazoe, M., Onogi, T., Sunako, Y., Niki, H., Yamanaka, K., Ichimura, T., and Hiraga, S. (1999). Complex formation of MukB, MukE and MukF proteins involved in chromosome partitioning in Escherichia coli. The EMBO journal *18*, 5873-5884.

Zimmerman, S.B. (2006). Shape and compaction of Escherichia coli nucleoids. Journal of structural biology *156*, 255-261.